ACTIVE TECTONICS AND KINEMATICS OF FETHİYE-GÖCEK BAY, SW TURKEY

A THESIS SUBMITTED TO
THE GRADUATE SCHOOL OF NATURAL AND APPLIED SCIENCES
OF
MIDDLE EAST TECHNICAL UNIVERSITY

BY

LEVENT TOSUN

IN PARTIAL FULFILLMENT FOR THE REQUIREMENTS
FOR
THE DEGREE OF MASTER OF SCIENCE
IN
GEOLOGICAL ENGINEERING

JANUARY 2018

Approval of the thesis:

ACTIVE TECTONICS AND KINEMATICS OF FETHİYE-GÖCEK BAY, SW TURKEY

Submitted by **LEVENT TOSUN** in partial fulfillment of the requirements for the degree of **Master of Science in Geological Engineering Department, Middle East Technical University** by,

Prof. Dr. Gülbin Dural Ünver _____
Dean, Graduate School of **Natural and Applied Sciences**

Prof. Dr. Erdin Bozkurt _____
Head of Department, **Geological Engineering**

Prof. Dr. Nuretdin Kaymakcı _____
Supervisor, **Geological Engineering Dept., METU**

Examining Committee Members:

Prof. Dr. Erdin Bozkurt _____
Geological Engineering Dept., METU

Prof. Dr. Hasan Sözbilir _____
Geological Engineering Dept., DEU

Prof. Dr. Nuretdin Kaymakcı _____
Geological Engineering Dept., METU

Prof. Dr. M. Cihat Alçiçek _____
Geological Engineering Dept., Pamukkale University

Assist. Prof. Dr. Erhan Gülyüz _____
Geological Engineering Dept., Yüzüncü Yıl University

Date: 31.01.2018

I hereby declare that all information in this document has been obtained and presented in accordance with academic rules and ethical conduct. I also declare that, as required by these rules and conduct, I have fully cited and referenced all material and results that are not original to this work.

Name, Last Name: Levent TOSUN

Signature:

ABSTRACT

ACTIVE TECTONICS AND KINEMATICS OF FETHİYE-GÖCEK BAY, SW TURKEY

Levent TOSUN
M.Sc., Department of Geological Engineering
Supervisor: Prof. Dr. Nuretdin KAYMAKCI

January 2018, 101 pages

Tomographic studies conducted in Eastern Mediterranean region reveal that Pliny-Strabo Trench corresponds to a tear known as "STEP" (Subduction Transform Edge Propagator) fault connecting the Aegean and Cyprean trenches along the northern edge of the northward subducting African lithosphere. Recently, it is claimed that Fethiye-Burdur Fault Zone, which interpreted as a sinistral transtensional shear zone, is the northeaster continuation of this fault.

In order to test this hypothesis, a rigorous study aiming at unravelling the characteristics and kinematic of the faults developed around the Fethiye-Göcek Bay located at the northeastern termination of the Pliny-Strabo Trench from off-shore to on-shore was conducted. In this context, totally 228 km long, 32 seismic lines collected from the Fethiye-Göcek Bay, are interpreted and faults cutting the seabed were mapped. In addition, the on-land continuation and characteristics of these faults were verified in the field. For this purpose, about 15.000 fault slip data from 222 locations within the bay and its vicinity were collected and analyzed.

According to obtained results, all of the faults are developed under approximately NW-SE directed extension, except some NW-SE-striking faults, which have strike-

slip components contrary to proposed sinistral nature of alleged Fethiye-Burdur Fault Zone. There is not any tangible evidence that supports the existence of a sinistral transtensional shear zone in the region. It is claimed that Pliny-Strabo Trench does not propagate on-land along a NE-SW striking major sinistral strike-slip shear zone in the region, and that existence and characteristics of the Fethiye-Burdur Fault Zone are therefore debatable.

Keywords: Fethiye-Burdur Fault Zone, Pliny-Strabo Trench, active faults, kinematic analysis, Fethiye-Göcek Bay

ÖZ

FETHİYE-GÖCEK KÖRFEZİ'NİN AKTİF TEKTONİĞİ VE KİNEMATİĞİ, GB TÜRKİYE

Levent TOSUN
Yüksek Lisans, Jeoloji Mühendisliği Bölümü
Tez Yöneticisi: Prof. Dr. Nuretdin KAYMAKCI

Ocak 2018, 101 sayfa

Doğu Akdeniz bölgesinde yapılan tomografi çalışmaları, batıdaki Ege Yayı'nı doğuda Kıbrıs Yayı'ndan ayıran Pliny-Strabo Hendeği'nin kuzeye dalmakta olan Afrika plakasının kuzey ucunda "STEP" (Subduction Transform Edge Propagator) fay olarak bilinen bir yırtılmaya karşılık geldiğini ortaya koymuştur. Son yıllarda yapılan çalışmalarda, sol yönlü transtansiyonel bir makaslama zonu olduğu iddia edilen Fethiye-Burdur Fay Zonu'nun bu fayın KD yönündeki devamı olduğu öne sürülmüştür.

Bu hipotezi test etmek amacıyla, Pliny-Strabo Hendeği'nin KD yönünde denizden karaya geçiş noktasında bulunan Fethiye-Göcek Körfezi ve yakın çevresinde gelişmiş fayların karakterleri ve kinematik özelliklerini ortaya koymayı hedefleyen titiz arazi çalışması tarafımızca gerçekleştirilmiştir. Bu kapsamda, körfez içerisinde toplam 228 km uzunluğunda 32 adet sismik hat yorumlanarak körfez tabanındaki güncel birimleri kesen aktif faylar haritalanmıştır. Buna ek olarak, haritalanan bu fayların karadaki devamlılıkları ve karakterleri arazide teyit edilmiştir. Bu amaçla körfez ve yakın civarındaki 222 farklı lokasyondan yaklaşık 15.000 fay çiziği verisi derlenmiş ve analiz edilmiştir.

Çalışmalar sonucu elde edilen verilere dayanılarak, sol yönlü hareket bileşeni olduğu ifade edilen Fethiye-Burdur Fay Zonu'nu boyunca iddia edilenin aksine, bölgede haritalanan fayların hemen hemen tamamının KB-GD yönlü bir genişlemeye bağlı olarak geliştikleri belirlenmiş olup az sayıdaki doğrultu atımlı fayın ise KB-GD yönlü olduğu saptanmıştır. Bölgede sol yönlü olduğu ileri sürülen transtansiyonel fay kuşağının varlığını destekleyecek herhangi bir veriye rastlanmamıştır. Pliny-Strabo Hendeği'nin karada KD-GB yönlü sol yanal atımlı makaslama zonu boyunca ilerlemediği belirlenmiştir. Bu sebeple, Fethiye-Burdur Fay Zonu'nun varlığı ve karakteri tartışmalıdır.

Anahtar Kelimeler: Fethiye-Burdur Fay Zonu, Pliniy-Strabo Hendeği, Aktif Fay, Kinematik Analiz, Fethiye-Göcek Körfezi

to my parents…

ACKNOWLEDGEMENTS

This thesis would not have been possible without the priceless contribution of many people over the last five month. I would like to take this opportunity to give my deepest thanks to all these people.

First of all, I am deeply grateful to my supervisor Prof. Dr. Nuretdin KAYMAKCI for his everlasting patience, invaluable guidance, encouragement and continued advice throughout the course of my M.Sc. studies. It has been an honour and a pleasure working with him. I would also like to thank to my co-supervisor Assist. Prof. Dr. Ulaş AVŞAR for his valuable guidance, continued advice and critical discussion throughout this study. I have been privileged to experience first-hand how a passionate person can make a difference.

I wish to thank my examining committee members, Prof. Dr. Erdin BOZKURT, Prof. Dr. Hasan SÖZBİLİR, Prof. Dr. M. Cihat ALÇİÇEK and Assist. Prof. Dr. Erhan Gülyüz for their valuable recommendations and criticism.

This study was carried out as part of the projects supported by The Scientific and Technological Research Council of Turkey (TÜBİTAK, Project Number 111Y239 & 112Y137).

I would like to thank to Prof. Dr. Derman DODURUR, the geophysicists, H. Mert KÜÇÜK, Özkan ÖZEL, Orhan ATGIN, who work at Dokuz Eylül University Institute of Marine Science and Technology, and the project coordinator Assist. Prof. Dr. Özgür AVŞAR, who has been involved in the seismic survey. Additionally, I would also like to thank to authorities of Chamber of Shipping-Fethiye for their collaboration and supports during seismic data collection.

I am heartily thankful to my roommate Fatih Seçkin ŞİŞ for his endless patience and answers to my numerous (and some insane) questions, to Mustafa KAPLAN from whom I have learned a lot before and throughout the study, especially with his theoretical support, to Zehra DEVECİ ARAL for her friendly and outgoing

friendship, to Abdul QAYYUM for his support in using SMT Kingdom software, to the research assistants of METU Geological Engineering Department; Felat DURSUN, Yavuz KAYA, Gamze TANIK, S. Görkem ATASOY and also to the graduate students; Akın ÇİL and Meryem Dilan İNCE for their support, friendship and endless encouragement throughout this study. It was enjoyable to work with them.

I would like to say a massive thank you all my long time friends who helped keep me sane during this rocky road including, M.Bedirhan KOYUNCU (Blue-eyed Giant), Ece Gizem KUBAT, Ezgi ÖZTEN, Hilal DOĞANÜLKER BERBEROĞLU and also Abidin Uğur YÜCEL and Selçuk İlkay ÇEVİK.

Special thanks are extended to Dr. Özcan DUMANLILAR and all Demir Export Exploration Department, who are my former teammates, for believing in me when I decided to build up an academic career.

At last but not the least, I wish to express my deepest thanks to my parents for their guidance, patience and care. This thesis belongs to them as much as it belongs to me. Their confidence on me gave me all the strength and courage I need to complete this work.

"Pluralitas non est ponenda sine necessitate."

Ockham's Razor

TABLE OF CONTENTS

LIST OF FIGURES

LIST OF TABLE

CHAPTER 1

INTRODUCTION

1.1 Purpose and Scope

The tectonic framework of the Western Anatolia has been shaped as result of two continuing tectonic processes since Early Miocene. The first is northward collision of the Arabian Plate causing westward extrusion of the Anatolian Plate along the North Anatolian and East Anatolian Fault Zones (Şengör et al., 1985). The latter is the northward subduction of African lithosphere along the south-westward retreating Aegean trench in the west and Cyprus trench in the east (McKenzie 1978; Le Pichon and Angelier 1979; Biryol et al. 2011). Due to slab tearing caused by the lateral variation in the nature of the subducted lithosphere, the Aegean and Cyprus trenches are segmented by a 100 km wide transform fault zone, called as Pliny-Strabo (Woodside et al., 2002; Govers and Wortel, 2005). In recent years, after the recognition of this large-scale sinistral transpressional shear zone based on seismic tomographic studies and geodetic measurements, it has been envisaged that Fethiye Burdur Fault Zone (FBFZ), which is an active sinistral transtensional shear zone, is the onland continuation of the Pliny Strabo trench in SW Anatolia (Dumond et al., 1979; Barka and Reilinger, 1997; Elitez 2010; Ocakoğlu, 2012; Tiryakioğlu et al., 2013; Hall et al., 2014; Aksoy et al., 2016).

This thesis presents an integrated study concerning the active tectonics and kinematics of the Fethiye-Göcek Bay, which is located at the transition zone between the Pliny-Strabo trench and the FBFZ (Figure 1), by using fault kinematic analysis

and interpretation of seismic sections. Kinematic analysis, based on fault slip data sets, is aimed at unravelling the paleostress orientations and their relative magnitudes that are responsible for style and pattern of the deformation in the investigated area. Additionally, seismic sections, combined with bathymetry, provide interpretation of the active faults and also provide means for the verification of the spatial distribution of faults in relation to the recent deformation in the region. The results will shed light on the understanding of link between Pliny-Strabo trench and their northwards continuation. This will allow us testing the hypothesis that (i) whether the active FBFZ is an active strike-slip fault zone developed in response to northwards propagation of the Pliny-Strabo STEP fault on land and accommodate differential motion between Aegean and Central Anatolian regions or (ii) it terminates around the Fethiye-Göcek Bay and connects Aegean and Cyprian trenches, like any other trench to trench connecting transform faults.

1.2 Geographic Position of the Study Area

The study area comprises the Fethiye-Göcek Bay and surroundings (Muğla, Turkey) (Figure 1). The area under investigation occupies approximately 1800 square kilometres between 36.30 N - 36.50 N latitudes and 28.45 E - 29.15 E longitudes and lies within O21b3,b4,c1,c2,c3,c4 and O22a3,a4,d1,d2,d3,d4 quadrangles of Turkish 1/25.000 scale topographic maps.

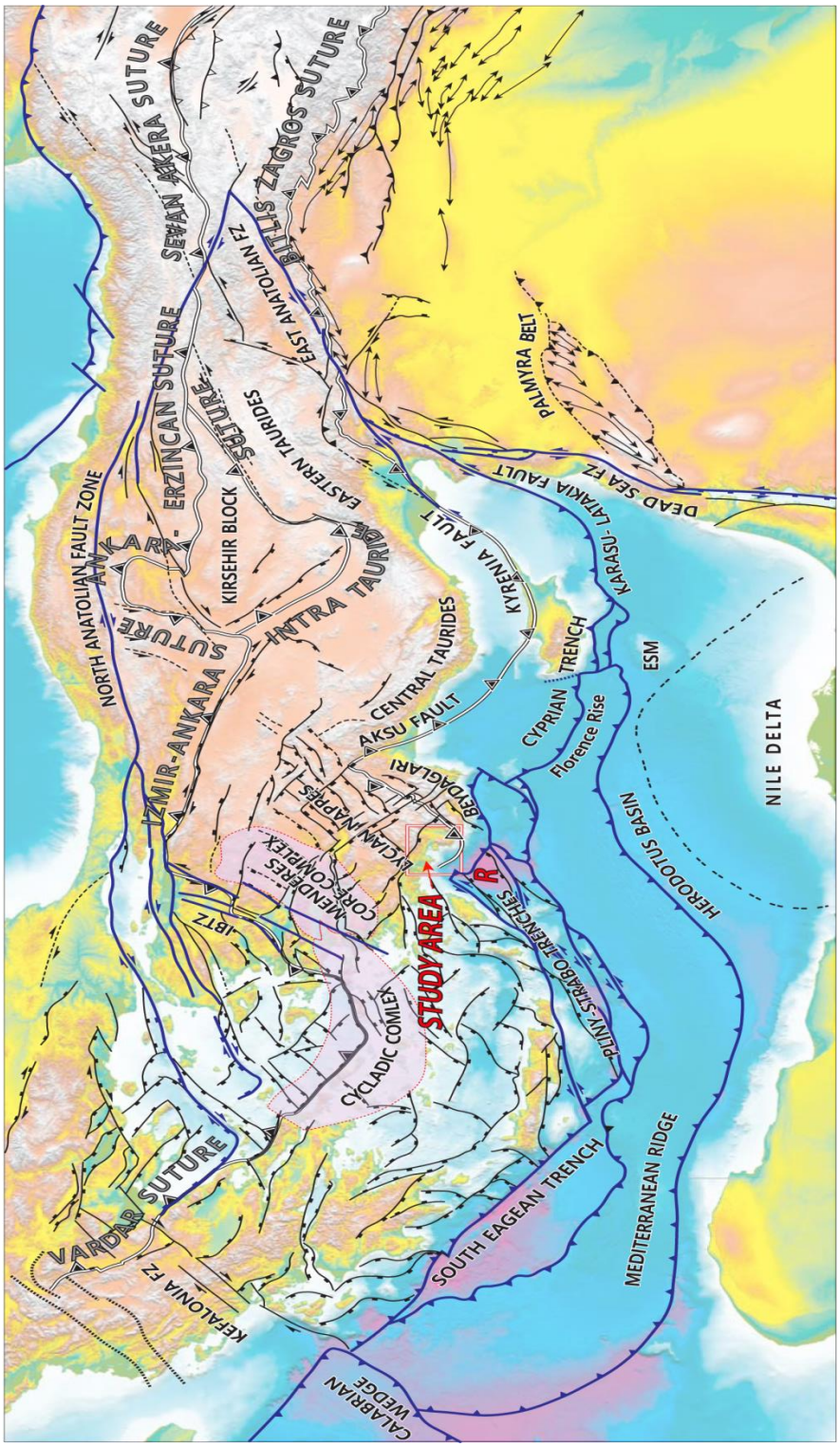

Figure 1 Simplified tectonic scheme of Eastern Mediterranean region (simplified from Le Pichon and Angelier 1981; Şengör et al., 1985; Bozkurt et al., 2001; Kaymakci, et al., 2007 and 2009, 2010; van Hinsbergen et al., 2010; Biryol et al., 2011).ESM: Eratosthenes Seamount , R: Rhodes basin. Note That Pliny-Strabo Trench Terminates at the northern end of Rhodes Basin.

1.3 Data and Method of the Study

This study was carried out in four main stages: 1) preliminary studies, 2) 2D seismic interpretation, 3) field studies and 4) office works. The preliminary studies include investigation and collection of available literature. For this purpose, the relevant documents, including topographical and geological maps, satellite images together with published reports, and research papers collected and scrutinized. During this stage, a detailed lineament map at digital elevation models was prepared for ground truthing.

The second stage was about interpretation of 32 2D seismic lines, a total of 228 km long sections. During this stage, the horizons and faults were picked in time domain and the surface intersection (trace) of the faults were mapped on plan view. Seismic interpretation was performed using SMT Kingdom software.

The third stage includes field studies, both on the mainland and islands in the bay area. Every island and all the shore line along the bay and its vicinity was visited by a 4.2 m fiberglass boat with 20 HP outboard motor (Figure 2). During this study, faults exposed on the cliffs and along the shoreline are studied in detail and fault-slip data was collected.

Figure 2 The boat used in marine side studies.

During field studies, total of 14877 slip data from 222 sites were collected and documented. Faults were identified and categorized, using slickensided surfaces, stratigraphic separations, where the basement units juxtaposed with younger sedimentary units, and available kinematic indicators help to identify direction of fault block movements. The slickenside lineations and orientations of fault planes were collected by using eGEO Compass Pro developed Marc Foi (http://www.mcfoi.it/egeo_compass; access: July 2017). It is a digital geological compass application specially designed for the Android mobile operating system.

The fourth and the last stage comprises integration and interpretation of all gathered information from previous stages. Reconstruction of paleostress configurations were performed in this stage. The collected data were processed by Win-Tensor (windows version of TENSOR) which is an interactive process of stress tensor calculation program developed based on Angelier's reduced stress tensor concept. Lastly, the structures and deformation styles of the area in question as well as their activities has been deduced from seismic interpretations and paleostress reconstruction studies in Fethiye-Göcek Bay.

1.4 Previous Studies

The tectonic evolution of the South Western Anatolia has been one of the most extensively studied region due to its role in the geodynamic evolution of the Eastern Mediterranean and its unique tectonic characteristics, extensional tectonics in particular. Similarly, this study is centred around the kinematics, characteristics, and activities of the faults around Fethiye-Göcek Bay and its relation to regional tectonics that governs SW Anatolia. Before going into details of the present study, previous works carried out around the bay area are summarized.

The previous studies conducted around the study area are categorized, based on the context of this study, into two groups. The first group is about the general geological characteristics of the region and includes paleotectonic and neotectonic evolution of south-western Anatolia. Studies including in this category will be given in detail in the regional tectonic setting part. The second group is active tectonics of the SW Anatolia, particularly the source mechanism of recent earthquakes. In this context, a

brief review of the key previous studies will be summarized in a chronological order below.

McKenzie (1972, 1978) investigated the active tectonics of Mediterranean region and Alpine-Himalayan belt including the Aegean Sea and surrounding regions based on moment tensor solutions of earthquakes, Landsat images, and seismotectonic characteristics of the region. He claimed that rapid extension is recently taking place in the northern and eastern parts of the Aegean Sea region.

Dumont et al. (1979) documented information about the formation mechanism of horst-graben systems in south-western Anatolia on account of faults cutting Miocene-Quaternary deposits. As a result, they proposed for the first time the alleged Fethiye Burdur Fault, a left lateral strike-slip fault that could be the NE continuation of Pliny-Strabo trench into the SW Anatolia.

Şaroğlu et al. (1987, 1992) mapped a number of NE-SW-trending active faults with sinistral strike-slip components within the alleged Fethiye-Burdur Fault Zone at a scale of 1:1,000,000 and they are included in the Active Fault Map of Turkey (Şaroğlu et al., 1992). During following years, this map was revised by Duman et al.(2016), using geographic information system based database includes maps of active faults, catalogues of instrumental and historical earthquakes, moment tensor solutions and data on crustal thickness, and they also claim that the NE-SW trending faults along Fethiye-Burdur Fault zone active and has been accommodating sinistral displacement.

Taymaz and Price (1992) determined the source parameters for May 12 1972 Burdur earthquake by using seismological and geological observations and suggest that the major earthquake fault was a normal fault with a listric geometry.

Price (1989), and Price and Scott (1994) proposed a basin evolution model for NE-SW trending Burdur-Acıgöl-Baklan basin. According to his study, each of these Quaternary basins has a half-graben geometry and active faults bounding them have a sinistral strike-slip component, with slip vectors indicating extension in an NW-SE direction.

Koçyiğit (1984) and Koçyiğit et al. (2000) studied the horst-graben system in SW Anatolia on the basis of field geological mapping. Orientations of local principal stress axes were reconstructed from fault slip data together with moment tensor solutions of recent large magnitude earthquakes in the region. They claimed that the basin-bounding NE-SW trending active faults bounding basins along FBFZ are orthogonal normal fault systems developed in a graben-type extensional depression without any significant evidence of basin formation in a strike-slip setting.

Yağmurlu et al. (1997) carried out a study, aimed at demonstrating the relationship between alkaline volcanism and active tectonism within the context of evolution of the Isparta Angle (IA). They claimed that the radiometric ages of alkaline volcanics, which were arranged contemporaneously along N-S trending faults at the apex of Isparta Angle, between Bucak and Afyon regions, are progressively become younger from north to south. The authors ascribed this pattern to the southward migration of the subduction zone. They also claimed that the NE-trending faults within the Burdur Basin are sinistral strike-slip faults and that these structures are the continuation of the Pliny-Strabo trench on land. The authors also claimed that these faults form the boundary between the Aegean and Mediterranean plates as was proposed by Dumont et al. (1979).

Akyüz and Altunel (1997, 2001) carried out a study to investigate the deformation of archaeological relics in the ancient city of Cibyra, which is located within the alleged FBFZ. They claimed that the NE-SW-oriented Cibyra fault can be traced within Pliocene sediments in the vicinity of the ancient city and slickenside lineations on exposed fault surfaces, which are also observed on the artifacts, indicate left-lateral motion combined with a minor normal component.

Alçiçek (2001), Alçiçek et al. (2002, 2004, 2005, 2006, 2007, 2008, 2013, 2015, 2018), Alçiçek and Ten Veen (2008) and studied the basin evolution combined with structural analysis and introduced the first detailed time-stratigraphic framework for the neotectonic development of Neogene grabens (i.e. Eşen, Çameli, Burdur) along the Fethiye-Burdur Fault Zone in south western Anatolia. They proposed a time-stratigraphic framework for the evolution of NE-SW-trending Neogene basins in FBFZ on the basis of bio-stratigraphically well constrained tectono-sedimentary

model. As a consequence, they stated that the FBFZ represents a broad zone of isolated or interconnected NE-SW-trending basins that formed under prevailing NW-SE extension, rather than being a significant strike-slip fault zone. In addition, based on the field observations from the Eşen, Çameli and Burdur areas, they suggested that the recent deformation is dominated by dextral shear along NE-SW-striking faults that are linked to the NW-SE extension in the region. In their interpretation, the dextral faults are local accommodation structures, which transfer NE-SW extensional strain in a system of bi-directional extension.

Şahin (2004) was claimed that there is an increase in the accumulated stress along the zone from Fethiye to Burdur based on coulomb stress distributions according to 24 earthquake solutions provided by Taymaz and Tan (2001) .

Gürer et al. (2004) provided first magnetotelluric images of a part of the crust in the south-western Taurides along the alleged FBFZ. They observed a broad vertical zone of high conductivity and attributed it to a deep-seated vertical fault zone.

Ten Veen et al. (2009) carried out a regional study in SW Anatolia, which provided structural evolutionary scenarios of the region from paleotectonic to neotectonic. According to their results, kinematic decoupling took place between the Lycian Nappes (to the south) and the Menderes Massif (in the north) in three tectonic phases from Early Miocene-Recent.

Hall et al. (2009, 2014) interpreted a number of multi-channel seismic reflection profiles from offshore areas and provided improved structural architecture of Rodos Basin where a number of NE-SW sinistral strike-slip faults dominate. As a result of these studies and combining published information they claimed that NE-trending Pliny-Strabo trench along the eastern edge of Aegean subduction zone continued along a zone collinear with the on-land alleged FBFZ in SW Anatolia. Therefore, they claimed that FBFZ is a sinistral strike-slip fault zone and is the NE continuation of the Pliny-Strabo STEP fault (c.f. Govers and Wortel 2005).

Elitez (2010) carried out a M.Sc study to investigate the Miocene-Quaternary geodynamics of Çameli and Gölhisar basins within the FBFZ. According to this study, the Neogene basins commenced in relation to a compressional regime in the

Early Miocene and followed by a left-lateral movement in the Middle-Late Miocene. The basins are currently situated within a Pliocene-Recent predominantly left-lateral extensional regime (Elitez et al., 2009; Elitez and Yaltırak, 2014a; Elitez and Yaltırak, 2014b; Elitez et al., 2015; Elitez et. al., 2016).

Karabacak (2001) carried out a study within the Cibrya segment of the alleged FBFZ, based on geological, geomorphological and archaeoseismological observations in the field. He claimed that Cibyra Fault is an active left -lateral fault capable of producing earthquakes of considerable magnitude and it is consistent with the sinistral nature of alleged FBFZ.

Biryol et al. (2011) modeled the African lithosphere beneath the Anatolian region based on the teleseismic P-wave tomography. They suggest that the northward subducting African lithosphere is segmented beneath Anatolia and this segmentation plays an important role in the active tectonics of Anatolia and controls the distribution of volcanic provinces and different deformation domains.

Ocakoğlu (2012) studied the seafloor morphology and sea-bottom deformation patterns in the region Fethiye-Marmaris Bay, using multi-beam bathymetric and seismic reflection data. The study mapped out some sinistral sea-bottom morphological patterns and that these faults are the manifestation of sinistral strike-slip faults in the region. These faults are interpreted as the indication of north-eastern extension of the Pliny-Strabo trench.

Özbakır et al. (2013) proposed that the NE-trending Pliny and Strabo trench in the eastern part of the Aegean trench represent the surface expression of a STEP-type plate boundary (c.f. Govers and Wortel, 2005), which is the boundary zone between the non-subducted African lithosphere and the Aegean lithosphere.

Över et al. (2013) studied the Plio-Quaternary to present day stress regime in the Burdur basin, which is located at the north-eastern end of the alleged FBFZ. He claimed that the region is predominated by a consistent normal faulting stress regime during Plio-Quaternary time based on the inversions of slip vectors recorded by brittle deformation and the seismic fault slip deduced from the earthquake focal mechanisms.

Özkaptan et al. (2014) and Kaymakcı et al. (2014) discussed the left-lateral transtensional nature of the FBFZ on the basis of paleomagnetic and kinematic studies. According to their study, there is no marked change in the rotation senses and amounts on the either side of the FBFZ implying no differential rotation within the zone. Additionally, the slickenside pitches and constructed paleostress configurations along the proposed FBFZ are normal in character and consistent with earthquake focal mechanisms, suggesting active extension in the region. Therefore, they claimed that there is no evidence for the presence of alleged FBFZ in the field.

Kürçer et al. (2016) carried out a paleoseismological survey in the Acıpayam Fault, which is an active fault segment located on the central part of the FBFZ. According to their paleoseismic data obtained from trench studies, the latest event recorded on the Acıpayam Fault was dated between 3030 ± 30 BP and 2410 ± 30 BP and, based on fault plane slip data measured from trenches, that the Acıpayam Fault is an active normal fault with minor sinistral strike-slip component.

Özbakır et al. (2017) carried out a numerical analysis comprising the active faults in the Anatolian-Aegean plate boundary region as constrained by seismicity, seismic reflection studies, tomographic studies, and geodetic measurements. The results of their analysis to testing the presence and nature of the FBFZ indicated that the any fault along the alleged FBFZ is effectively locked or inactive at present

1.5 Regional Geological Setting

The land mass underlying most parts of Turkey consists of several continental fragments derived from the margins of two ancient mega continents, Gondwana in the south and Laurasia in the north. These continental fragments, once separated by Tethys ocean, were amalgamated into a single landmass by orogenic processes since at least early Mesozoic times. Presently, Turkey is lying within the Alpine-Himalayan mountain belt near the junction of Eurasian, African and Arabian plates. The relative motion and interaction between these plates resulted in four major structures, which operate side by side and govern the major neotectonic configuration of Turkey. They are the dextral North Anatolian Fault Zone, the sinistral East Anatolian Fault Zone, the sinistral Dead Sea Fault Zone and the South

Aegean-Cyprus Subduction Arc, a convergent plate boundary where the African plate on the south is subducting beneath the Anatolian plate to the north (e.g., Bozkurt and Mittwede, 2001).

According to the Eurasia fixed Global Positioning System (GPS) derived velocities, Arabian plate has been moving towards north near South Aegean-Cyprus trench at a rate of 8 mm/yr, meanwhile, the movement rate of western Anatolia is 35 mm/yr towards southwest (McClusky et al., 2000). As is known, the relative motion between these plates is associated with south-westward migration of trench, which is governed by roll-back of the remnant Neotethyan slab beneath Anatolia (Le Pichon and Angelier, 1979; Moores et al., 1984; Royden, 1993; Govers and Fichtner, 2016). On the other hand, following collision between Arabia and Eurasia, the north-south striking left-lateral Dead Sea Fault signifies the northward movement of the Arabian plate with respect to Eurasia at a rate of 15 mm/yr (Kahle et al., 1998, Reilinger et al., 2006). Collectively, the available data indicate that the Anatolia has been escaping westward with at a rate of ~25 mm/yr along both the dextral North Anatolian and the sinistral East Anatolian fault zones; the westward escape is accompanied by overall counter-clockwise rotation of the Anatolian Block (Şengör, 1979; Jackson and McKenzie, 1984; Rotstein, 1984; Dewey et al., 1986; Oral et al., 1992; Reilinger et al., 1997 and 2006; McClusky et al., 2000).

On the other hand, the eastern Mediterranean region has long been recognized as one of the best natural laboratories owing to its variety in terms of tectonic processes, such as rifting, passive margin development, contractional deformation and associated subduction, and ophiolite emplacement. The present tectonic framework of the region has been shaped by the collision between the Arabian and African plates, and the Eurasian Plate since late Miocene (Şengör et al., 1985). Presently, the Aegean trench in the west and the Cyprus trench in the east mark the boundary between the African Plate and Aegean-Anatolian microplate. Due to the lateral variation in the nature of the oceanic lithosphere arrived at the trench, the Aegean and Cyprus trenches are segmented by a 100 km wide transform fault zone, called as Pliny-Strabo trench, at this convergent plate boundary (Woodside et al., 2000; Govers and Wortel, 2005; van Hinsbergen et al., 2010; Biryol et al. 2011).

Indeed, the evolution history of the grabens in the SW Turkey has long been subject of a profound debate due to the fact that it is located in a transitional zone where various slab-edge processes, such as subduction, roll-back, slab tear, back arc extension and escape tectonics interact. Several competing and contrasting geodynamic models have been postulated. These are: (a) tectonic escape model resulted from westward movement of the Anatolian plate along the North and East Anatolian fault zone since 12 Ma (e.g., Dewey and Şengör, 1979; Şengör and Yılmaz, 1981; Şengör et al., 1985; Görür et al., 1995) while some researchers suggest a time interval between 3 and 7 Ma (Barka and Kadinsky-Cade, 1988) (b) Back-arc spreading model caused by south-westward migration of the Aegean-Cyprian subduction zone due to slab roll-back initiated between 13-5 Ma ago (e.g., McKenzie, 1978; Le Pichon and Angelier, 1979; Meulenkamp et al., 1988). (c) Orogenic-collapse model, which refers to gravitational collapse of over-thickened western Anatolian crust since 18 Ma (Dewey, 1988; Seyitoğlu and Scott, 1991, 1992; McClusky et al., 2000). (d) Episodic two-stage graben model suggested the existence of two differently originated extensional period separated by a short phase of compression as a combination of both the orogenic collapse and tectonic escape model (e.g., Bozkurt and Park, 1994; Koçyiğit et al., 1999; Bozkurt, 2002; Yılmaz et al., 2000; Koçyiğit and Özacar, 2003; Bozkurt and Sözbilir, 2004; Purvis and Robertson, 2004, 2005; Bozkurt and Rojay, 2005; Koçyiğit, 2005). This is not an exhaustive list of the models, but they represent the end member models proposed for the region. For alternative models, Hetzel et al. (1995), Gessner et al. (2001), Doglioni et al. (2002), Sözbilir (2002), Gürer and Yılmaz (2002), Westaway (2003), Agostini et al. (2010), Jolivet and Brun (2010) are referred.

1.6 The Geology of the Study Area

The paleotectonic basement of SW Turkey comprises three major tectonostratigraphic units. From northwest to southeast, they are the Menderes Massif, the Lycian Nappes, and the Beydağları Autochthon (Figure 1). These units, marked by structural contacts, constitute an entirely exposed section as a product of subduction, obduction and collision processes associated with the closure of a

northern branch of Neotethys ocean (Şengör and Yılmaz, 1981; Collins and Robertson, 1999; Okay et al., 2001). In the study area, the understanding of the emplacement and juxtaposition of these units is crucial since the collinearity of neotectonic structures with those implies that the pre-existing structures affected the orientations of the latter ones (Bozkurt and Mittwede, 2005).

The Menderes Massif represents a relatively autochthonous Panafrican basement as a metamorphic core complex (Bozkurt and Park, 1994). It is overlain by a pre-Devonian-Eocene metasedimentary cover, which is predominated by a passive margin carbonate platforms of Mesozoic-Early Cenozoic age in the upper part (Özer et al., 2001). The location of the original depositional realm of this platform has been a subject of long lasting debate (e.g., Graciansky, 1972; Dürr et al., 1978; Gutnic et al., 1979; Sengör and Yılmaz, 1981; Collins and Robertson, 1999; Poisson, 1977; Özkaya, 1990; Collins and Robertson, 1997; Robertson and Pickett, 2000; Okay, 2001; ten Veen et al., 2009). Those rocks constitutes, together with Lycian ophiolites generated by supra-subduction zone spreading in the late Early Cretaceous (Collins and Robertson, 1997), the Lycian Nappes. These NE-SW trending allochthonous units overlie tectonically the Eocene flysch of the Menderes Massif as an evidence of emplacement (Okay, 2001). The Lycian Nappes and the Eocene flysch overlies the Bey Dağları Autochthon in southwest, which forms the western limb of the so-called Isparta Angle (Blumenthal, 1963).

From structurally lower to higher, Beydağları Autochthon, exposed in Göcek Window (Hayward, 1984), the Eocene flysch of Menderes Massif, which underlies the nappes, and the Lycian Nappes. The nappes, which are made up of platform carbonates and ophiolite units, are the main rock units cropping out in the study area (Figure 3). Although the aim of this study is to contribute to the style and pattern of recent deformation of the region, there are not any sedimentary record within the on land borders of study area like as deposited in Neogene grabens (i.e. Eşen, Çameli, Burdur) along the Fethiye-Burdur Fault Zone. Nevertheless, in the bay, the recent sedimentation under water enable to interpret the neotectonic deformation in the region.

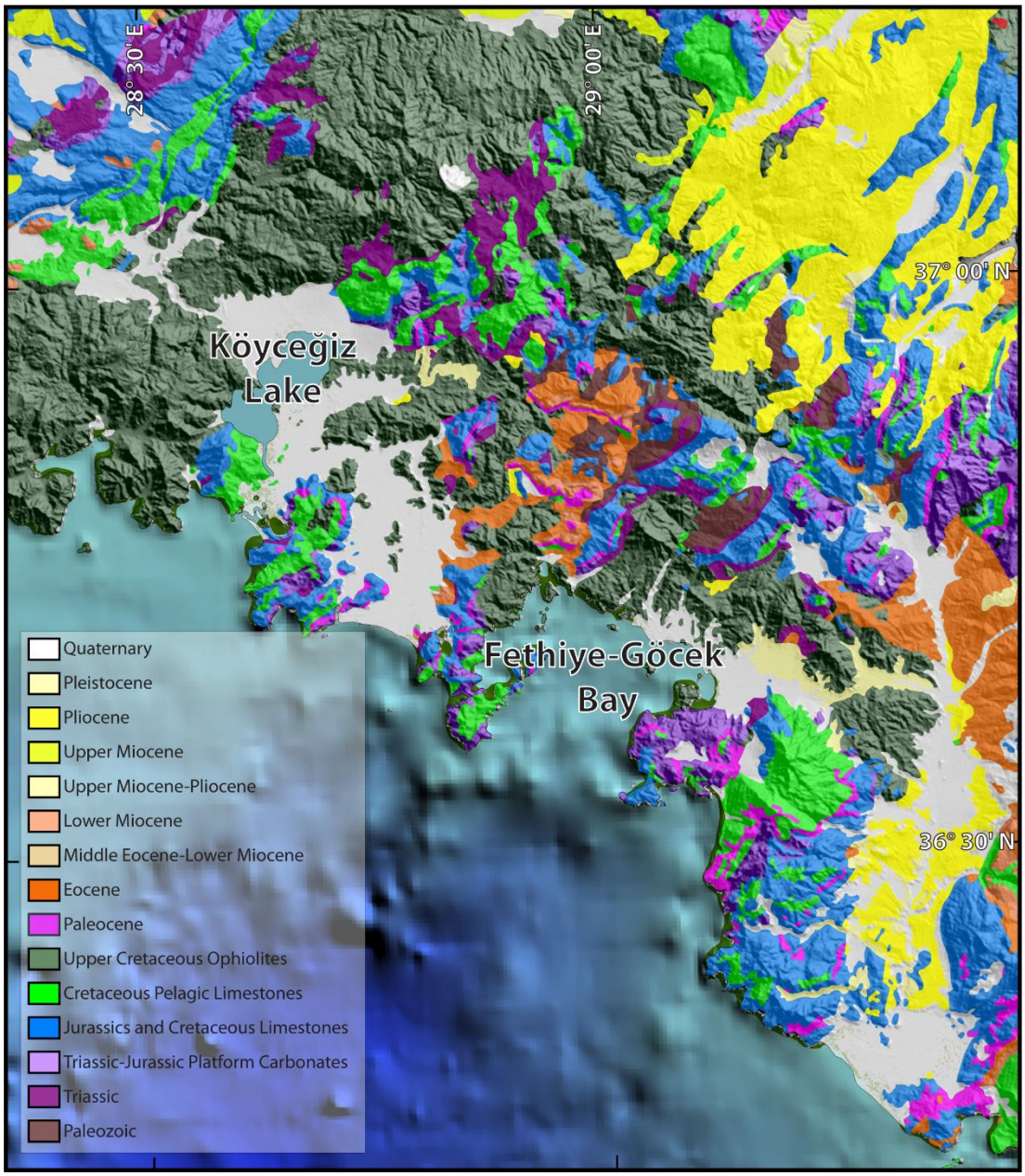

Figure 3 Simplified geological map of SW Turkey showing the location of study area (adopted from 1:500.000 geological map of MTA, 2002)

1.7 The Seismicity of the Study Area

The study area is situated at the south-western edge of alleged FBFZ which is one of the seismically active parts of SW Turkey. It extents along NE-SW direction between the Fethiye-Göcek Bay and Sultan Mountains for a length of about 310 km with a width of 40 to 50 km (Poisson et al., 2003; Elitez, 2009). The fault zone lacks a

continuous master fault on the surface; instead, it comprises various linear, near vertical fault segments trending in NE-SW direction with an oblique-slip normal faults, even though the kinematics of the fault zone has been still a controversial issue (e.g., Dumont et al., 1979; Eyidoğan and Barka, 1996; Barka et al., 1997; Taymaz et al., 1991; Taymaz and Price, 1992; Koçyiğit et al., 2000; Alçiçek et al., 2006; Hall et al., 2014; Ocakoğlu, 2009; Tiryakioğlu et al., 2013; Över et al., 2013; Kaymakcı et al., 2014; Özbakır et al, 2017). Another notable active structural element of the region is a WNW-ESE-trending fault zone, which is formed as a combination of numerous en-échelon normal faults transecting the NE-SW-trending faults and is referred as Gökova-Yeşilüzümlü Fault Zone (Elitez and Yaltırak, 2014).

According to the Disaster and Emergency Management Authority (AFAD) earthquake catalogues, the hundreds of earthquakes (M>=4) occurred in and around Fethiye-Göcek Bay and during the instrumental period covering a time slice between 1900 and 2017 years (Appendix A). During the past century, five large/high magnitude earthquakes (M>=5) were recorded and they might have resulted in severe ground motions at the study area. These are (1) Ms 5.2 earthquake in 1905, (2) Ms 5.4 earthquake in 1943, (3) Ms 5.3 earthquake in 1959, (4) Ms 5.3 earthquake in 1963, and (5) Ms 5.0 earthquake in 1967. Moreover, according to the European Archive of Historical Earthquake Data (AHEAD), there are also historical earthquakes which were reported in and near environ of the study area. 1851 (M=6.8) and 1870 (M=6.0) earthquakes are the prominent ones among these earthquakes. Figure 4 shows the distribution of both instrumentally recorded and historical earthquakes in the region. All these reveal that the spatial distribution of seismicity in the study area is consistent with the distribution of active faults, and based on their focal mechanisms, the earthquakes occurred on almost pure normal faults in the Fethiye-Göcek Bay and its vicinity, whereas the offshore earthquakes are associated with strike-slip faults.

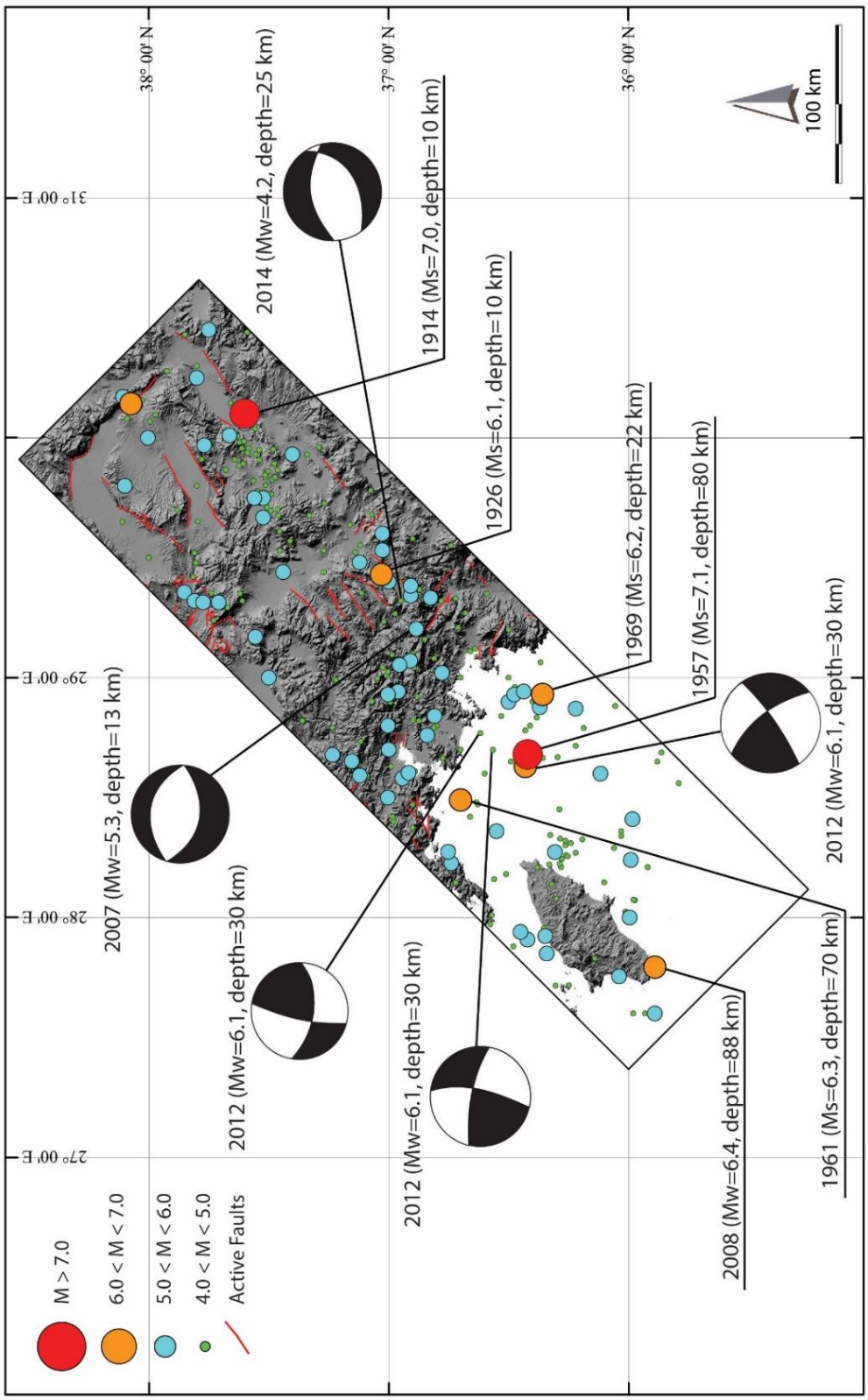

Figure 4 Spatial distribution of earthquake (M>4) and the focal mechanism solutions recorded for the major earthquakes

CHAPTER 2

PALEOSTRESS ANALYSIS

In order to unravel the kinematic characteristics of faults and their spatial distributions, paleostress analyses were performed. This procedure involves collection of fault data sets in the field and reconstruction of paleostress configurations for each sampling site. Within the scope of this thesis, fault data includes the fault plane and slicken line orientations as well as their relative sense of movement. In addition, a detailed lineament map of the study area was also prepared in order to embody the continuities, orientations and spatial distributions of fault on map view. As a result, paleostress orientations and their relative magnitudes (i.e. shape of stress ellipsoid) were determined by using the reduced stress tensor concept. These outcomes were used to improve the understanding of the kinematic and characteristics of faults developed in the Fethiye-Göcek Bay and its vicinity.

2.1 Paleostress Analysis from Fault Slip Data

Paleostress analysis is a structural analysis, which provide a dynamic interpretation to kinematic analysis of faults in tectonic regimes operated in the past. Paleostress analysis has been widely used and regionally consisting results have been obtained from several applications in various tectonic settings over the last three decades. Therefore, paleostress analysis is accepted as a favourable structural analysis to determine the stress tensors and associated tectonic regimes operated in the past.

It is important to be aware of what have been obtained as outcomes of the analysis, because, contrary to what the name implies, paleostress analysis does not directly

yield a true magnitude of paleostresses (i.e. instantaneous forces applied at a per unit area in the past). Instead, it gives the orientation and relative magnitudes of the principle stresses (Angelier et al., 1979, 1984, and 1989, Lisle 1987).

There are several graphical, i.e. M-Plane (Arthaud, 1969; Aleksandrowski, 1985) and Right-Dihadra method (McKenzie, 1969; Angelier and Mechler, 1977; Lisle, 1987), and numerical (Carey and Brunier, 1974; Etchecopar et al., 1981; Armijo et al., 1982; Angelier, 1984, 1989; Marrett and Allmendinger, 1990) methods, which have been proposed for inferring paleostress orientations and their relative magnitudes from populations of fault since the premise study of Wallance (1951) and Bott (1959). These methods involve orientation of fault plane and movement direction of displacement that can be deduced from the fault planes (slicken side), the focal mechanisms of seismic events (Gephart and Forsyht, 1984) and the mechanical twinning in calcite minerals (Spang, 1972) associated with the motion.

The graphical methods are based on finding the orientations of the stress tensor of each measurement and representing the results on the unit sphere. In addition, they are useful to separate heterogeneous data, which may resulted from multiple tectonic events or fault interactions. However, the shape parameter (i.e. relative magnitude of paleostresses) of the stress ellipsoid cannot be deduced directly from graphical methods. Otherwise, the numerical methods are more robust and favoured in that manner, since they yield the full stress tensor result by using empirical relations pertaining to brittle deformation. Each method hinges on various assumptions and boundary conditions. Therefore, user must be aware of the advantages and limitations of used method for paleostress analysis.

In this study, the direct inversion method (INVD) of Angelier (1979, 1984, 1994) has been applied as a numerical paleostress reconstruction technique developed based on reduced stress tensor concept and thereby paleostress orientations and relative paleostress magnitudes were revealed based on some assumptions that prevailed during the time of faulting. These assumptions include; 1) the fault blocks move independently along the maximum resolved shear stress with negligible block rotation, 2) maximum resolved shear stress directions are parallel to the slickensides formed on a planar fault surface (Wallace and Bott hypothesis), 3) the movement of

faults obey Mohr-Coulomb failure criterion i.e: frictional envelope governs the failure and motion of the faults (Coulomb, 1776; Mohr, 1900) , 4) faults are activated under a single phase of uniform stress field 5) pore-water pressure does not alter intrinsic properties of faults, i.e. orientations and normal versus shear stress ratios are independent from the pore-water pressure changes. In other words, Coulomb-Mohr relationship is not altered due to pore-water pressure changes.

Angelier's method is based on aforementioned assumptions which are idealization and simplification of local heterogeneities and inconsistencies existing in the deformed medium. For instance, the uniform intensity and orientation of stress field operating on isotropic masses of curst is a very broad approximation. Furthermore, the fact that the faults are not perfectly planer on any scale (e.g listric fault geometry) is in contradiction with an implicit assumption in paleostress analysis assuming that faults are uniformly dipping planar structures. However, despite all assumptions, when the previous application of the technique is taken into consideration, it has been proved that obtained results of paleostress analysis are consistent and empirically valid with certain limitations.

Angelier's reduce stress tensor concept is a numerical method for iteratively determining of paleostress tensor for a given fault population. The method implies that the shape of the principle stress ellipsoid can be partly but conveniently described by a single number Φ ($\Phi= \sigma_2- \sigma_3/ \sigma_1- \sigma_2$) which varies between 0 and 1, as $\sigma_{1>}\ \sigma_{2>}\ \sigma_3$ in positive compression. Therefore, in areas where the stress ratio (Φ) approximates 0 (i.e. prolate stress ellipsoid) and 1 (i.e. oblate stress ellipsoid), uniaxial compression ($\sigma_2=\sigma_3$) and uniaxial tension ($\sigma_1=\sigma_2$) conditions prevail respectively and faults can form in any direction. Otherwise, when stress condition is tri-axial which means that all of the principal stress magnitudes are significantly different from each other, the fault orientations can be constrained along parallel to intermediate principle stress (σ_2) directions. In this case, the mechanism of faulting approximate to Anderson's Theory (1951) which basically implies that Earth's surface is a principle plane of stress across which one of the three-principle stress operates perpendicular while the other two are parallel to it. In this regard, the calculated Φ -value and the direction of paleostresses, which are the four unknown of

reduced stress tensor found out after a series of calculations, make users able to manifest the kinematic characteristics of fault based on the shape and orientation of stress ellipsoid with respect to Earth's surface.

Theoretically, determination of paleostress orientations enables the indirect measurement of each paleostress magnitudes, which include vertical one with respect to Earth's surface, that is directly proportional to thickness of the overburden, average density of the rock column and acceleration due to gravity (Bergerat, 1987, Angelier, 1989). However, it is not easy to obtain the information about the depth of faulting and the determination of the amount of deposition and erosion, which are the requirements for estimating the thickness of overburden. Furthermore, such data has been easily eroded away and this missing parts of the rock record make it difficult to get information about post depositional changes such as the amount of compaction and density variations, water content, etc. (Kaymakcı, 2006). Therefore, indirect measurement of true magnitude of paleostresses is not a favoured technique especially in continental areas.

2.2 Lineament map of the study Area

Lineaments are defined as mapable rectilinear or slightly curvilinear surface features, which are recognizably different from the patterns of adjacent ones and presumably reflect subsurface phenomena (O'Leary et al., 1976). The lineaments on map or satellite images provides a method of detecting the tectonic trends as a preliminary study before going to the field. In this regard, a detailed lineament map of the study area were prepared prior to collection of fault data aiming to schedule field study (Figure 5). During the field study, the major structural trends and probable fault locations were visited in order to verify those structures in the field, which is known as ground truthing procedure.

As shown in the Figure 5, two group of lineaments were detected based on their orientations, trending NE-SW and WNW-ESE. It is clear that the NE-SW-trending lineaments dominate the entire region and they are consistent with either the orientation of units in paleotectonic basement or the structures developed in the Neogene grabens situated along the FBFZ. On the other hand, WNW-ESE-trending

lineaments transects the NE-SW ones and mainly clusters with a lower frequency in the northern part of the bay. That lineaments and their spatial distribution in the study area are equivalent to en-échelon normal faults, which is referred to as Gökova-Yeşilüzümlü Fault Zone (Elitez and Yaltırak, 2014). Moreover, the consistency between the onshore lineaments and surface projection of interpreted faults in seismic sections in terms of their orientations will be discussed in Chapter 3.

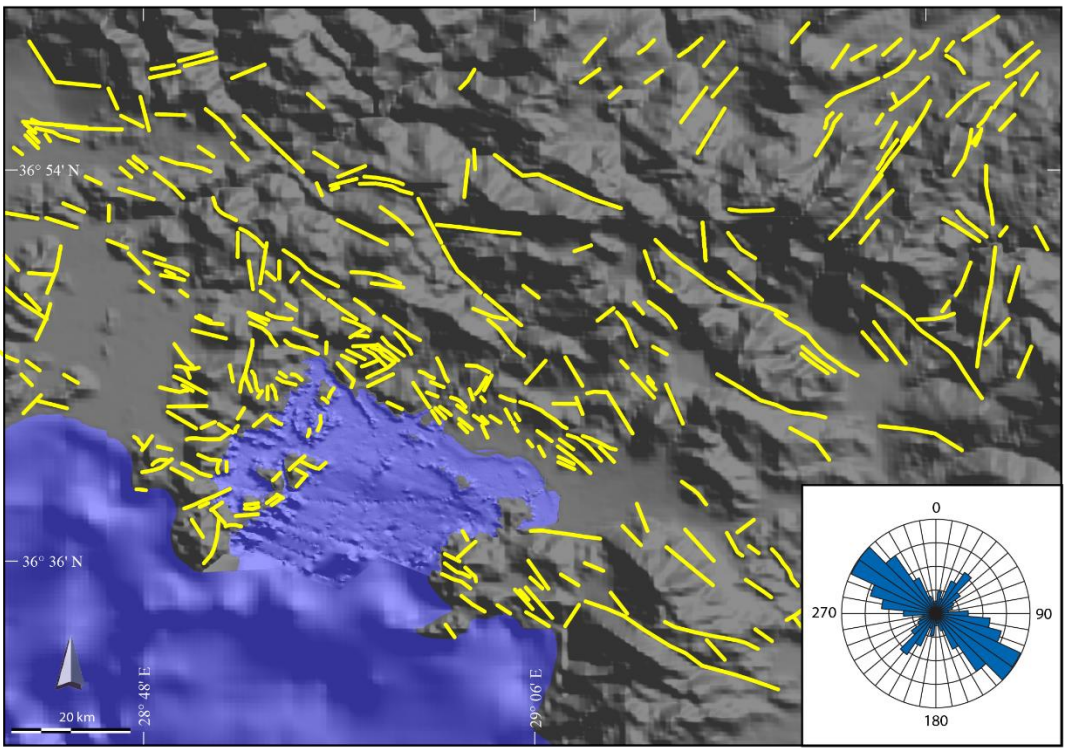

Figure 5 Lineament map of the study area and length weighted rose diagram of lineaments.

2.3 Fault Data and Sampling

The size of the stations, where fault data were collected from, were kept as small as possible for the purpose of obtaining structurally homogeneous domains (Hancock, 1985). At least three different location along the same fault plane were sampled in order to represent the consistency of analyses. For each sampling side, the attitude of fault plane, the orientation of slickenside and the relative sense of movement were noted with their geographic locations and the faults were documented by taking photograph Figure 6. The direction of relative displacement on fault plane were

inferred from frictional grooves or fibrous lineations (Fleuty, 1975). Additionally, The fault measurements taken from the surface where the structurally higher and lower units juxtaposed along hanging wall and foot wall block respectively also imply normal fault in the region (Figure 7)

Figure 6 Slickenside lineations on fault planes. Arrows indicate the sense of slip on fault planes.

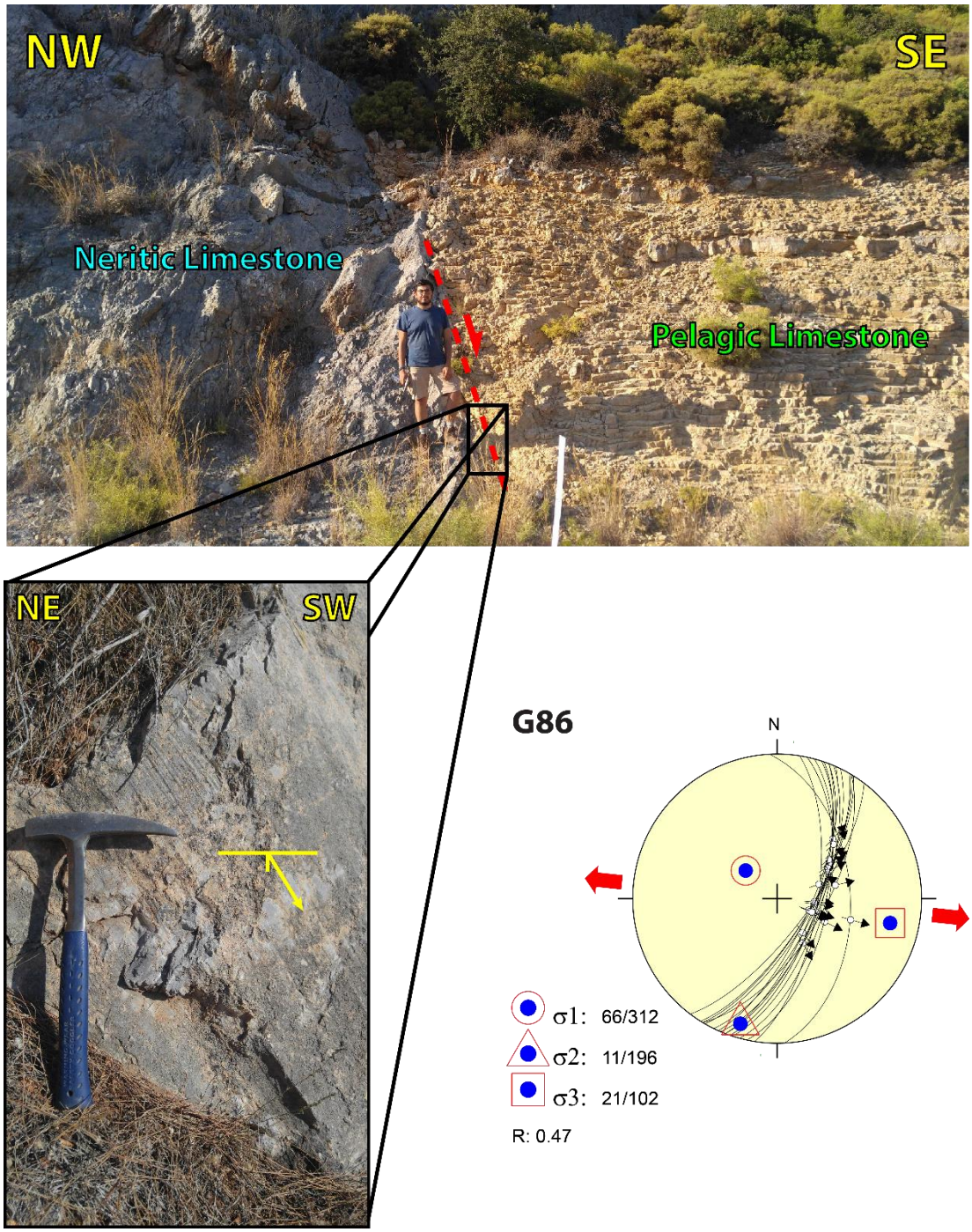

Figure 7 The fault juxtaposing structurally higher and lower units at the site G86 along the hanging wall and footwall blocks respectively and its constructed paleostress orientations.

In total, 14877 slip data on fault planes from 222 different locations were collected in order to reveal the stress conditions responsible for the brittle deformation (Figure 8). Among these, the stations, where the over printing slickensides are encountered, fault data were collected separately for each slickenside orientation (Figure 9).

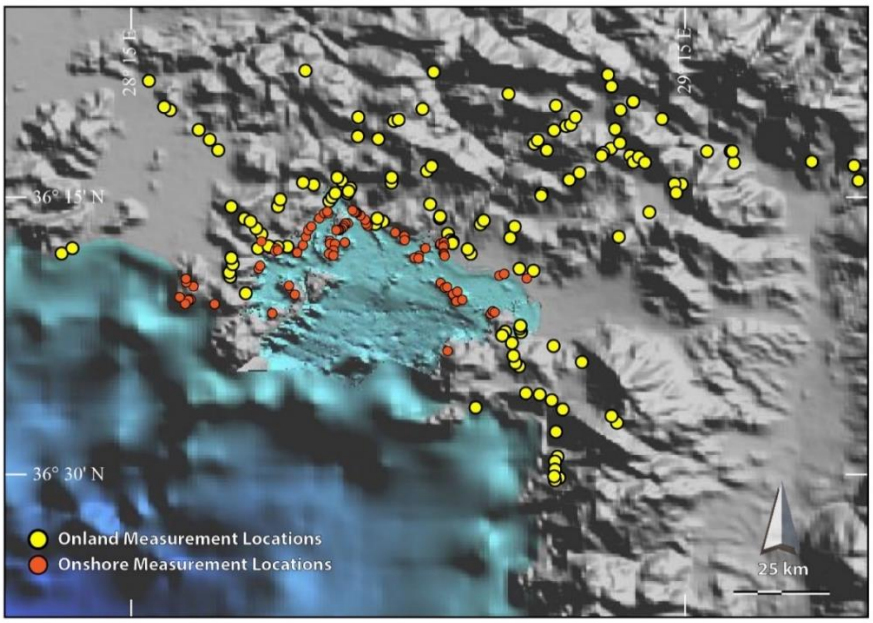

Figure 8 The spatial distribution of fault surface sampling sides in the Fethiye-Göcek Bay and its vicinity.

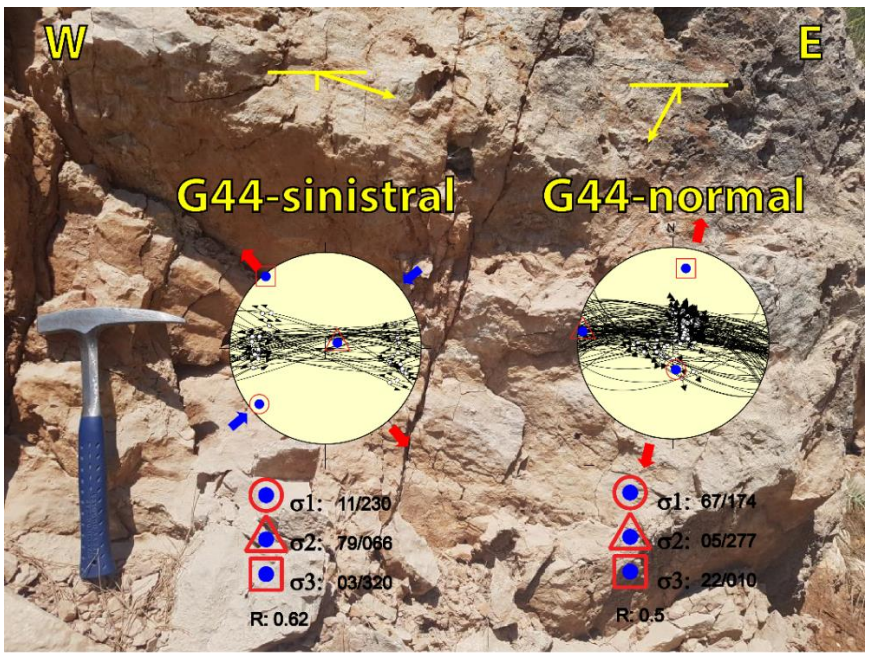

Figure 9 Overprinting slickensides and their paleostress reconstruction result

3.4 Paleostess Reconstruction Results

The data were processed by Win-Tensor (windows version of TENSOR) which is an interactive process of stress tensor calculation software developed based on Angelier's reduced stress tensor concept (Delvaux and Sperner 2003). The output data consists of the orientation of the three principle stress axes and their relative magnitudes as well as the R ratio (corresponding to Φ in Angelier (1975) (Appendix C) and misfit angle for each measurement. In addition, the software plots each fault plane with slicken line orientations on an equal-area lower hemisphere diagram and it shows the distribution of fault planes in a dimensionless Mohr diagram including the relative values of the principle stresses. Another feature of the software is its "Optimization" module, which allows minimizing the angular deviation between the observed and theoretical slip directions and maximizes the precision of the resolved shear stress. During the inversion process, the allowable maximum misfit angle F1 was taken as 25°. In this regard, the fault-slip data exceeding this limit was separated from the main data set and then reprocessed as a separate tensor for the same location, which may indicate multiple phase of deformation or stress permutations (Homberg et al. 2002, Hu and Angelier 2004). Otherwise, they are treated as spurious and deleted out from the data set, which comprises only less than 2 % of the total data, pointing out that the collected data for each fault set correspond to a single event in the region.

A total of 222 paleostress configurations constructed using fault slip data indicates that the individual datasets are consistent among most of the data in entire region (Figure 10). Among these, almost all yielded an approximately NE-SW direction of extensions even though a few of them are both dextral and sinistral strike-slip faults parallel to NW-SE direction that transects the NE-SW ones.

The analysis shows that the fault slip measurements deduced from NE-SW trending normal faults have steeply plunging σ_1 axes (>70°) and gently plunging σ_2 and σ_3 axes (~20° and ~15° respectively), whereas the NW-SE trending strike-slip faults have nearly vertical σ_2 (>80°) and nearly horizontal σ_1 and σ_3 axes (~15° and ~10° respectively). In essence, the paleostress configuration suggests that NE-SW-directed extensional deformation predominates the region and strike-slip faults, whose tips

terminate against NE-SW-trending normal faults, are observed generally on the NW-SE direction. These faults were interpreted as transfer faults that accommodates extension and normal motion (Figure 11).

Due to the lack of stratigraphic record of the Neogene units in the region, the temporal order of the fault motions were not established using fault-slip data set. However, in terms of their orientations, the consistency of the measured faults with the faults, which bound the NE-SW-trending Neogene basins along north-eastern continuation of the study area, indicates that those faults developed under the influence of the same tectonic regime. Based on the previous studies conducted in NE-SW-trending Neogene grabens along northern termination of the study area, the present day geometry of faults developed around Fethiye-Göcek Bay are the result of Miocene onset of extensional deformation in the region. In this regard, any tangible evidence to support the existence of NE-trending sinistral transtensional FBFZ (or shear zone) has not been encountered during this comprehensive field study. Therefore, it was revealed that the region is dominated by extensional deformation and strike-slip components are observed on both NW-SE and NE-SW-striking faults. Moreover, the minor amount of NE-SW-trending strike-slip faults have dextral character contrary to sinistral nature of alleged Fethiye-Budur Fault Zone (Figure 12).

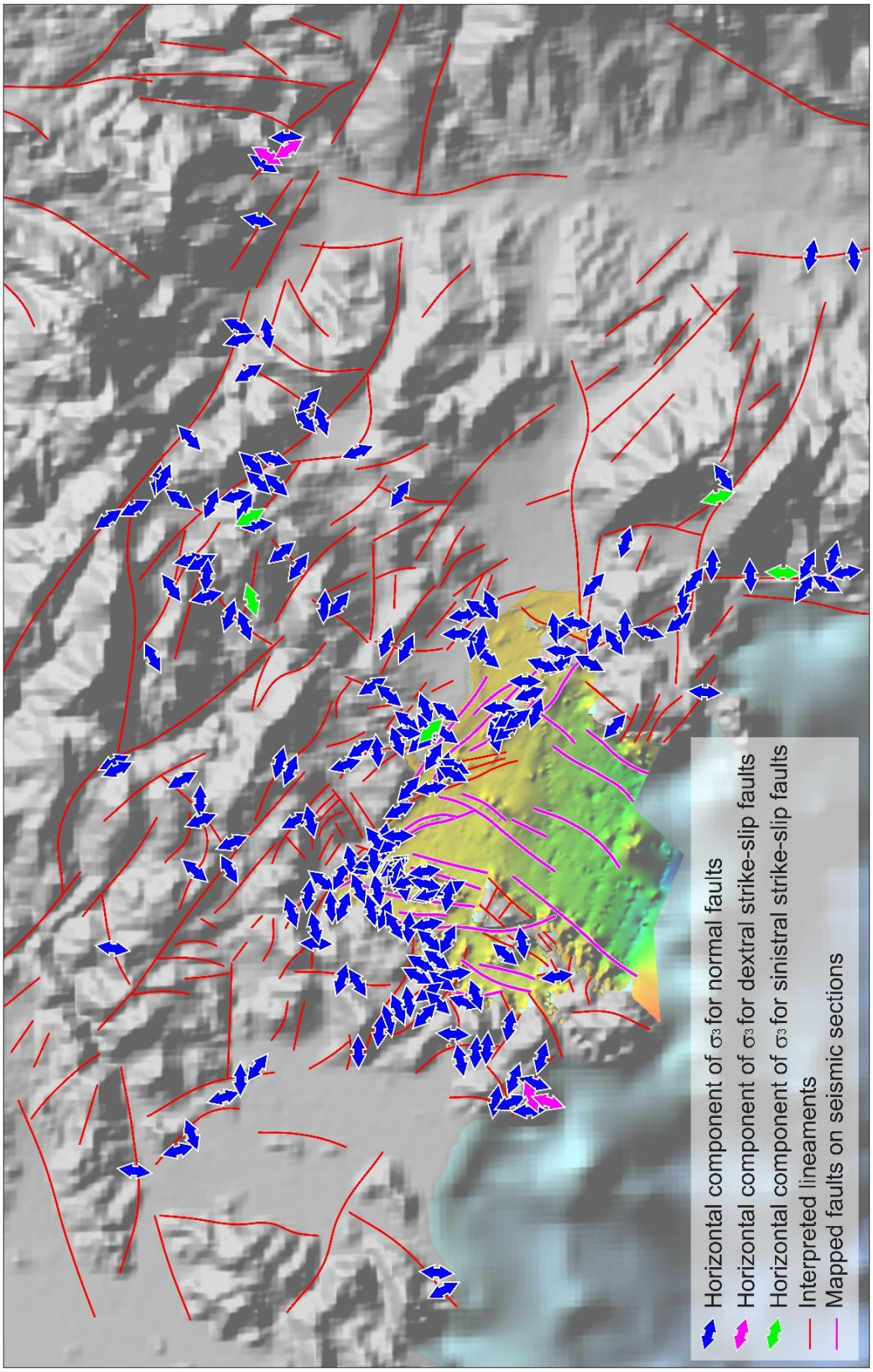

Figure 10 Paleostress reconstruction analysis results and their spatial distributions in the Fethiye-Göcek Bay.

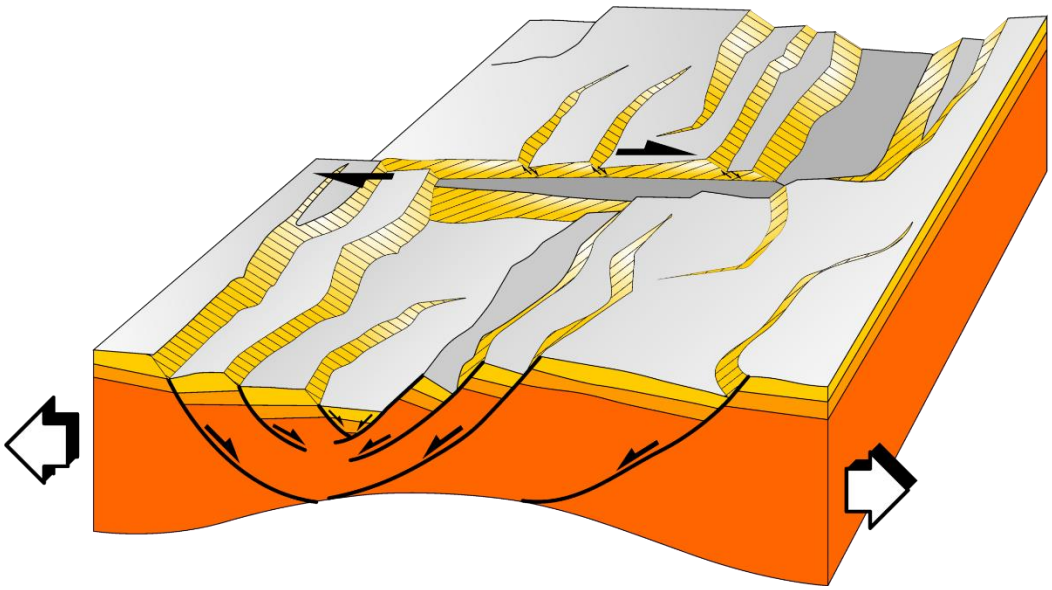

Figure 11 Schematic block diagram illustrating the transfer faults developed in extensional tectonic regimes (modified from Van der Pluijm and Marschak 2004).

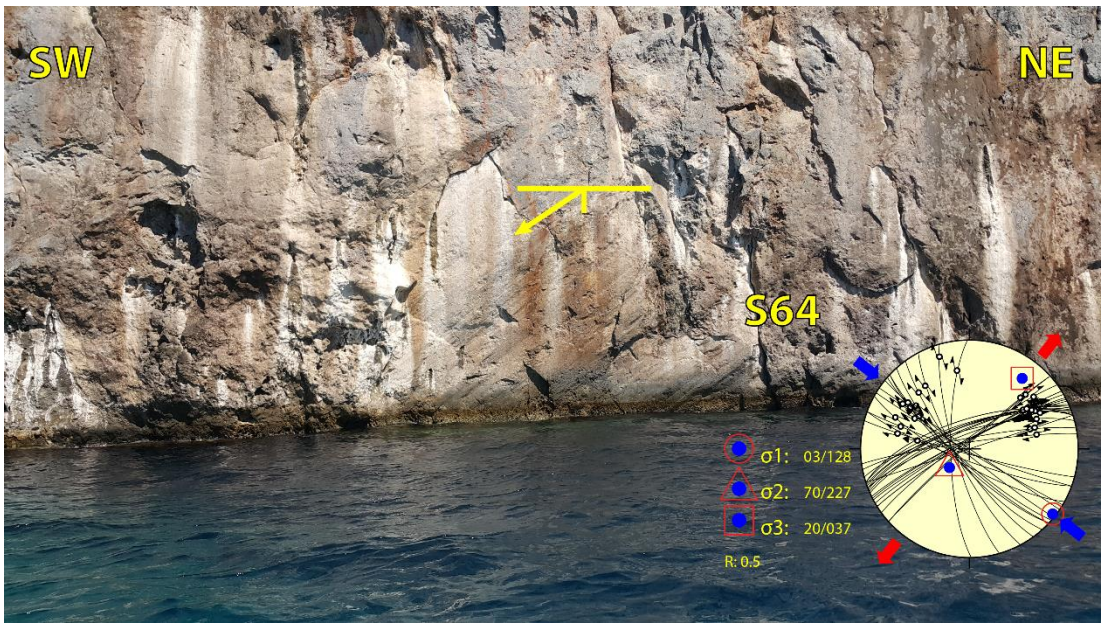

Figure 12 NE-SW-trending dextral strike-slip fault on cliffs and its paleostress reconstruction result.

CHAPTER 3

SEISMIC INTERPRETATION

In order to unravel the activity and orientation of the faults developed in Fethiye-Göcek Bay, 2D seismic reflection data, which were collected as transecting the probable geological structures developed in the bay, were interpreted. During this interpretation, the key horizons were determined based on their distinct seismic characteristics throughout the survey area and they were picked on seismic sections in time domain. Similarly, the faults were also interpreted on each individual seismic section mainly by utilizing picked horizons and seismic layer terminations, and they were correlated from one section to another throughout the bay. As a result, the sea-bottom projection of the faults were mapped out and they were used to improve the understanding of spatial distributions and activity of the faults developed in the Fethiye-Göcek Bay.

3.1 Data Collection and Processing

The seismic reflection data interpreted in this study were collected for a project supported by the Scientific and Technological Research Council of Turkey (TÜBİTAK) (Grand Number 112Y137), which aimed at determining the spatial distribution and hydrogeochemical properties of the subaqueous thermal springs at the bottom of Fethiye-Göcek Bay, Köyceğiz, Alagöl, Sülüngür, Kocagöl lakes that are located in a geothermally active area in Muğla Province (SW Turkey). In the context of this project, the high-resolution seismic reflection data were collected and processed based on cooperation protocol signed between Muğla Sıtkı Koçman

University, Department of Geological Engineering and Dokuz Eylül University, Institute of Marine Sciences and Technology. The equipment and data collection parameters, which were used during data collection process, are given in Appendix B.

In this context, totally 228 km long seismic reflection data were collected along 32 lines, which are intersecting each other in NE-SW and NW-SE directions. The starting and ending points of lines in UTM35 coordinate system, and the length and azimuth of each line were listed in Appendix B. Figure 13 shows the distribution of lines in the Fethiye-Göcek Bay.

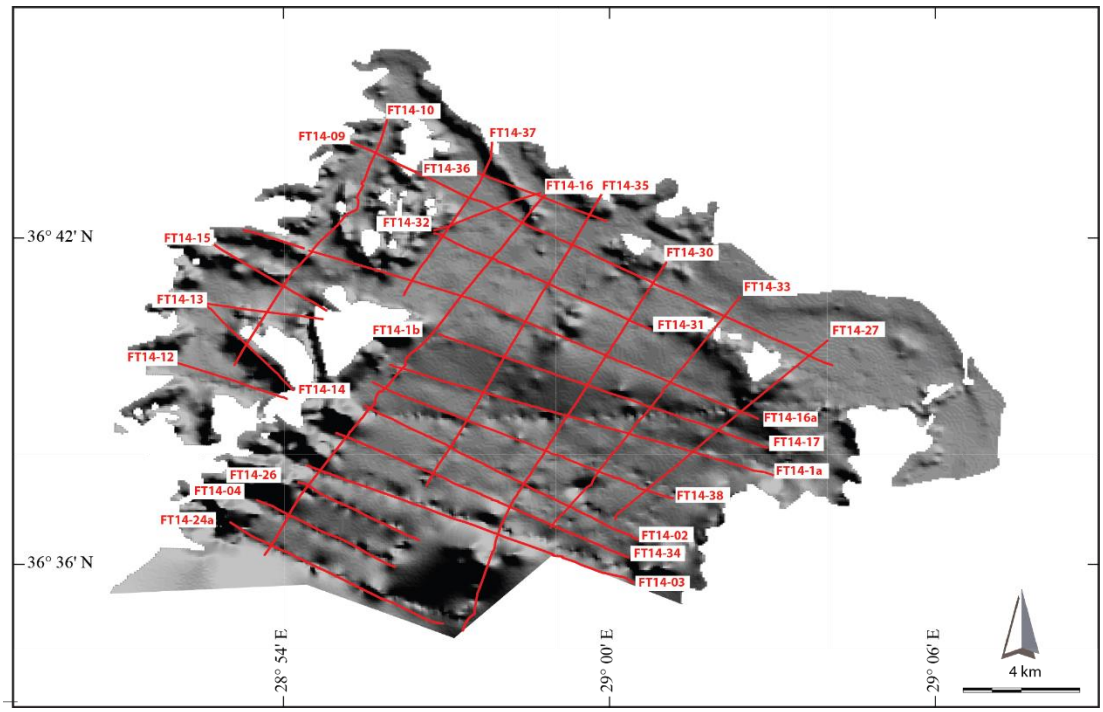

Figure 13 The orientations and distributions of seismic lines interpreted in Fethiye-Göcek Bay

The obtained single channel seismic reflection data were processed by Dokuz Eylül University, Institute of Marine Sciences and Technology. SeisSpace/Promax software developed by Landmark/Halliburton was used. The data processing procedure carried out to increase the signal strength and to decrease signal to noise ratio and remove multiple reflections within the limits of the available software. As a result, after a series of data processing procedures, the data qualities were considerably improved on each seismic section. In this context, the horizontal offset

between traces kept in 2 m (horizontal resolution), which means that seabed and units below were sampled in each of 2 m along seismic lines while the vertical resolution is ~40 cm since applied dominant frequency value was 1000 Hz. This means that even thin sedimentary layers can be distinguished from the seismic sections.

The position of the survey was determined by using GPS measurements taken simultaneously during the survey and a rough bathymetry map of the bay is produced by using linear interpolation techniques (Figure 14). Based on this map, the shelf break is located a distance at ~7 km from coastline where the depth of bathymetry rapidly decreases from 170 m to 270 m. In addition, the small local highs on seismic section corresponding to high velocity basement units is also seen in the bathymetry map of the bay.

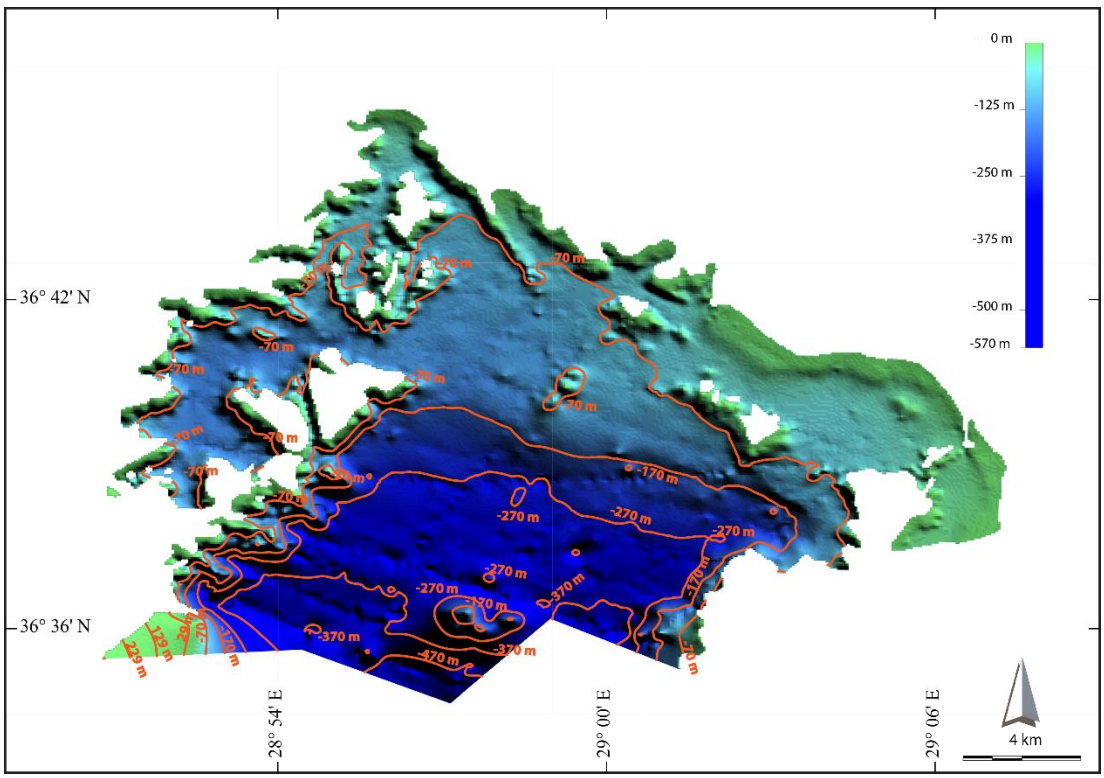

Figure 14 The colour coded bathymetry map of the Fethiye-Göcek Bay.

3.2 Seismic Interpretation

The seismic interpretations including the horizon picking and fault tracing as well as extraction of surface map projection of faults were performed by Kingdom Software acquired from IHS-SMT company through Academic License Act. These interpretation processes were carried out in two main stages: defining and picking the key horizons, and fault interpretation.

3.2.1 Defining and Picking the Key Horizons

Due to the lack of well data, seismic reflection data could not have been tied to an absolute vertical data. Nevertheless, the selection of the key horizons was performed by considering the appraisal of the seismic characteristics of horizons through the survey area, which give region-wide traceable high amplitude reflections and seismic stratigraphic characteristics and seismic facies such as on-lap, down-lap, shingle patterns etc. In this context, the candidate horizons were correlated at the intersection points of seismic sections.

Based on the aforementioned criteria, in total six interface were picked in order to reveal the recent sedimentary record of the Fethiye-Göcek Bay (Figure 15). As a result, 6 main seismic stratigraphic units, which display traceable reflections, were recognized. As it is excepted that whole record above basement unit is seen on the sections situated southern side of shelf break, which is deeper side of the bay (Figure 16). On the other hand, as getting close to the shoreline, basement units are overlaid by sediments, which were deposited during high stand of sea level with respect to shelf break (Figure 17).

3.2.2 Fault Interpretation

The faults were identified and mapped out by means of reflection offsets in seismic sections and the morphological expressions of the time surfaces. In this context, first of all, each faults on individual seismic sections were traced by utilizing picked horizons and seismic layer terminations (e.g Figure 15, Figure 16, Figure 17). Then, they were correlated from one section to another in order to reveal their orientations throughout the bay. The on land terminations of faults and the morphology of

seafloor, which were deduced from bathymetry, were considered during this correlation process. As the orientation of a fault is revealed, the surface projection of the faults were extracted from seismic section (Figure 18). As a result, a total number of 108 faults were digitized on seismic section in the study area. During correlations of major faults, smaller antithetic or synthetic faults, which are not persistent across seismic sections, were neglected. Therefore, out of more than hundred faults interpreted in the area, 84 of them were chosen to be eligible for mapping of large scale fault representing the characteristics of deformation in the region.

3.3 Seismic Interpretation Results

The produced map showing the surface projection of the major fault geometry for Fethiye-Göcek Bay indicates that the faults interpreted on seismic sections are consistent with the faults developed on land, in terms of their orientations and collinearity. Two sets of faults trending NE-SW and WNW-ESE directions were determined and are similar to the patterns obtained on the lineament map of the study area (Figure 18). Based on this similarity, the faults detected in seismic sections are presumed to have continuity with the faults mapped on-land during field studies. This match further implies that all the faults were resulted from the same tectonic regimes.

The paleostress reconstruction analysis performed on on-land faults revealed that almost all faults are normal in character and associated with dominant NW-SE oriented extensional deformation. Likewise, the type of the faults which were interpreted from seismic sections have very strong vertical normal components which most probably are also normal faults as also manifested by normal drag fold features. Therefore, the characteristics of faults especially bounding mini basins, where the basement units juxtaposed with younger sedimentary units, were deduced by means of those morphological features (Figure 19a-b).

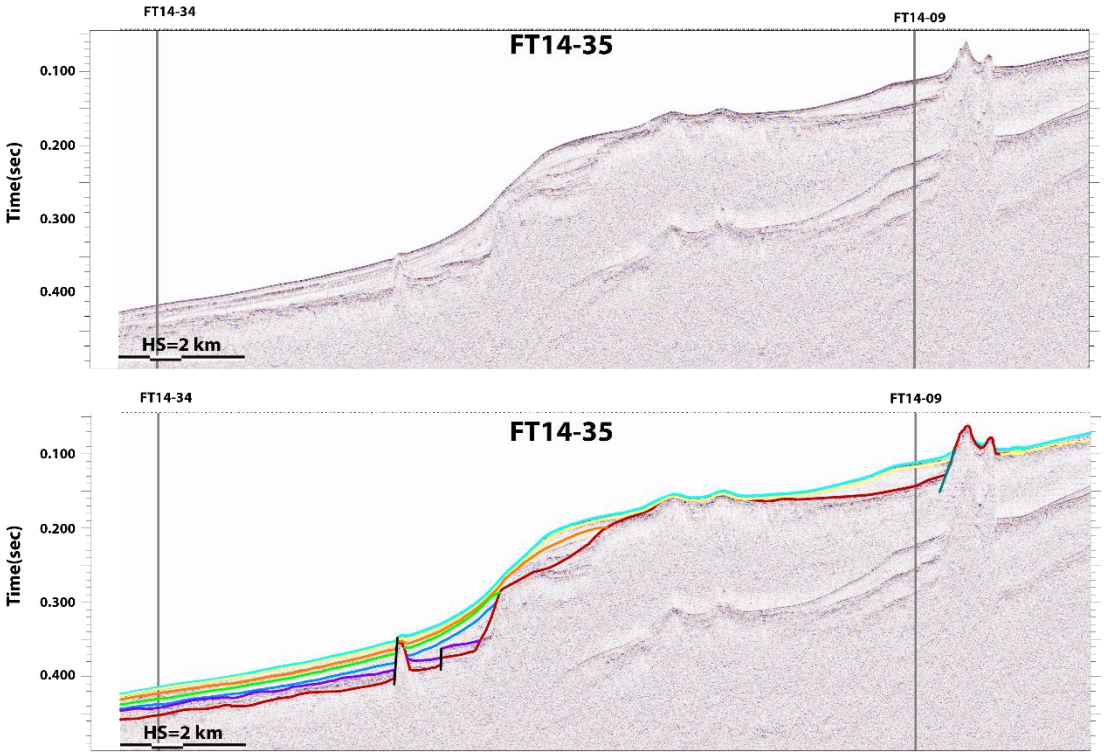

Figure 15 Picked horizons and the interpreted faults on seismic line FT14-35

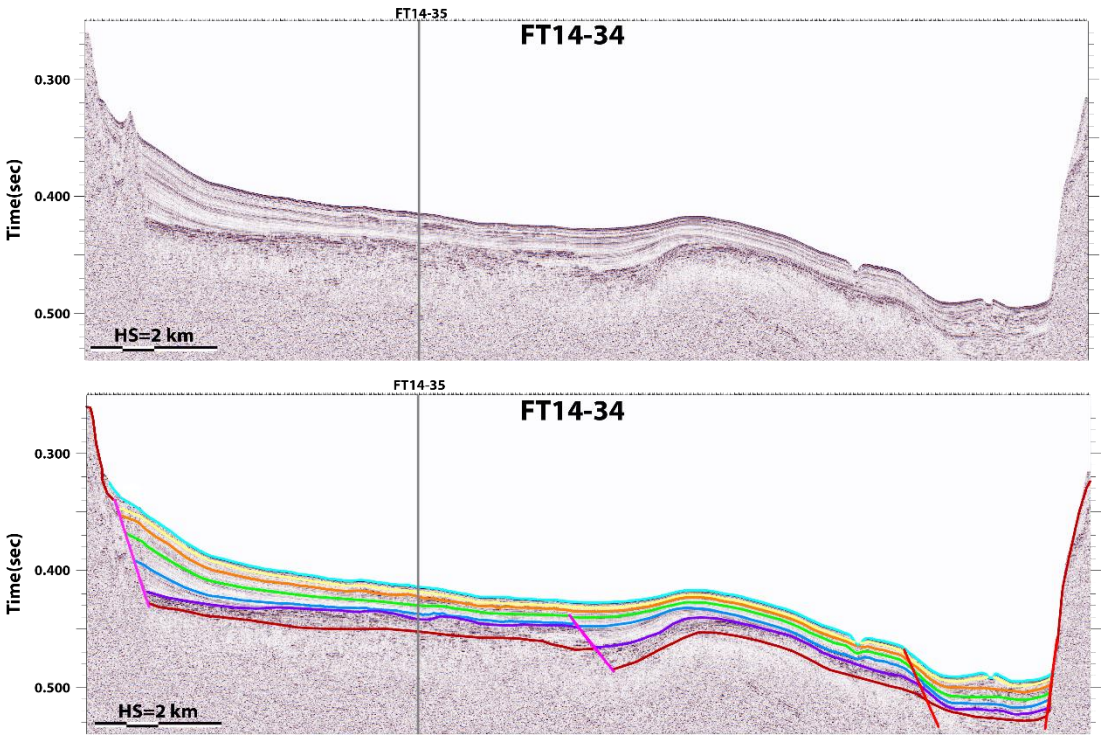

Figure 16 Picked horizons and the interpreted faults on seismic line FT14-34

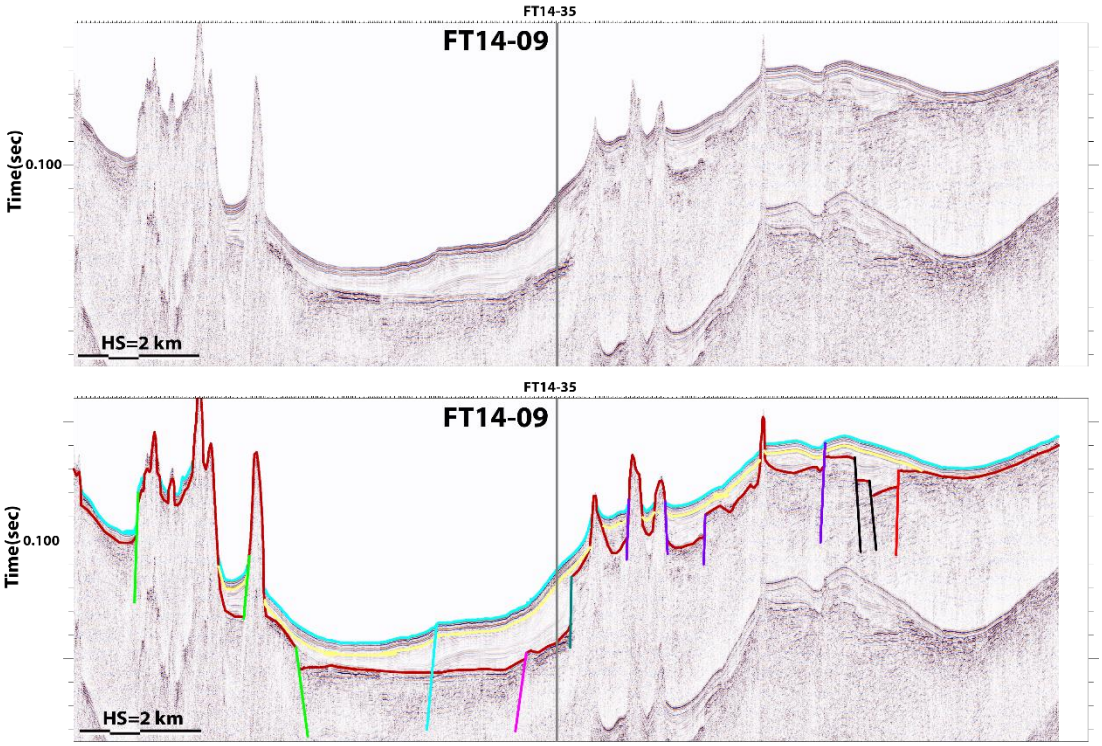

Figure 17 Picked horizons and the interpreted faults on seismic line FT14-09

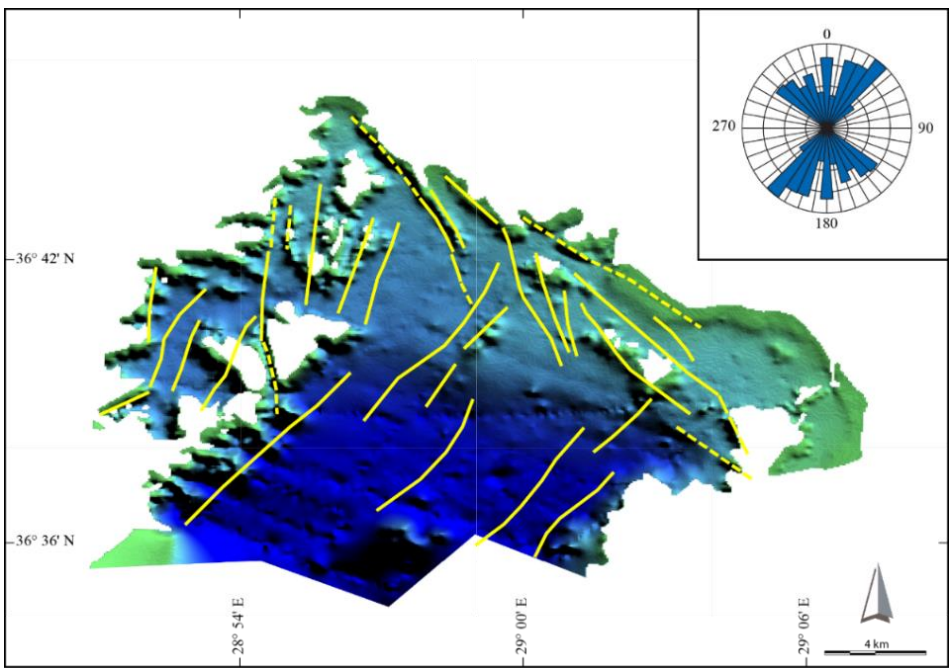

Figure 18 Surface projections of faults execrated from seismic sections within the Fethiye-Göcek Bay and the length weighted rose diagram of the lineaments.

During field studies, the activities of the faults developed in the Fethiye-Göcek Bay and vicinity could not deduced from kinematic analysis of faults due to lack of Neogene units in the region. In such a case, there are two suitable approach that can be used for the speculation of the fault activity. The first one is using the earthquakes solutions deduced from instrumentally recorded seismic activities in the region. Their spatial distributions and consistency with the faults measured in the study area have been discussed in Chapter 1. The latter approach is the using of faults on seismic sections, which cut the recent sedimentary units and even the seabed. The existence of those faults are the clear evidence of fault activity in the vicinity.

For this purpose, the seismic line FT14-9 was chosen to be eligible for the discussion of fault activity since it passes close to the only available core data (Depth of core: 90 cm; Coordinates (UTM): 682.059 E, 4.061.094 N), which is taken in an attempt to estimate recent sedimentation rate in the bay (Figure 21a). Based on the outcomes obtained from this core, U. Avşar (personal communication, October 26, 2017) calculated a recent sedimentation rate of 3.5 mm/yr in the upper 90 cm of unconsolidated sediments from the surface. From this point of view, the core was projected to seismic line 9 in order to estimate an average sedimentation rate for the units which unconformably overlays the basement. When the compaction of sediment, which depends on the increase in overburden load, is taken into consideration, it is predicted that the sedimentation rate may range from 3.5 mm/yr to 2.5 mm/yr with depth. For this reason, it was assumed that the average sedimentation rate of 3.00 mm/yr is a reliable rate near the shoreline of Fethiye-Göcek Bay. Moreover, the depth of water and the depth of interface between basement and recent sedimentary units were calculated as 43.5 m. The top of the horizon is encountered at 0.058 seconds while base of the horizon is 0.072 seconds. The time difference between the top and bottom layers of the most recent sediments is 0.072-0.058= 0.014 seconds. The seismic velocity of water and the average interval velocity of unconsolidated dry sediments were taken as 15000 m/sec and 2000 m/sec respectively (Sharma, 1997). Therefore, the total thickness of the horizon is 14 m and the time required for its deposition with a rate of 3.00 mm/ yr is around 4.600 years.

This implies that, the faults cutting the recent sedimentary units must have been active during Holocene Epoch (Figure 20).

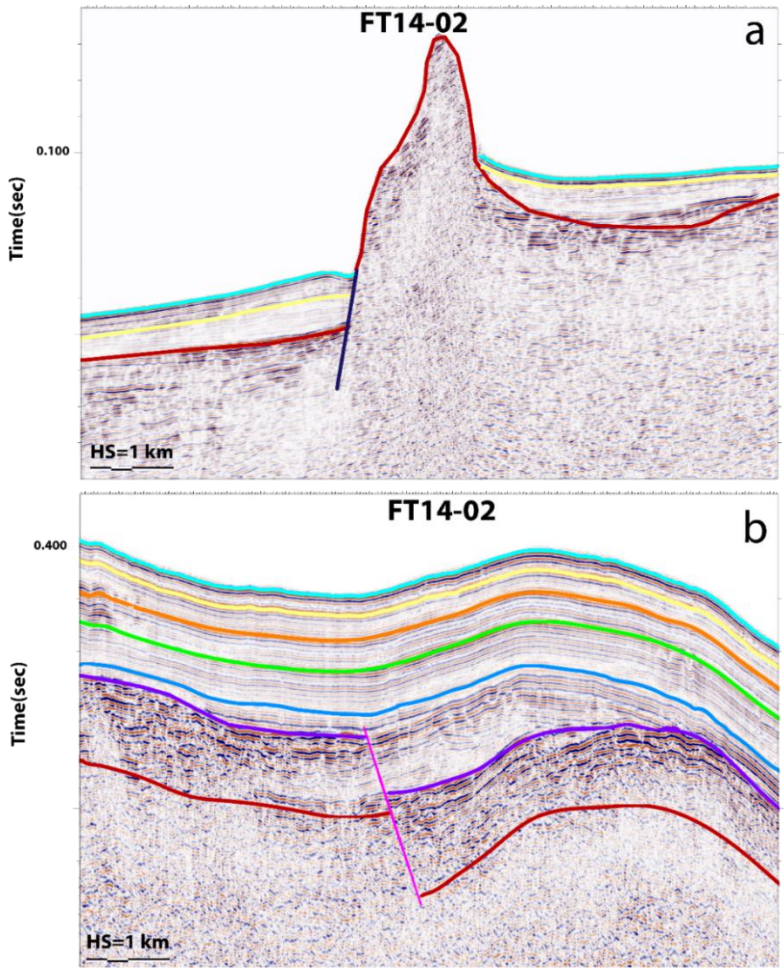

Figure 19 Seismic facies characteristics used for interpretation of faults.

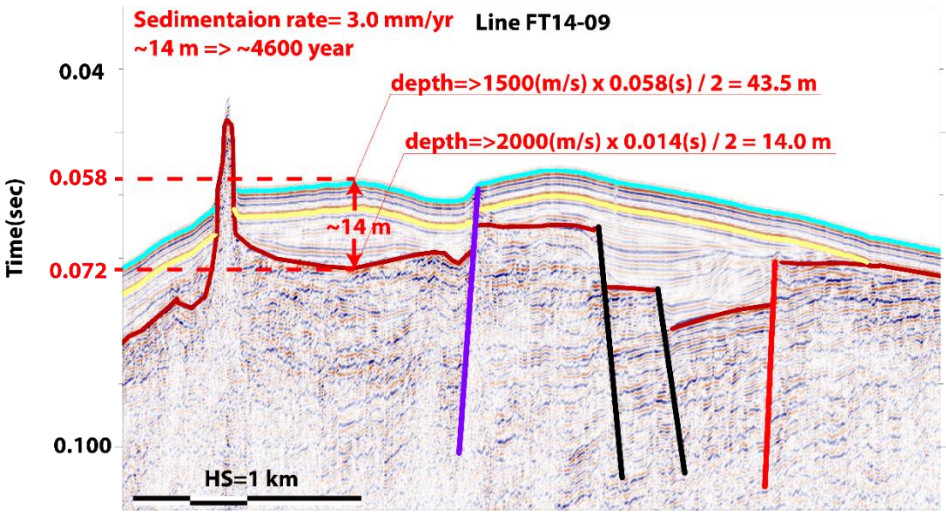

Figure 20 Active faults cutting seabed and recent sedimentary units in seismic line FT14-09 (Interval velocity of the water and sediments taken as 1500 m/s and 2000 m/s respectively).

The studies aiming at estimating the mean sea level variation in the Mediterranean region reveals that, following to last glacial maximum ended around 19,000 years ago, the global sea level has started to rise rapidly all over the world (Clark et al., 2009). The Figure 21b shows the estimated change of mean sea level as a function of time in Mediterranean (McGuire et al., 1997). As shown in the sea level variation graph, during the last 19.000 year, the sea level has risen by around 120 m. For this reason, the shelf break detected on seismic lines, where the depth of bathymetry rapidly decreases from 170 m to 270 m, corresponds to paleo-shoreline. Therefore, according to principle of crosscutting relationship, the fault cutting the sediments, which had been deposited during high stand of sea level with respect to shelf break, cannot be older than mentioned period of sea level rise. This situation is another clear evidence to indicate fault activity in the region.

Additionally, the locations with anomalous temperature values were detected during the study conducted to find subaqueous hot springs in the Fethiye-Göcek Bay. Among these anomalies one of them was confirmed as subaqueous hot spring in the bay (Figure 21a). The location of this hot spring (Coordinates (UTM): 675.787 E 4,066.071 N) is around İnlice Cove where the frequency of active faults detected in seismic sections increases (Avşar et al., 2017). This coincidence further corroborates the existence of active faults in the Fethiye-Göcek Bay.

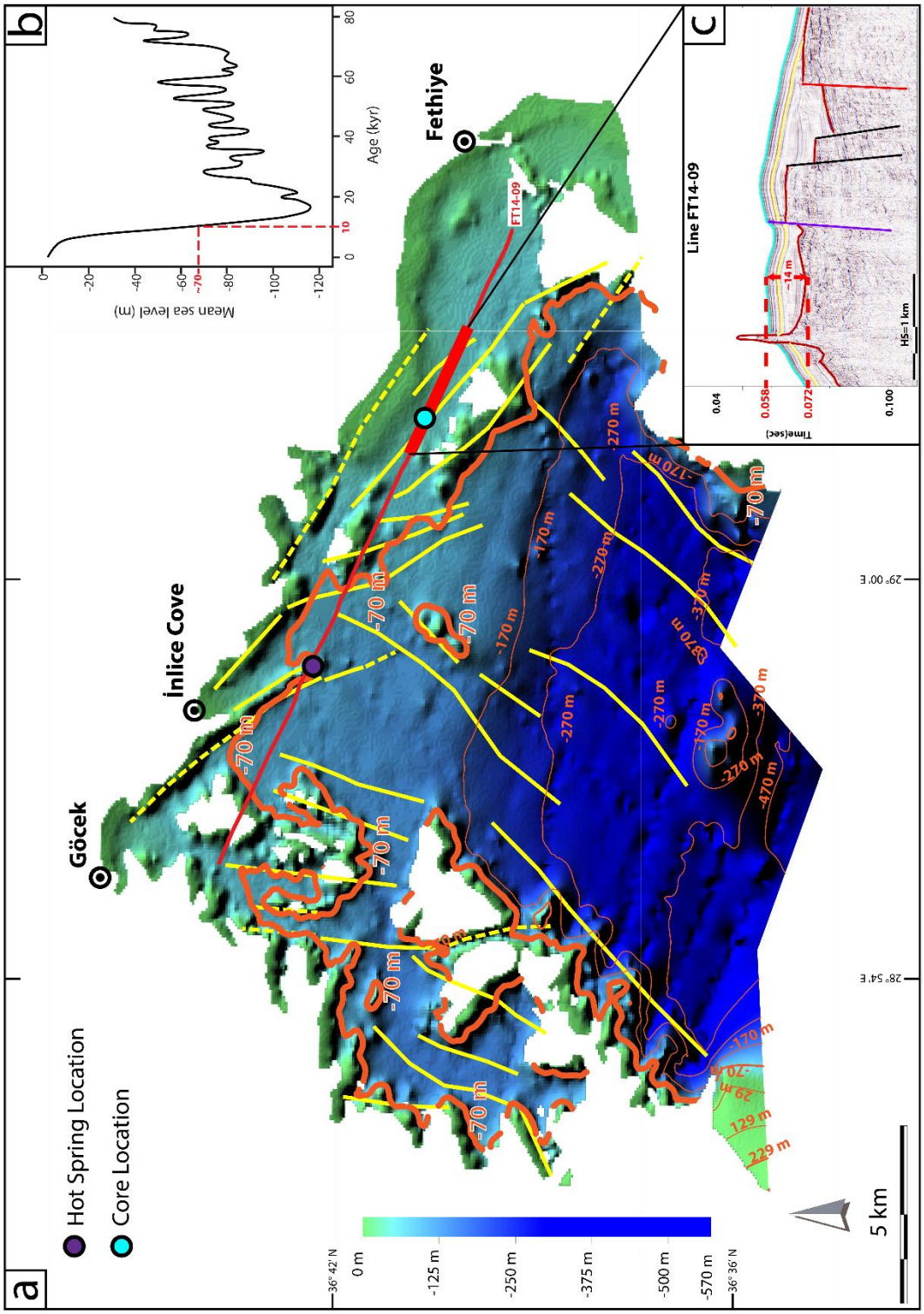

Figure 21 a) Colour coded bathymetry, depth contours (70 m is highlighted), and location of subaqueous hot spring and the core in the Fethiye-Göcek Bay; b) Mediterranean sea level variation chart (modified from McGuire et al., 1997); c) Active faults on seismic line FT14-09.

CHAPTER 4

DISCUSSIONS

4.1. Regional Tectonic Implications

Integration of seismic interpretation and field studies aimed at unravelling the paleostress configurations and on-land continuation of faults interpreted faults on the seismic sections revealed that the Fethiye-Göcek Bay area is under the influence of dominantly NW-SE directed extensional tectonics. Most of the structures both on-land and off shore are normal faults with minor strike-slip components. Strike-slip components are not constrained to any particular directions, on the contrary both dextral and sinistral components are observed on the faults having same direction and temporal relationships. This feature indicates that the strike-slip faults are simple accommodation structures transferring and linking the extensional deformation between two or more near orthogonal normal faults. Similarly, absence of any consistent and reliable strike-slip kinematic characteristics on a regional basis and absence of any flower structure on the seismic sections, which could indicate strike-slip faults, indicate lack of a regional strike-slip fault in the region. In other words, the region is dominated by normal faults and regional strike-slip faults are absent or have never been developed. The paleostress configurations also indicate absence of any transcurrent tectonics in the region. This implies that alleged Fethiye-Burdur Fault Zone does not exist or does not extend into the study area.

The other implication, the results of this study are that the Pliny-Strabo trench is not extending to the Fethiye-Göcek Bay, although, Ocakoğlu (2012) argued that it is extending as north as to the Turkish shores near the Fethiye-Göcek Bay based on

multibeam ecosounder images of sea bottom. These geometric manifestations of the sea bottom are either haphazard coincidence of sea bottom features or they correspond to the northernmost manifestations of the trench. This means that the Pliny-Strabo Trench terminates somewhere around the northern tip of Rhodes island (Figure 1).

This argument further implies that the Pliny-Strabo trench is a typical trench-trench connecting transform-like fault (STEP Fault, sensu Govers and Wortel 2005), a structure extending from the SE corner of South Aegean trench up to northern margin of Rhodes Basin and connecting the South Aegean and Cyprian trenches. Therefore, it cannot be linked up with the alleged Fethiye-Burdur Fault Zone existence of which is heavily debated.

The paleostress configurations, nature of on-land and off-shore faults all collectively indicate that the study area is under extensional deformation. Having extension vectors in almost all directions, although they are dominated in NW-SE, indicate that the region is under the influence of multidirectional extensional deformation while NW-SE directions dominates over the other directions. Similar extensional style was already been proposed by Alçiçek et al. (2006 and 2013), Kaymakçı (2006), and Verhaert et al. (2006).

CHAPTER 5

CONCLUSIONS

The fault orientations and their activities facilitated to unravel the characteristics of deformation styles around Fethiye-Göcek Bay. Using Angelier's reduced stress tensor procedure, the paleostress configurations and their relative magnitudes (i.e. shape of stress ellipsoid) were deduced from fault slip data set collected in the field. In the contest of seismic interpretation studies, the seismic horizons, which give region-wide traceable high amplitude reflection, were picked in time domain, and subsequently faults on each seismic sections were traced by utilizing picked horizons and seismic layer terminations. Then, the faults were correlated through the survey area and surface projection of major faults were mapped out in the bay. Moreover, using cross-cutting relationship, it was verified that these faults are the active faults, which have moved during the past 10,000 years of the Holocene Epoch. As a result, it was revealed that NW-SE directed extensional deformation predominates in the region and resulted in NE-SW striking active normal faults. Apart from those faults, a few number of NW-SE trending strike-slip faults were identified, which were developed almost perpendicular to NE-SW trending normal faults. They were interpreted as transfer faults, which accommodates differential displacement between two adjacent segments of the normal faults. Hence, based on the aforementioned findings, almost all the faults developed around the Fethiye-Göcek Bay located at the north-eastern termination of the Pliny-Strabo trench from off-shore to on-shore are nearly pure normal faults similar to earthquake focal mechanisms suggesting active extension in the region.

The hypothetic idea of sinistral transtensional FBFZ as onland termination of Pliny-Strabo trench was formed based upon the concept of STEP faults. By definition, STEP faults are the large-scale faults where the subducting lithosphere are laterally decoupled from non-subducting lithosphere in a scissor type of fashion, and therefore, they display considerably similar deformation pattern of strike-slip faults characterized by an array of subsidiary brittle fractures (e.g. Riedel and P shears). Moreover, depending on the tectonic setting, type of deformation occurring in STEP fault zones can vary from transpression to transtension. In this context, following the recognition of tearing of the subducting and retreating African lithosphere based on tomographic studies, the further subsurface studies revealed that Pliny-Strabo trench is a transpressional STEP fault connecting the Aegean and Cyprean trenches along the northern edge of the northwards subducting African lithosphere. Based on the collinearity between Pliny-Strabo fault zone and the NE-SW trending faults elongating from Fethiye to Burdur, it was proposed that FBFZ is a sinistral strike-slip fault zone as the NE propagation of Pliniy-Strabo trench in to the SW Anatolia. Subsequently, based on GPS velocities, it was also stated that the FBFZ is an active fault zone and accommodates sinistral displacements. However, the proposed hypothetic model of FBFZ is not valid for two reasons considering evolution model of STEP faults. First of all, according to the evolution model of STEP faults, as the tear propagated, STEP faults peruse the tear towards the trench side. From this point of view, propagation direction of Pliny-Strabo STEP fault culminates towards eastern tip of Aegean subduction. This means that, the FBFZ have already been experienced the effect of tear as a shear zone situated on the overriding plate above the subducted African lithosphere. However, any tangible evidence to support the existence of neither transtensional nor transpressional sinistral fault zone has not been encountered within the scope of this study. On the contrary, to proposed sinistral nature of the FBFZ, all of the faults are developed under approximately NW-SE directed extensions in the study area. Secondly, if the proposed model of FBFZ was valid, position of the Cyprian trench would be located somewhere in the Central Anatolia. However, based on tomographic studies, the present location of the both Aegean and Cyprus trenches are clear. Therefore, presence of FBFZ, which is supposed to accommodate at least 100 km sinistral displacement between the

Menderes Massif and the Beydağları Autochthon, is either kinematically or hypothetically debatable.

In consequence, overall kinematics of faults, fault plane solutions of earthquakes, and subsurface data through area in question manifests that the hypothetic idea of FBFZ as onland termination of Pliny-Strabo trench is not valid. Considering the fact that the SW Anatolia is a territory of multi-directional extensional deformation hosting arrays of NE-SW and NW-SE trending graben-type depressions, the kinematic characteristics of alleged NE-SW trending faults are no different from the faults having about the same trend which have been developed under the influence of the same tectonic regime in the region.

REFERENCES

Agostini, S., Doglioni, C., Innocenti, F., Manetti, P., Tonarini, S. (2010). On the geodynamics of the Aegean rift. Tectonophysics, 488(1), 7-21.

Aksu, A. E., Hall, J., Yaltırak, C. (2005). Miocene to Recent tectonic evolution of the eastern Mediterranean: New pieces of the old Mediterranean puzzle. Marine Geology, 221(1), 1-13.

Aksoy, R., Aksarı, S. (2016). Neogene-Quaternary evolution of the Tefenni basin on the Fethiye-Burdur fault zone, SW Anatolia-Turkey. Journal of African Earth Sciences, 118, 137-148.

Akyüz, H. S., Altunel, E. (1997). 417 Cibyra depremi: Burdur-Fethiye Fay Zonu'nun sol-yanal hareketine ait veriler (GB Anadolu). Aktif Tektonik Araştırma Grubu Birinci Toplantısı, İTÜ, İstanbul, 8-9. (In Turkish).

Akyüz, H. S., Altunel, E. (2001). Geological and archaeological evidence for post-Roman earthquake surface faulting at Cibyra, SW Turkey. Geodinamica Acta, 14(1-3), 95-101.

Alçiçek, M. C. (2001). Sedimentological investigation of Çameli Basin (late Miocene-late Pliocene, Denizli, SW Anatolia). Ankara University. Unpublished PhD thesis.

Alçiçek, M. C., Kazancı, N., Çemen, I., Özkul, M. (2002, October). Strikeslip faulting in the Çameli basin, southwestern Turkey: implications for inland transform prolongation of the Hellenic subduction zone. In Denver Annual Meeting (Vol. 2730).

Alçiçek, M. C., Kazancı, N., Özkul, M., Şevket, Ş. (2004). Çameli (Denizli) Neojen Havzasının tortul dolgusu ve jeolojik evrimi. Maden Tetkik ve Arama Dergisi, 128(128). (In Turkish).

Alçiçek, M. C., Kazancı, N., Özkul, M. (2005). Multiple rifting pulses and sedimentation pattern in the Çameli Basin, southwestern Anatolia, Turkey. Sedimentary Geology, 173(1), 409-431.

Alçiçek, M. C., Özkul, M. (2005). Extensional faulting induced tufa precipitation in the Neogene Çameli Basin of south-western Anatolia, Turkey. In travertine, Proceedings of 1st International Symposium on travertine (pp. 120-127).

Alçiçek, M. C., Ten Veen, J. H., Özkul, M. (2006). Neotectonic development of the Çameli basin, southwestern Anatolia, Turkey. Geological Society, London, Special Publications, 260(1), 591-611.

Alçiçek, M. C. (2007). Tectonic development of an orogen-top rift recorded by its terrestrial sedimentation pattern: the Neogene Eşen Basin of southwestern Anatolia, Turkey. Sedimentary Geology, 200(1), 117-140.

Alçiçek, M. C., Johan, H. (2008). The late Early Miocene Acıpayam piggy-back basin: refining the last stages of Lycian nappe emplacement in SW Turkey. Sedimentary Geology, 208(3), 101-113.

Alçiçek, M. C., Mayda, S., Titov, V. (2013). Lower Pleistocene stratigraphy of the Burdur basin of SW Anatolia. Comptes Rendus Palevol, 12(1), 1-11.

Alçiçek, M. C. (2015). Comment on "The Fethiye-Burdur Fault Zone: A component of upper plate extension of the subduction transform edge propagator fault linking Hellenic and Cyprus Arcs, Eastern Mediterranean. Tectonophysics 635, 80-99" by J. Hall, AE Aksu, İ. Elitez, C. Yaltırak, G. Çiftçi. Tectonophysics, 664, 1-4.

Alçiçek, H., Bülbül, A., Brogi, A., Liotta, D., Ruggieri, G., Capezzuoli, E., Alçiçek, M. C. (2018). Origin, evolution and geothermometry of the thermal waters in the Gölemezli Geothermal Field, Denizli Basin (SW Anatolia, Turkey). Journal of Volcanology and Geothermal Research, 349, 1-30.

Aleksandrowski, P. (1985). Graphical determination of principal stress directions for slickenside lineation populations: an attempt to modify Arthaud's method. Journal of Structural Geology, 7(1), 73-82.

Anderson, E. M. (1951). The dynamics of faulting and dyke formation with applications to Britain. Hafner Pub. Co.

Angelier, J. (1979). Determination of the mean principal directions of stresses for a given fault population. Tectonophysics, 56(3-4), T17-T26.

Angelier, J. (1984). Tectonic analysis of fault slip data sets. Journal of Geophysical Research: Solid Earth, 89(B7), 5835-5848.

Angelier, J. (1989). From orientation to magnitudes in paleostress determinations using fault slip data. Journal of structural geology, 11(1-2), 37-50.

Angelier, J. (1994). Fault slip analysis and paleostress reconstruction. Continental deformation, 53-101.

Angelier, J. T., Mechler, P. (1977). Sur une methode graphique de recherche des contraintes principales egalement utilisables en tectonique et en seismologie: la methode des diedres droits. Bulletin de la Société géologique de France, 7(6), 1309-1318.

Armijo, R., Carey, E., Cisternas, A. (1982). The inverse problem in microtectonics and the separation of tectonic phases. Tectonophysics, 82(1-2), 145-160.

Arthaud, F. (1969). Methode de determination graphique des directions de raccourcissement, d9allongement et intermediaire d9une population de failles. Bulletin de la Société géologique de France, 7(5), 729-737.

Avşar, Ö., Avşar, U., Arslan, Ş., Kurtuluş, B., Niedermann, S., Güleç, N. (2017). Subaqueous hot springs in Köyceğiz Lake, Dalyan Channel and Fethiye-Göcek Bay (SW Turkey): Locations, chemistry and origins. Journal of Volcanology and Geothermal Research, 345, 81-97.

Barka, A. A., Kadinsky- Cade, K. (1988). Strike- slip fault geometry in Turkey and its influence on earthquake activity. Tectonics, 7(3), 663-684.

Barka, A., Reilinger, R. (1997). Active tectonics of the Eastern Mediterranean region: deduced from GPS, neotectonic and seismicity data. Annals of Geophysics, 40(3).

Bergerat, F. (1987). Stress fields in the European platform at the time of Africa-Eurasia collision. Tectonics, 6(2), 99-132.

Biryol, C. B., Beck, S. L., Zandt, G., Özacar, A. A. (2011). Segmented African lithosphere beneath the Anatolian region inferred from teleseismic P-wave tomography. Geophysical Journal International, 184(3), 1037-1057.

Blumenthal, M.M., (1963). Le système structural du Taurus sud Anatolies. Bill. Soc. Géol. Fr. In: Livre à Mémoire de Professor P. Fallot. Mém. Soc. Géol. Fr. 1 (2), 611-662.

Bott, M. H. P. (1959). The mechanics of oblique slip faulting. Geological Magazine, 96(2), 109-117.

Bozkurt, E. (2001). Neotectonics of Turkey-a synthesis. Geodinamica Acta, 14(1-3), 3-30.

Bozkurt, E. and Park, R. G., (1994). Southern Menderes Massif: an incipient metamorphic core complex in western Anatolia, Turkey. Journal of the Geological Society, London 151, 213-216.

Bozkurt, E. and Rojay, B., (2005). Episodic, Two-Stage Neogene Extension and Short-Term Intervening Compression in Western Anatolia: Field Evidence from the Kiraz Basin and Bozdağ Horst. Geodinamica Acta, 18, 299-312.

Bozkurt, E. and Sözbilir, H., (2004). Tectonic Evolution of the Gediz Graben: Field Evidence for an Episodic, Two-Stage Extension in Western Turkey. Geological Magazine, 141, 63-79.

Bozkurt, E., Mittwede, S. K. (2001). Introduction to the geology of Turkey—a synthesis. International Geology Review, 43(7), 578-594.

Bozkurt, E., (2002) Discussion on the Extensional Folding in the Alaşehir (Gediz) Graben, Western Turkey. Journal of Geological Society, 179, p.105-109.

Bozkurt, E., Mittwede, S. K., (2005) Introduction: Evolution of continental extensional tectonics of western Turkey. Geodinamica Acta, 18.3-4: 153-165.

Carey, M. E. Brunier, B. (1974). Analyse théorique et numérique d'un modèle mécanique élémentaire appliqué à l'étude d'une population de failes. Compte Rendus Hebdomadaires des Seances de l'Academie des Science, 279, 891-894.

Clark, P. U., Dyke, A. S., Shakun, J. D., Carlson, A. E., Clark, J., Wohlfarth, B., ... McCabe, A. M. (2009). The last glacial maximum. Science, 325(5941), 710-714.

Collins, A. S., Robertson, A. H. (1997). Lycian melange, southwestern Turkey: an emplaced Late Cretaceous accretionary complex. Geology, 25(3), 255-258.

Collins, A. S., Robertson, A. H. (1999). Evolution of the Lycian Allochthon, western Turkey, as a north- facing Late Palaeozoic to Mesozoic rift and passive continental margin. Geological Journal, 34(12), 107-138.

Coulomb, C.A. (1776), "Sur une application des regles maximis et minimis a quelques problems de statique, relatives a l'architecture", Acad. Sc.i Paris Mem. Math. Phys., 7, 343-382.

de Graciansky, P. C. (1972). Recherches géologiques dans le Taurus Lycien. Universite de Paris-Sud, Centre d'Orsay.

Delvaux, D. and Sperner, B., (2003). Stress tensor inversion from fault kinematic indicators and focal mechanism data: the TENSOR program. New insights into structural interpretation and modelling, 212, pp.75-100.

Dewey, J. F., Hempton, M. R., Kidd, W. S. F., Saroglu, F. A. M. C., Şengör, A. M. C. (1986). Shortening of continental lithosphere: the neotectonics of Eastern Anatolia—a young collision zone. Geological Society, London, Special Publications, 19(1), 1-36.

Dewey, J.F. and Sengor, A.M.C., (1979). Aegean and surrounding regions: complex multiplate and continuum tectonics in a convergent zone: Geol. Soc. Amer. Bull., 90, 84-92.

Dewey, J.F., (1988). Extensional collapse of orogens: Tectonics, v. 7, p. 1123-1139.

Doglioni, C. , Agostini, S., Crespi, M., Innocenti, F., Manetti, P., Riguzzi, Fç, Savascin, Y., (2002). On the extension in western Anatolia and the Aegean Sea. Journal of the Virtual Explorer, 8, 169-183.

Duman, T. Y., Çan, T., Emre, Ö., Kadirioğlu, F. T., Baştürk, N. B., Kılıç, T., Karakaya, F. (2016). Seismotectonic database of Turkey. Bulletin of Earthquake Engineering, 1-40.

Dumont, J.F., Uysal, Ş., Şimşek, Ş., Karamanderesi, I.H. ve Letouzey, J., (1979). Güneybatı Anadolu'daki Grabenlerin Oluşumu. Maden Tetkik ve Arama Dergisi, 97, p. 7-17. (In Turkish).

Dürr, S., Altherr, R., Keller, J., Okrusch, M., Seidel, E., (1978). The Median Aegean Crystalline Belt: Stratigraphy, Structure, Metamorphism, Magmatism. Alps, Apennines, Hellenides. Edited by H. Closs-D. Roeder-K. Schmidt, Int. Un. Com on Geod., Sc. Rep., 38, 455-477

Elitez, İ. (2010). The Miocene-Quaternary Geodynamics of Çameli and Gölhisar Basins, Burdur-Fethiye Fault Zone. Istanbul Technical University, unpublished MSc Thesis.

Elitez, İ., Yaltırak, C. (2014). Miocene-Quaternary Geodynamics of Çameli Basin, Burdur-Fethiye Shear Zone (SW Turkey). Geological Bulletin of Turkey, 57(3), 41-67.

Elitez, I., Yaltirak, C. (2014, May). Burdur-Fethiye Shear Zone (Eastern Mediterranean, SW Turkey). In EGU General Assembly Conference Abstracts (Vol. 16).

Elitez, İ., Yaltırak, C., Akkök, R. (2009, September). Morphotectonic Evolution of the Middle of Burdur-Fethiye Fault Zone: Acıpayam, Gölhisar and Çameli Area, SW Turkey. In International Symposium on Historical Earthquakes and Conservation of Monuments and Sites in the Eastern Mediterranean Region 500th Anniversary Year of the 1509 September (Vol. 10, pp. 10-12).

Elitez, İ., Yaltırak, C., Hall, J., Aksu, A. E., Çifçi, G. (2015). Reply to the comment by MC Alçiçek on "The Fethiye-Burdur Fault Zone: A component of upper plate extension of the subduction transform edge propagator fault linking Hellenic and Cyprus Arcs, Eastern Mediterranean," Tectonophysics, 635, 80-99, by J. Hall, AE Aksu, İ. Elitez, C. Yaltirak and G. Çifçi. Tectonophysics, 664, 5-13.

Elitez, İ., Yaltırak, C., Aktuğ, B. (2016). Extensional and compressional regime driven left-lateral shear in southwestern Anatolia (eastern Mediterranean): The Burdur-Fethiye Shear Zone. Tectonophysics, 688, 26-35.

Etchecopar, A., Vasseur, G., Daignieres, M. (1981). An inverse problem in microtectonics for the determination of stress tensors from fault striation analysis. Journal of Structural Geology, 3(1), 51-65.

Eyidoğan, H., Barka, A. (1996). The 1 October 1995 Dinar earthquake, SW Turkey. Terra Nova, 8(5), 479-485.

Fleuty, M. J. (1975). Slickensides and slickenlines. Geological Magazine, 112(3), 319-322.

Gephart, J. W., Forsyth, D. W. (1984). An improved method for determining the regional stress tensor using earthquake focal mechanism data: application to the San Fernando earthquake sequence. Journal of Geophysical Research: Solid Earth, 89(B11), 9305-9320.

Gessner, K., Ring, U., Johnson, C., Hetzel, R., Passchier, C. W., Güngör, T. (2001). An active bivergent rolling-hinge detachment system: Central Menderes metamorphic core complex in western Turkey. Geology, 29(7), 611-614.

Görür, N., Sengör, A. M. C., Sakinü, M., Akkök, R., Yiğitbaş, E., Oktay, F. Y., Ersoy, Ş. (1995). Rift formation in the Gökova region, southwest Anatolia: implications for the opening of the Aegean Sea. Geological Magazine, 132(6), 637-650.

Govers, R., Wortel, M. J. R. (2005). Lithosphere tearing at STEP faults: response to edges of subduction zones. Earth and Planetary Science Letters, 236(1), 505-523.

Govers, R., Fichtner, A. (2016). Signature of slab fragmentation beneath Anatolia from full-waveform tomography. Earth and Planetary Science Letters, 450, 10-19.

Gürer, Ö. F., Yılmaz, Y. (2002). Geology of the Ören and surrounding areas, SW Anatolia. Turkish Journal of Earth Sciences, 11(1), 1-13.

Gürer, A., Bayrak, M., Gürer, Ö. F. (2004). Magnetotelluric images of the crust and mantle in the southwestern Taurides, Turkey. Tectonophysics, 391(1), 109-120.

Gutnic, M., Monod, O., Poisson, A. and Dumont, J., (1979). Géologie des Taurides Occidentales (Turquie). Mémoires de la Société Géologique de France (Nouvelle Série), Mémoire, 137, 109.

Hall, J., Aksu, A. E., Yaltırak, C., Winsor, J. D. (2009). Structural architecture of the Rhodes Basin: a deep depocentre that evolved since the Pliocene at the junction of Hellenic and Cyprus Arcs, eastern Mediterranean. Marine Geology, 258(1), 1-23.

Hall, J., Aksu, A. E., Elitez, I., Yaltırak, C., Çifçi, G. (2014). The Fethiye-Burdur Fault Zone: A component of upper plate extension of the subduction transform edge propagator fault linking Hellenic and Cyprus Arcs, Eastern Mediterranean. Tectonophysics, 635, 80-99.

Hayward, A.B., (1984). Miocene clastic sedimentation related to the emplacement of the Lycian Nappes and the Antalya Complex, S.W. Turkey. In: Dixon, J.E., Robertson, A.H.F. (Eds.), The Geological Evolution of the Eastern Mediterranean. Geol. Soc. London, Spec. Publ., No. 17, 287-300.

Hancock, P. L. (1985). Brittle microtectonics: principles and practice. Journal of structural geology, 7(3-4), 437-457.

Hetzel, R., Passchier, C. W., Ring, U., Dora, Ö. O. (1995). Bivergent extension in orogenic belts: the Menderes massif (southwestern Turkey). Geology, 23(5), 455-458.

Homberg, C., Bergerat, F., Philippe, Y., Lacombe, O. and Angelier, J., (2002). Structural inheritance and cenozoic stress fields in the Jura fold-and-thrust belt (France). Tectonophysics, 357, 137-158.

Hu, J.C. and Angelier, J., 2004. Stress permutations: Three- dimensional distinct element analysis accounts for a common phenomenon in brittle tectonics. Journal of Geophysical Research: Solid Earth, 109(B9).

Jackson, J., McKenzie, D. (1984). Active tectonics of the Alpine-Himalayan Belt between western Turkey and Pakistan. Geophysical Journal International, 77(1), 185-264.

Jolivet, L., Brun, J. P. (2010). Cenozoic geodynamic evolution of the Aegean. International Journal of Earth Sciences, 99(1), 109-138.

Kahle, H. G., Straub, C., Reilinger, R., McClusky, S., King, R., Hurst, K., Cross, P. (1998). The strain rate field in the eastern Mediterranean region, estimated by repeated GPS measurements. Tectonophysics, 294(3), 237-252.

Karabacak, V. (2011). Geological, geomorphological and archaeoseismological observations along the Cibyra Fault and their implications for the regional tectonics of SW Turkey. Turkish Journal of Earth Sciences, 20(4), 429-447.

Kaymakci, N. (2006). Kinematic development and paleostress analysis of the Denizli Basin (Western Turkey): implications of spatial variation of relative paleostress magnitudes and orientations. Journal of Asian Earth Sciences, 27(2), 207-222.

Kaymakci, N., Aldanmaz, E., Langereis, C., Spell, T. L., Gurer, O. F., Zanetti, K. A. (2007). Late Miocene transcurrent tectonics in NW Turkey: evidence from palaeomagnetism and 40Ar–39Ar dating of alkaline volcanic rocks. Geological Magazine, 144(2), 379-392.

Kaymakci, N., Özçelik, Y., White, S. H., Van Dijk, P. M. (2009). Tectono-stratigraphy of the Çankırı Basin: late Cretaceous to early Miocene evolution of the Neotethyan suture zone in Turkey. Geological Society, London, Special Publications, 311(1), 67-106.

Kaymakçı, N., Özacar, A., Özkaptan, M., Koç, A., Gülyüz, E., Lefebvre, C., Sözbilir, H. (2014, October). Fethiye-Burdur fault zone: a myth. In the 8th International Symposium on Eastern Mediterranean Geology (ISEMG-8) (pp. 13-17).

Kaymakci, N., Inceöz, M., Ertepinar, P., Koç, A. (2010). Late Cretaceous to recent kinematics of SE Anatolia (Turkey). Geological Society, London, Special Publications, 340(1), 409-435.

Koçyigit, A. (1984). Intra-plate neotectonic development in southwestern Turkey and adjacent areas. Bull Geol Soc Turkey, 27, 1-16.

Koçyiğit, A., Yusufoğlu, H. ve Bozkurt, E. (1999). Evidence from the Gediz graben for episodic two-stage extension in western Turkey. Journal of the Geological Society, London 156, 605-616.

Koçyiğit, A. and Özacar, A., (2003). Extensional Neotectonic Regime through the NE Edge of the Outer Isparta Angle, Sw Turkey: New Field and Seismic Data. Turkish Journal of Earth Sciences 2, 67-90.

Koçyiğit, A., (2005). Denizli Graben-Horst System and the Eastern Limit of the West Anatolian Continental Extension: Basin Fill, Structure, Deformational Mode, Throw Amount and Episodic Evolutionary History, Sw Turkey. Geodinamica Acta. 18, 167-208.

Kürçer, A., Özdemir, E., Güldoğan, Ç. U., Duman, T. Y. (2016). The Fırst Paleoseısmıc Trench Data From Acıpayam Fault, Fethiye Burdur Fault Zone, Sw Turkey. Bulletin of the Geological Society of Greece, 50(1), 75-84.

Le Pichon, X., Angelier, J. (1979). The Hellenic arc and trench system: a key to the neotectonic evolution of the eastern Mediterranean area. Tectonophysics, 60(1), 1-42.

Lisle, R. J. (1987). Principal stress orientations from faults: an additional constraint. In Annales Tectonicae (Vol. 1, No. 2, pp. 155-158).

Marrett, R., Allmendinger, R. W. (1990). Kinematic analysis of fault-slip data. Journal of structural geology, 12(8), 973-986.

McClusky S, Balassanian S, Barka A, Demir C, Ergintav S, Georgiev I, Gurkan O, Hamburger M, Hurst K, Kahle H, Kastens K, Kekelidze G, King R, Kotzev V, Lenk O, Mahmoud S, Mishin A, Nadariya M, Ouzounis A, Paradissis D, Peter Y, Prilepin M, Reilinger R, Sanli I, Seeger H, Tealeb A, Toksoz MN, Veis G., (2000). Global Positioning System constraints on plate kinematics and dynamics in the eastern Mediterranean and Caucasus. Journal of Geophysical Research-Solid Earth, 105 (B3): 5695-5719.

McClusky, S., Balassanian, S., Barka, A., Demir, C., Ergintav, S., Georgiev, I., Kastens, K. (2000). Global Positioning System constraints on plate kinematics and dynamics in the eastern Mediterranean and Caucasus. Journal of Geophysical Research: Solid Earth, 105(B3), 5695-5719.

McGuire, W. J., Howarth, R. J., Firth, C. R., Solow, A. R., Pullen, A. D., Saunders, S. J., ... Vita-Finzi, C. (1997). Correlation between rate of sea-level change and frequency of explosive volcanism in the Mediterranean. Nature, 389(6650), 473-476.

McKenzie, D. P. (1969). The relation between fault plane solutions for earthquakes and the directions of the principal stresses. Bulletin of the Seismological Society of America, 59(2), 591-601.

McKenzie, D. (1972). Active tectonics of the Mediterranean region. Geophysical Journal International, 30(2), 109-185.

McKenzie, D. (1978). Active tectonics of the Alpine—Himalayan belt: the Aegean Sea and surrounding regions. Geophysical Journal International, 55(1), 217-254.

Meulenkamp, J.E., Wortel, M.J.R., Van Wamel, W.A., Spakman, W. Stratıng, E.H. (1988). On the Hellenic subduction zone and the geodynamic evolution of Crete since the late Middle Miocene. Tectonophysics, 146, 203-215.

Mohr, O. (1900). Welche Umstände bedingen die Elastizitätsgrenze und den Bruch eines Materials. Zeitschrift des Vereins Deutscher Ingenieure, 46(1524-1530), 1572-1577.

Moores, E. M., Robinson, P. T., Malpas, J., Xenophonotos, C. (1984). Model for the origin of the Troodos massif, Cyprus, and other mideast ophiolites. Geology, 12(8), 500-503.

MTA, (2002). Geological map of Turkey, 1 / 500,000 scaled Zonguldak quadrangle. MTA Genel Mudurlugu, Ankara, Turkey.

Ocakoğlu, N. (2012). Investigation of Fethiye-Marmaris Bay (SW Anatolia): seismic and morphologic evidences from the missing link between the Pliny Trench and the Fethiye-Burdur Fault Zone. Geo-Marine Letters, 32(1), 17-28.

Okay, A. I., Tansel, İ., Tüysüz, O., (2001). Obduction, subduction and collision as reflected in the Upper Cretaceous-Lower Eocene sedimentary record of western Turkey. Geological Magazine, 138(2), 117-142.

O'leary, D. W., Friedman, J. D., Pohn, H. A. (1976). Lineament, linear, lineation: some proposed new standards for old terms. Geological Society of America Bulletin, 87(10), 1463-1469.

Oral, M.B., Reilinger, R., Toksoz, R., (1992). Deformation of the Anatolian block as deduced from GPS measurements. Transactions, American Geophysical Union, EOS 73, 120.

Özkaptan, M., Koç, A., Lefebvre, C., Gülyüz, E., Uzel, B., Kaymakci, N., Sözbilir, H. (2014, May). Kinematics of SW Anatolia implications on crustal deformation above slab tear. In EGU General Assembly Conference Abstracts (Vol. 16).

Özbakır, A. D., Şengör, A. M. C., Wortel, M. J. R., Govers, R. (2013). The Pliny-Strabo trench region: A large shear zone resulting from slab tearing. Earth and Planetary Science Letters, 375, 188-195.

Özbakır, A. D., Govers, R., Wortel, R. (2017). Active faults in the Anatolian-Aegean plate boundary region with Nubia. Turkish Journal of Earth Sciences, 26(1).

Özer, S., Sözbilir, H., Özkar, Ý., Toker, V., Sarı, B., (2001). Stratigraphy of Upper Cretaceous- Palaeogene sequences in the southern and eastern Menderes Massif (western Turkey). Int. J. Earth Sci., 2001, 852-866.

Özkaya, İ. (1990). Origin of the allochthons in the Lycien Belt, Southwest Turkey. Tectonophysics, 177(4), 367-379.

Över, S., Yılmaz, H., Pınar, A., Özden, S., Ünlügenç, U. C., Kamacı, Z. (2013). Plio-quaternary stress state in the Burdur Basin, SW-Turkey. Tectonophysics, 588, 56-68.

Poisson, A., (1977). Recherches Géologiques dans les Taurides Occidentales (Turquie). Doctorat d'Etat thesis, Université de Paris-Sud, Orsay, France.

Poisson, A., Yağmurlu, F., Bozcu, M. and Senturk, M., (2003). New insight on the tectonic setting and evolution around the apex of the Isparta Angle (SW Turkey). Geological Journal, 38, p. 257-282.

Price, S. P. (1989). Sedimentation and neotectonics of the Burdur region, SW Turkey. Unpublished Ph.D. thesis, University of Leicester.

Price, S. P., Scott, B. (1994). Fault-block rotations at the edge of a zone of continental extension; southwest Turkey. Journal of Structural Geology, 16(3), 381-392.

Purvis, M. and Robertson, A.H.F., (2004). A pulsed extension model for the Neogene-Recent E-W trending Alaşehir Graben and the NE-SW trending Selendi and Gördes Basins, western Turkey. Tectonophysics 391, 171- 201.

Purvis, M. and Robertson, A.H.F., (2005). Miocene sedimentary evolution of the NE-SW-trending Selendi and Gördes Basins, Western Turkey: implications for extensional processes. Sedimentary Geology 174, 31-62.

Reilinger, R., McClusky, S., Vernant, P., Lawrence, S., Ergintav, S., Cakmak, R., Nadariya, M. (2006). GPS constraints on continental deformation in the Africa- Arabia- Eurasia continental collision zone and implications for the dynamics of plate interactions. Journal of Geophysical Research: Solid Earth, 111(B5).

Reilinger, R. E., McClusky, S. C., Oral, M. B., King, R. W., Toksoz, M. N., Barka, A. A., Sanli, I. (1997). Global Positioning System measurements of present-day crustal movements in the Arabia- Africa- Eurasia plate collision zone. Journal of Geophysical Research: Solid Earth, 102(B5), 9983-9999.

Robertson, A. H. (1998). Mesozoic-Tertiary tectonic evolution of the easternmost Mediterranean area: integration of marine and land evidence. Proceedings of the Ocean Drilling Program, Scientific Results, Vol. 160; Chapter 54.

Robertson, A. H., Pickett, E. A. (2000). Palaeozoic-early Tertiary Tethyan evolution of melanges, rift and passive margin units in the Karaburun Peninsula (western Turkey) and Chios Island (Greece). Geological Society, London, Special Publications, 173(1), 43-82.

Rotstein, Y. (1984). Counterclockwise rotation of the Anatolian block. Tectonophysics, 108(1-2), 71-91.

Royden, L. H. (1993). The tectonic expression slab pull at continental convergent boundaries. Tectonics, 12(2), 303-325.

Şahin, Ş. (2004). Güneybatı Anadolu'da Gerilme Dağılımı ve Burdur Fayına Olan Etkisi. İstanbul Yerbilimleri Dergisi, 17(1). (In Turkish).

Saroglu, F., Boray, A., Emre, O. (1987). Active faults of Turkey. General Directorate of the Mineral Research and Exploration, Ankara, Turkey, 1(2), 000.

Saroglu, F., Emre, O., Kuscu, I. (1992). Active fault map of Turkey. General Directorate of Mineral Research and Exploration, Ankara.

Şengör, A. M. C., Kidd, W. S. F. (1979). Post-collisional tectonics of the Turkish-Iranian plateau and a comparison with Tibet. Tectonophysics, 55(3-4), 361-376.

Şengör, A. M. C., Yilmaz, Y. (1981). Tethyan evolution of Turkey: a plate tectonic approach. Tectonophysics, 75(3-4), 181193203-190199241.

Şengör, A.M.C., Görür, N, Şaroğlu, F., (1985). Strike-slip faulting and related basin formation in zones of tectonic escape: Turkey as a case study: in Biddle, K.T. and Christie-Blick, N., edts, Strike-slip Deformation, Basin Formation, and Sedimentation, Soc. Econ. Paleont. Min. Spec. Pub. 37 (in honor of J.C. Crowell), p. 227-264.

Seyitoglu, G. Scott, B. C., (1991). Late Cenozoic crustal extension and basin formation in west Turkey. Geological Magazine, 128, 155-166.

Seyitoglu, G. Scott, B. C., (1992). The age of Buyiik Menderes Graben (west Turkey) and its tectonic implications. Geological Magazine, 129,239-242.

Sharma, P. V. (1997). Environmental and engineering geophysics. Cambridge university press.

Sözbilir, H. (2002). Geometry and origin of folding in the Neogene sediments of the Gediz Graben, western Anatolia, Turkey. Geodinamica Acta, 15(5-6), 277-288.

Spang, J. H. (1972). Numerical method for dynamic analysis of calcite twin lamellae. Geological Society of America Bulletin, 83(2), 467-472.

Taymaz, T., Price, S. (1992). The 1971 May 12 Burdur earthquake sequence, SW Turkey: a synthesis of seismological and geological observations. Geophysical Journal International, 108(2), 589-603.

Taymaz, T., Jackson, J., McKenzie, D. (1991). Active tectonics of the north and central Aegean Sea. Geophysical Journal International, 106(2), 433-490.

Taymaz, T. ve Tan, 0., (2001). Sultandag1 Depremi ve Göller Bölgesinin depremselligi, Cumhuriyet Bilim ve Teknik, 719, 18-19.

Ten Veen, J. T., Boulton, S. J., Alçiçek, M. C. (2009). From palaeotectonics to neotectonics in the Neotethys realm: The importance of kinematic decoupling and inherited structural grain in SW Anatolia (Turkey). Tectonophysics, 473(1), 261-281.

Tiryakioğlu, İ., Floyd, M., Erdoğan, S., Gülal, E., Ergintav, S., McClusky, S., Reilinger, R. (2013). GPS constraints on active deformation in the Isparta Angle region of SW Turkey. Geophysical Journal International, 195(3), 1455-1463.

Van der Pluijm, B.A. and Marshak, S., 2004. Earth structure. New York.

van Hinsbergen, D. J. (2010). A key extensional metamorphic complex reviewed and restored: the Menderes Massif of western Turkey. Earth-Science Reviews, 102(1-2), 60-76.

Verhaert, G., Similox-Tohon, D., Vandycke, S., Sintubin, M. and Muchez, P., (2006). Different stress states in the Burdur-Isparta region (SW Turkey) since Late Miocene times: a reflection of a transient stress regime. Journal of structural geology, 28(6), pp.1067-1083.

Wallace, R. E. (1951). Geometry of shearing stress and relation to faulting. The Journal of Geology, 59(2), 118-130.

Westaway, R. (2003). Kinematics of the Middle East and Eastern Mediterranean Updated. Turkish Journal of Earth Sciences, 12(1).

Woodside, J. M., Mascle, J., Zitter, T. A. C., Limonov, A. F., Ergün, M., Volkonskaia, A. (2002). The Florence Rise, the western bend of the Cyprus Arc. Marine Geology, 185(3), 177-194.

Woodside, J., Mascle, J., Huguen, C., Volkonskaia, A., (2000). The Rhodes Basin, a postMiocene tectonic trough. Marine Geology. 165, 1-12.

Yağmurlu, F., Savaşçın, Y., Ergün, M. (1997). Relation of alkaline volcanism and active tectonism within the evolution of the Isparta Angle, SW Turkey. The journal of geology, 105(6), 717-728.

Yılmaz, Y., Genç, Ş.C., Gürer, F., Bozcu, M., Yilmaz, K., Karacik, Z., Altunkaynak, Fi. and Elmas, A., (2000). When Did The Western Anatolian Grabens Begin To Develop? In: Bozkurt, E., Wınchester, J.A. and Piper, J.D.A. (Eds), Tectonics and Magmatism In Turkey and The Surrounding Area. Geological Society, London, Special Publications 173, 353-384.

APPENDIX A

SELECTED SEISMIC RECORD

Table A-1 Seismic parameters of the earthquakes with magnitudes larger than 4.5 occurred in the period of 1900-2017.

Id	Longitude	Latitude	M/D/Y	Time	M	Depth	Ref
1	28° 36' 16"E	37° 06' 52"N	11/24/2017	9:49 PM	5.1	24.46	1
2	28° 35' 31"E	37° 07' 14"N	11/22/2017	8:22 PM	5	24.75	1
3	28° 26' 37"E	36° 18' 58"N	11/7/2017	2:4 AM	4.4	41.89	1
4	28° 11' 13"E	36° 43' 57"N	11/4/2017	9:54 PM	4.2	66.78	1
5	28° 01' 29"E	36° 00' 44"N	9/1/2017	4:48 PM	4.8	61.98	1
6	28° 38' 49"E	37° 09' 11"N	4/13/2017	4:22 PM	5	11.33	1
7	28° 38' 30"E	37° 06' 14"N	12/15/2016	4:43 PM	4.2	18.11	1
8	28° 09' 19"E	36° 17' 11"N	9/6/2016	5:27 AM	4.2	49.58	1
9	27° 58' 42"E	36° 35' 33"N	3/12/2016	3:44 PM	4.2	51.57	1
10	29° 22' 01"E	36° 56' 55"N	2/5/2016	1:25 PM	4	8.03	1
11	28° 52' 40"E	37° 06' 03"N	9/13/2015	2:57 AM	4.4	21.36	1
12	28° 41' 18"E	37° 08' 35"N	7/25/2015	6:35 PM	4.2	15.05	1
13	28° 32' 22"E	37° 03' 25"N	4/28/2015	7:59 AM	4	16.92	1
14	27° 54' 14"E	36° 31' 10"N	3/16/2015	8:9 PM	4	18.22	1
15	28° 48' 57"E	36° 25' 40"N	11/15/2014	8:23 PM	4.2	6.02	1
16	28° 45' 28"E	37° 08' 50"N	11/10/2014	9:2 AM	4.3	10.34	1

Table A-1 (continued)

17	28° 44' 04"E	37° 06' 58"N	11/10/2014	6:16 AM	4.8	14.46	1
18	29° 22' 10"E	36° 57' 39"N	10/1/2014	7:16 AM	4.2	25.37	1
19	28° 06' 22"E	35° 54' 23"N	8/14/2014	12:27 PM	4	21.39	1
20	28° 06' 36"E	36° 44' 33"N	7/20/2014	2:46 AM	4	37.97	1
21	28° 34' 31"E	36° 21' 52"N	6/20/2014	1:59 PM	4.3	49.42	1
22	28° 51' 47"E	36° 19' 39"N	5/3/2014	4:46 AM	4.1	32.25	1
23	28° 52' 41"E	37° 02' 04"N	4/19/2014	11:39 PM	4	14.17	1
24	27° 55' 54"E	36° 37' 27"N	6/21/2013	6:26 PM	4.2	83.41	1
25	28° 22' 17"E	37° 01' 18"N	5/16/2013	9:26 PM	4.2	16.61	1
26	28° 24' 36"E	37° 00' 19"N	5/16/2013	9:21 PM	4.4	20.87	1
27	28° 25' 14"E	36° 58' 57"N	5/16/2013	3:2 AM	4.6	25.43	1
28	28° 11' 41"E	36° 11' 33"N	4/21/2013	1:45 AM	4.4	50.96	1
29	28° 51' 22"E	36° 11' 41"N	12/27/2012	4:9 PM	4	16.9	3
30	27° 57' 15"E	36° 37' 47"N	12/2/2012	7:2 PM	4	4.05	1
31	28° 38' 25"E	37° 12' 31"N	11/30/2012	2:32 AM	4.2	20.27	1
32	27° 57' 08"E	36° 37' 03"N	11/26/2012	5:35 PM	4.8	7.4	1
33	27° 55' 19"E	36° 35' 44"N	11/25/2012	8:51 AM	4	10.77	1
34	27° 56' 40"E	36° 37' 01"N	11/24/2012	9:35 PM	4.1	4.45	1
35	27° 55' 39"E	36° 35' 17"N	11/24/2012	9:31 PM	4.2	20.59	1
36	27° 56' 19"E	36° 36' 00"N	11/24/2012	9:4 PM	4.3	11.66	1
37	28° 14' 30"E	36° 31' 43"N	11/13/2012	6:25 PM	4	8.4	3
38	27° 57' 36"E	36° 40' 48"N	11/9/2012	4:46 AM	4	2	5
39	28° 14' 33"E	36° 33' 00"N	10/20/2012	1:9 AM	4.1	2.9	3
40	28° 56' 31"E	36° 26' 31"N	6/25/2012	1:5 PM	5	27	3
41	29° 03' 51"E	36° 21' 58"N	6/14/2012	4:46 PM	4.8	32.89	1
42	28° 54' 04"E	36° 28' 50"N	6/13/2012	8:59 AM	4.5	27.33	1
43	28° 55' 41"E	36° 27' 28"N	6/12/2012	9:58 PM	4.5	28.02	1
44	28° 59' 01"E	36° 27' 27"N	6/11/2012	7:51 PM	4.3	27.87	1

Table A-1 (continued)

45	28° 59' 26"E	36° 24' 40"N	6/11/2012	5:35 PM	4.4	27.94	1
46	29° 00' 19"E	36° 25' 36"N	6/11/2012	2: PM	4	28.69	1
47	28° 58' 43"E	36° 25' 32"N	6/11/2012	2:6 AM	4.4	28.19	1
48	28° 56' 39"E	36° 25' 27"N	6/10/2012	10:31 PM	4	28.32	1
49	28° 57' 38"E	36° 28' 25"N	6/10/2012	6:28 PM	4.5	28.64	1
50	28° 57' 40"E	36° 29' 28"N	6/10/2012	12:5 PM	4.4	7.13	1
51	28° 55' 46"E	36° 28' 34"N	6/10/2012	12:49 PM	5	26.85	1
52	28° 55' 48"E	36° 21' 36"N	6/10/2012	12:44 PM	6.1	30	5
53	28° 28' 56"E	37° 02' 19"N	6/9/2012	2:33 PM	4.2	20.92	1
54	28° 12' 07"E	36° 54' 58"N	6/4/2012	2:19 PM	4.6	12.11	1
55	28° 31' 43"E	37° 02' 07"N	5/8/2012	7:31 AM	4.3	23.36	1
56	28° 09' 57"E	36° 46' 27"N	4/10/2012	6:1 AM	4	53.5	3
57	28° 42' 56"E	36° 13' 11"N	2/15/2012	2:34 AM	4.5	63.6	3
58	28° 28' 47"E	36° 08' 35"N	1/23/2012	6:23 PM	4	19.6	3
59	28° 26' 24"E	36° 09' 37"N	1/20/2012	1:36 AM	4.1	8.1	3
60	28° 28' 48"E	35° 55' 48"N	11/29/2011	2:7 PM	4	22	3
61	28° 42' 27"E	36° 31' 23"N	10/24/2011	10:14 AM	4.2	23.32	1
62	28° 40' 25"E	36° 32' 02"N	10/24/2011	10:6 AM	4	25.83	1
63	28° 47' 51"E	36° 11' 48"N	9/5/2011	11:42 AM	4.3	50.79	1
64	28° 46' 27"E	36° 35' 48"N	6/15/2011	6:23 PM	4	25.98	1
65	28° 41' 24"E	36° 20' 24"N	4/27/2011	2:4 AM	4	2	3
66	28° 49' 12"E	36° 27' 00"N	4/10/2011	11:11 AM	4	6	3
67	28° 46' 12"E	36° 29' 24"N	4/3/2011	11:42 PM	4	5	3
68	28° 03' 11"E	36° 35' 54"N	12/14/2010	11:1 PM	4.1	66.5	2
69	27° 58' 27"E	36° 34' 22"N	8/8/2010	12:24 AM	4.3	22.3	2
70	29° 20' 08"E	36° 55' 28"N	1/31/2010	4:18 AM	4	6.92	1
71	28° 37' 04"E	36° 29' 01"N	12/12/2009	3:23 PM	4.4	56.3	2
72	29° 34' 10"E	37° 24' 38"N	12/4/2009	5:19 PM	4.7	19.5	2

Table A-1 (continued)

73	29° 09' 02"E	37° 01' 09"N	1/1/2009	7:1 PM	4.1	22.52	1
74	27° 55' 11"E	35° 54' 51"N	12/14/2008	7:27 AM	4.4	70.1	2
75	28° 13' 24"E	36° 37' 57"N	11/24/2008	11:34 AM	4	73.2	2
76	28° 09' 56"E	36° 52' 12"N	11/9/2008	1:2 PM	4	63.6	5
77	27° 57' 55"E	36° 08' 19"N	11/9/2008	7:48 AM	4	69.9	2
78	28° 25' 23"E	36° 04' 53"N	10/6/2008	5:19 AM	4.1	76.7	2
79	29° 10' 27"E	36° 58' 25"N	10/1/2008	3:53 AM	4.1	5.4	2
80	29° 12' 40"E	36° 58' 32"N	8/25/2008	2:57 AM	4.3	10	2
81	29° 12' 03"E	36° 57' 19"N	8/24/2008	10:52 PM	4	10	2
82	27° 47' 34"E	35° 53' 24"N	7/15/2008	3:26 AM	6.4	52	4
83	29° 09' 35"E	37° 02' 33"N	7/11/2008	2:11 PM	4.3	4.8	2
84	29° 14' 02"E	37° 01' 10"N	7/3/2008	5:37 PM	4.5	13.2	2
85	29° 12' 17"E	36° 56' 34"N	5/30/2008	5:34 AM	4	1.2	2
86	29° 16' 01"E	36° 55' 24"N	5/28/2008	10:35 PM	4	9.2	2
87	29° 14' 09"E	36° 55' 42"N	1/8/2008	3:57 PM	4.3	10	5
88	29° 14' 35"E	36° 54' 48"N	12/28/2007	10:34 AM	4	12.9	2
89	29° 17' 31"E	36° 57' 50"N	12/9/2007	8:29 PM	4.3	20	4
90	27° 54' 29"E	36° 18' 30"N	12/7/2007	12:57 PM	4.1	81.7	2
91	29° 19' 15"E	36° 56' 56"N	12/2/2007	8:21 PM	4.6	27.4	4
92	29° 22' 58"E	36° 54' 32"N	11/16/2007	9:8 AM	5.1	20	4
93	29° 16' 01"E	36° 58' 22"N	11/12/2007	3:2 PM	4.5	10	4
94	29° 23' 31"E	36° 53' 52"N	10/31/2007	5:58 PM	4.4	20	4
95	29° 22' 04"E	36° 52' 19"N	10/29/2007	7:41 PM	4.5	20	4
96	29° 20' 31"E	36° 54' 28"N	10/29/2007	9:23 AM	5.3	20	4
97	27° 58' 37"E	36° 37' 55"N	10/10/2007	9:27 PM	4.4	89.6	4
98	28° 23' 22"E	35° 53' 23"N	4/9/2007	2:29 PM	4	14	2
99	28° 45' 06"E	36° 29' 10"N	4/2/2007	12:38 PM	4	13	2
100	28° 32' 58"E	37° 05' 54"N	3/6/2007	3:34 AM	4.4	4.7	2

Table A-1 (continued)

101	28° 48' 21"E	36° 23' 27"N	8/24/2006	4:3 AM	4.2	10	2
102	28° 12' 07"E	35° 58' 15"N	7/2/2006	6:55 AM	4.2	15.8	4
103	28° 11' 05"E	36° 52' 49"N	4/18/2006	1:21 AM	4	16.9	2
104	28° 15' 00"E	36° 54' 14"N	4/17/2006	8:18 PM	4.2	5.6	4
105	28° 16' 50"E	36° 54' 56"N	4/17/2006	11:53 AM	4.1	10	2
106	28° 16' 39"E	36° 23' 30"N	3/15/2006	3:17 AM	4	74.6	5
107	28° 15' 57"E	36° 51' 28"N	1/20/2006	10:4 AM	4	12.4	4
108	28° 06' 10"E	36° 25' 26"N	7/11/2005	5:2 PM	4	58.9	4
109	28° 21' 10"E	36° 55' 59"N	1/14/2005	7:8 PM	4.2	16.8	2
110	28° 18' 10"E	37° 00' 36"N	12/28/2004	8:34 PM	4.5	13.7	4
111	28° 16' 56"E	36° 57' 51"N	12/21/2004	12:23 AM	4.1	42	2
112	28° 20' 42"E	36° 57' 00"N	12/20/2004	11:2 PM	5.3	28.3	4
113	28° 16' 15"E	35° 56' 18"N	10/26/2004	1:18 PM	4	72.6	2
114	28° 04' 22"E	35° 58' 03"N	9/27/2004	4:5 AM	4	93.1	2
115	29° 12' 20"E	37° 41' 48"N	9/16/2004	1:4 AM	4.3	11.7	2
116	27° 57' 21"E	36° 21' 07"N	8/20/2004	11:12 AM	4.6	78.9	4
117	27° 58' 19"E	36° 30' 54"N	7/29/2004	5:35 AM	4.2	80.9	4
118	28° 15' 56"E	36° 07' 07"N	5/20/2004	11:26 AM	4	74.5	2
119	28° 41' 24"E	36° 57' 25"N	2/19/2004	4:9 AM	4.1	9.8	4
120	27° 51' 24"E	35° 52' 21"N	1/3/2004	5:18 PM	4.1	80.1	2
121	28° 23' 31"E	35° 55' 45"N	2/24/2003	12:19 AM	4.2	57	2
122	27° 50' 45"E	36° 10' 19"N	10/2/2002	4:31 AM	4.2	73.8	4
123	27° 58' 19"E	36° 34' 33"N	9/26/2002	8:44 PM	4.6	23.6	4
124	28° 22' 01"E	36° 00' 00"N	8/14/2002	9:1 PM	4.2	55.3	2
125	29° 17' 31"E	37° 40' 15"N	7/30/2002	12:2 PM	4.7	17.3	4
126	27° 45' 18"E	36° 17' 02"N	7/24/2002	9: AM	4.2	89.8	2
127	27° 55' 22"E	36° 21' 00"N	2/17/2002	12:23 PM	5	88	2
128	28° 04' 15"E	36° 17' 31"N	12/31/2001	1:32 PM	4	70.1	2

Table A-1 (continued)

129	28° 07' 26"E	36° 30' 43"N	12/29/2001	11:12 PM	4	100.3	2
130	28° 10' 22"E	36° 43' 58"N	10/8/2001	11:38 AM	4	87.7	2
131	27° 54' 43"E	36° 20' 49"N	7/25/2001	4:52 PM	4	75.4	2
132	28° 40' 26"E	36° 30' 21"N	4/9/2001	8:5 PM	4	63.3	2
133	28° 24' 43"E	36° 56' 09"N	10/30/2000	7:37 PM	4.1	9.5	2
134	28° 44' 16"E	36° 11' 09"N	10/18/2000	10:55 PM	4.4	25.3	4
135	29° 17' 27"E	37° 46' 33"N	4/21/2000	12:29 PM	4	10	2
136	28° 01' 58"E	36° 32' 52"N	12/26/1999	3:37 AM	4.1	89	2
137	28° 07' 37"E	36° 47' 02"N	10/5/1999	1:4 AM	4.2	6.3	2
138	28° 13' 33"E	36° 44' 20"N	10/5/1999	12:53 AM	5.2	19	4
139	29° 13' 30"E	36° 29' 52"N	8/2/1999	4:58 PM	4.3	47.1	2
140	28° 47' 34"E	37° 07' 19"N	3/29/1999	4:5 AM	4.2	21.9	4
141	28° 24' 36"E	35° 58' 58"N	3/9/1998	11:21 AM	5.1	60.3	4
142	28° 13' 15"E	36° 19' 48"N	2/24/1998	3:11 PM	4.5	31.5	4
143	28° 27' 03"E	36° 17' 16"N	2/13/1998	7:18 AM	4.8	72.6	4
144	27° 54' 28"E	36° 25' 15"N	4/26/1996	7:1 AM	5.4	72.3	4
145	28° 19' 27"E	36° 25' 18"N	2/2/1996	11:3 PM	4	33.1	2
146	28° 09' 05"E	36° 30' 38"N	10/30/1995	3:45 PM	4.1	17.8	2
147	29° 22' 30"E	36° 37' 57"N	9/28/1995	1:16 AM	4.4	22.3	2
148	28° 37' 22"E	36° 23' 55"N	6/30/1995	5:34 AM	4.1	56.2	2
149	28° 32' 52"E	35° 59' 56"N	5/27/1995	9:35 PM	4.2	77.4	2
150	28° 21' 15"E	36° 03' 03"N	4/19/1995	1:4 AM	4	86	2
151	27° 53' 52"E	36° 24' 03"N	4/2/1995	6:35 PM	4.4	75.9	4
152	28° 57' 36"E	36° 54' 09"N	2/27/1995	4:12 AM	4	13	2
153	28° 58' 03"E	36° 52' 25"N	1/23/1995	8:37 AM	4	15	2
154	29° 01' 08"E	36° 53' 49"N	1/22/1995	7:46 PM	4.3	16.2	2
155	28° 58' 09"E	36° 57' 09"N	11/13/1994	11:38 AM	4.1	4.1	2
156	29° 05' 42"E	36° 59' 06"N	11/13/1994	8:15 AM	4.8	41.4	4

Table A-1 (continued)

157	29° 01' 30"E	37° 00' 07"N	11/13/1994	7:58 AM	4.9	44	4
158	29° 02' 27"E	36° 53' 38"N	11/13/1994	7:13 AM	4.5	48	4
159	29° 03' 10"E	36° 57' 18"N	11/13/1994	6:56 AM	5.3	20	4
160	29° 07' 37"E	37° 00' 43"N	11/9/1994	5:9 AM	4.3	30	4
161	28° 57' 36"E	37° 13' 12"N	4/3/1994	6:56 AM	4.1	5	7
162	28° 03' 43"E	36° 43' 26"N	8/26/1993	10:3 AM	5.2	37	4
163	27° 48' 55"E	36° 15' 32"N	6/1/1993	4:33 PM	4.1	104.8	2
164	27° 56' 27"E	36° 21' 35"N	4/19/1993	4:58 AM	4.3	33.7	2
165	27° 55' 32"E	36° 30' 20"N	4/7/1993	3:22 AM	4.2	106.6	2
166	29° 22' 24"E	37° 14' 49"N	9/30/1992	12:1 AM	4.1	10.1	2
167	28° 01' 12"E	36° 37' 43"N	8/5/1992	2:2 PM	4.3	30	2
168	28° 54' 52"E	37° 09' 24"N	7/29/1992	10:5 PM	4	10	2
169	28° 48' 34"E	36° 58' 08"N	7/29/1992	9:59 PM	4	10	2
170	28° 18' 23"E	36° 42' 17"N	6/29/1992	7:43 PM	4	70.2	2
171	28° 00' 26"E	36° 36' 25"N	6/9/1992	8:6 PM	4	114.5	2
172	28° 18' 16"E	36° 02' 46"N	6/1/1992	3:44 PM	4.2	88.6	2
173	28° 46' 29"E	36° 17' 15"N	4/19/1992	10:12 PM	4	117.7	2
174	28° 18' 28"E	35° 59' 55"N	3/27/1992	2:9 AM	4.1	90.6	2
175	27° 48' 26"E	35° 57' 57"N	3/16/1992	4:2 AM	4.2	10	2
176	29° 33' 34"E	37° 03' 08"N	11/18/1991	1:35 PM	4.2	26.6	2
177	28° 05' 00"E	36° 00' 38"N	11/16/1991	9:48 AM	4	33	2
178	28° 01' 43"E	36° 33' 09"N	8/13/1991	10:1 AM	4.1	91.1	2
179	28° 12' 38"E	36° 19' 23"N	7/30/1991	4:5 AM	4.3	47.7	2
180	29° 13' 48"E	36° 56' 24"N	7/29/1991	5:1 PM	4	10	2
181	29° 42' 57"E	37° 17' 06"N	7/27/1991	3:4 PM	4	27.8	2
182	29° 44' 16"E	37° 17' 52"N	7/27/1991	2:43 PM	4.2	1.1	2
183	29° 43' 33"E	37° 16' 04"N	7/27/1991	11:38 AM	4.6	36.8	4
184	28° 28' 14"E	36° 24' 45"N	6/2/1991	3:11 AM	4.2	14.3	2

Table A-1 (continued)

185	27° 50' 48"E	36° 06' 10"N	3/28/1991	2:49 AM	4	95.6	2
186	28° 50' 06"E	36° 58' 55"N	1/25/1991	9:3 AM	4.3	2.3	2
187	29° 29' 12"E	37° 05' 54"N	1/16/1991	5:8 PM	4	14	2
188	29° 28' 51"E	37° 07' 15"N	1/15/1991	9:1 PM	5.3	1	2
189	29° 33' 06"E	37° 07' 05"N	1/13/1991	5:11 AM	4.9	6.5	2
190	29° 30' 44"E	37° 03' 16"N	1/10/1991	10:55 PM	4.1	28.5	2
191	27° 47' 48"E	36° 08' 14"N	12/13/1990	12:57 AM	4	71.9	2
192	29° 36' 02"E	37° 01' 36"N	11/21/1990	2:2 PM	5	19	2
193	29° 02' 49"E	36° 47' 32"N	11/19/1990	9:36 AM	4.2	6.4	2
194	29° 50' 02"E	37° 06' 10"N	10/28/1990	5:12 PM	4.4	10	6
195	29° 28' 04"E	37° 01' 59"N	10/4/1990	4: PM	4	40.2	2
196	28° 13' 22"E	36° 26' 47"N	9/29/1990	4:28 PM	4.1	76.6	2
197	29° 31' 20"E	37° 08' 21"N	9/8/1990	9:1 PM	4.7	10	2
198	29° 36' 19"E	37° 04' 31"N	9/3/1990	7:56 AM	4.1	18.7	2
199	29° 32' 01"E	37° 02' 27"N	9/3/1990	12:4 AM	4.2	19.7	2
200	29° 25' 33"E	37° 04' 52"N	9/2/1990	4:2 AM	4	10	2
201	28° 04' 26"E	35° 58' 44"N	8/25/1990	2:58 PM	4.8	57.2	4
202	29° 35' 09"E	36° 59' 53"N	8/20/1990	10:55 PM	4.4	35.6	2
203	29° 36' 38"E	37° 03' 43"N	8/17/1990	11:49 PM	4	10	2
204	29° 33' 28"E	37° 01' 39"N	8/7/1990	1:9 PM	4	13.2	2
205	29° 31' 46"E	37° 00' 06"N	8/2/1990	7:12 PM	4	13.3	2
206	29° 29' 00"E	37° 04' 40"N	8/1/1990	7:17 AM	4.1	4.6	2
207	29° 32' 38"E	37° 03' 26"N	7/18/1990	2:56 PM	4.2	19.7	2
208	29° 31' 51"E	37° 01' 33"N	7/18/1990	11:29 AM	5.5	40.4	4
209	29° 13' 58"E	37° 19' 39"N	6/26/1990	4:48 AM	4.2	19.1	2
210	28° 38' 25"E	36° 53' 39"N	5/25/1990	10:22 PM	4.2	10	2
211	28° 00' 46"E	36° 43' 21"N	7/8/1989	5:45 AM	4.1	65.7	2
212	29° 17' 14"E	37° 47' 34"N	6/4/1989	4:49 AM	4.1	10	2

Table A-1 (continued)

213	28° 05' 25"E	36° 13' 08"N	5/8/1989	5:54 PM	4	81	2
214	29° 14' 15"E	37° 43' 44"N	2/24/1989	12:3 PM	4.5	22.7	2
215	29° 15' 47"E	37° 43' 04"N	2/24/1989	1:17 AM	4.4	19.3	2
216	29° 18' 50"E	37° 42' 32"N	2/24/1989	12:4 AM	5.3	14.4	4
217	28° 08' 47"E	36° 06' 03"N	10/29/1988	4:13 AM	4.7	4.1	2
218	28° 20' 50"E	36° 43' 23"N	10/23/1988	5:21 PM	4.2	111	2
219	28° 07' 24"E	36° 02' 39"N	5/24/1988	2:16 PM	4.2	7	2
220	29° 38' 32"E	36° 55' 28"N	5/6/1988	12:18 PM	4.4	24.2	2
221	28° 13' 25"E	36° 17' 11"N	1/30/1988	7:1 PM	4.5	1	2
222	28° 17' 05"E	36° 46' 55"N	12/12/1987	6:24 PM	4.3	77.8	2
223	28° 19' 33"E	36° 11' 31"N	10/27/1987	2:48 PM	4.6	6	2
224	28° 12' 32"E	36° 22' 47"N	10/25/1987	4:19 PM	4.5	18.2	2
225	28° 10' 28"E	36° 16' 48"N	10/25/1987	2:4 PM	4.2	8.1	2
226	28° 20' 38"E	36° 19' 33"N	10/25/1987	1:2 PM	4.6	34.9	4
227	28° 18' 03"E	36° 15' 47"N	10/12/1987	2:44 AM	4.6	10	2
228	28° 18' 34"E	36° 14' 25"N	10/9/1987	12:9 PM	4.6	8	2
229	28° 21' 06"E	36° 16' 30"N	10/9/1987	11:22 AM	4.4	10	2
230	28° 19' 43"E	36° 17' 04"N	10/6/1987	9:25 PM	4.7	14	2
231	28° 14' 40"E	36° 16' 40"N	10/6/1987	8:45 PM	4.5	20.3	2
232	28° 15' 21"E	36° 15' 11"N	10/6/1987	12:7 PM	4.5	36	2
233	28° 07' 22"E	36° 26' 15"N	10/6/1987	11:31 AM	4.4	4.1	2
234	28° 19' 12"E	36° 15' 46"N	10/6/1987	11:28 AM	4.6	32.8	4
235	28° 16' 22"E	36° 18' 32"N	10/5/1987	9:27 AM	5.1	42.1	4
236	28° 14' 18"E	36° 08' 55"N	7/18/1987	2:3 PM	4.2	51.2	2
237	28° 09' 32"E	36° 46' 37"N	6/19/1987	6:45 PM	5.3	76.1	4
238	28° 22' 26"E	36° 54' 00"N	4/4/1987	3:59 PM	4.6	18.5	4
239	28° 07' 03"E	36° 04' 52"N	2/1/1987	7:42 PM	4.4	25.1	2
240	28° 01' 14"E	36° 13' 26"N	2/1/1987	6:2 PM	4.1	10	2

Table A-1 (continued)

241	27° 53' 36"E	36° 18' 48"N	2/1/1987	4:48 PM	4.1	10	2
242	28° 01' 22"E	36° 15' 51"N	2/1/1987	4:27 AM	4.1	1	2
243	28° 00' 18"E	36° 14' 24"N	2/1/1987	1:43 AM	4	6	2
244	28° 08' 24"E	36° 09' 41"N	1/31/1987	4:6 PM	4.3	17.4	2
245	28° 06' 24"E	36° 10' 04"N	1/7/1987	8:3 PM	4.2	35.2	2
246	28° 07' 19"E	36° 09' 02"N	1/6/1987	7:54 AM	4.4	15.5	2
247	28° 02' 04"E	36° 11' 38"N	1/6/1987	6:55 AM	4.3	6.8	2
248	27° 59' 08"E	36° 14' 51"N	1/1/1987	10:36 PM	4.1	10	2
249	28° 29' 29"E	35° 54' 23"N	1/31/1986	11:28 PM	4.2	10	2
250	28° 53' 49"E	36° 59' 34"N	12/6/1985	10:35 PM	4.6	7.8	4
251	28° 50' 02"E	36° 22' 55"N	9/11/1985	11:8 AM	4.6	56.5	4
252	28° 47' 29"E	37° 14' 03"N	8/23/1985	8:38 PM	4.5	11	2
253	27° 55' 36"E	36° 11' 18"N	7/8/1985	7: AM	4.2	34.9	2
254	27° 54' 01"E	36° 11' 43"N	6/5/1985	8:48 AM	4.3	43.9	2
255	28° 47' 24"E	36° 11' 13"N	5/20/1985	10:33 AM	4.8	50.3	4
256	28° 24' 05"E	35° 55' 28"N	10/16/1984	3:18 AM	4	10	2
257	28° 49' 46"E	36° 28' 27"N	7/31/1984	12:44 PM	4.1	5	2
258	28° 43' 17"E	37° 13' 33"N	6/7/1984	11:37 PM	4.3	10	2
259	28° 04' 20"E	35° 58' 21"N	4/20/1984	2:21 PM	4.6	84.6	2
260	28° 38' 08"E	36° 26' 27"N	2/29/1984	2:7 PM	4.3	13	2
261	28° 34' 45"E	36° 03' 26"N	2/22/1984	7:52 AM	4.1	10	2
262	28° 21' 04"E	36° 05' 38"N	2/11/1984	4:15 PM	4	76.3	2
263	28° 40' 40"E	37° 14' 02"N	2/5/1984	12:2 AM	5	32.5	4
264	28° 49' 12"E	36° 52' 25"N	11/18/1983	7:13 AM	4.5	15	2
265	28° 26' 18"E	36° 26' 07"N	6/14/1983	3:55 AM	4.1	93.5	2
266	28° 47' 27"E	37° 06' 33"N	5/28/1983	3:27 PM	4.1	10	2
267	28° 11' 12"E	36° 53' 18"N	5/24/1983	7:39 AM	4.1	11.2	2
268	28° 04' 35"E	36° 09' 21"N	5/16/1983	9:7 AM	4.1	5	2

Table A-1 (continued)

269	29° 21' 13"E	37° 06' 47"N	3/24/1983	10:55 AM	4.6	10	2
270	29° 14' 21"E	37° 00' 48"N	3/22/1983	11:19 AM	4.4	10	2
271	29° 31' 45"E	37° 27' 10"N	11/23/1982	11:49 AM	4.5	17.1	2
272	28° 51' 44"E	36° 55' 56"N	5/11/1982	10:25 AM	4.2	12	2
273	29° 46' 47"E	37° 04' 27"N	11/23/1981	10:56 AM	4.6	20.7	2
274	29° 32' 39"E	37° 17' 43"N	8/15/1981	5:46 AM	4.2	10	2
275	28° 52' 02"E	36° 13' 10"N	6/8/1981	9:6 PM	4.1	68.3	2
276	29° 00' 29"E	37° 29' 44"N	5/28/1981	9:4 PM	4.2	10	2
277	28° 08' 42"E	36° 43' 12"N	5/11/1981	7:15 PM	4.7	15.2	4
278	28° 36' 08"E	36° 54' 12"N	1/3/1981	6:1 AM	4.8	10	2
279	28° 44' 58"E	36° 53' 42"N	11/11/1980	1:45 AM	4.1	1.2	2
280	28° 49' 16"E	36° 53' 53"N	11/11/1980	1:22 AM	4.9	10	2
281	28° 48' 00"E	37° 00' 00"N	10/4/1980	3:12 PM	5.1	26	9
282	27° 46' 19"E	36° 03' 45"N	6/11/1980	5:16 PM	4.3	108	2
283	28° 43' 51"E	37° 04' 01"N	4/29/1980	9:19 PM	4.4	31.7	2
284	28° 14' 16"E	36° 00' 39"N	3/29/1980	3:58 AM	4.5	69.6	4
285	29° 02' 02"E	36° 48' 00"N	6/22/1979	10:34 AM	4.1	10.5	2
286	28° 22' 51"E	36° 35' 51"N	12/22/1978	3:53 AM	4.2	12.3	2
287	29° 16' 48"E	36° 54' 36"N	9/18/1978	5:34 PM	4	29	2
288	28° 59' 24"E	37° 13' 12"N	4/3/1978	3:44 PM	4.9	10	2
289	28° 51' 36"E	37° 28' 48"N	1/11/1978	3:57 AM	5	5	9
290	27° 45' 18"E	36° 02' 20"N	11/28/1977	2:59 AM	5.4	79.1	4
291	28° 54' 36"E	36° 59' 24"N	6/13/1977	8:59 AM	4	10	2
292	28° 50' 24"E	36° 13' 48"N	6/8/1977	4:49 AM	4	64	2
293	28° 32' 21"E	36° 32' 26"N	3/8/1977	3:1 AM	4.1	64.8	2
294	27° 51' 45"E	36° 25' 32"N	12/8/1975	11:3 PM	4.3	4.8	2
295	28° 08' 20"E	36° 19' 12"N	11/12/1975	9:3 AM	4.8	61.7	4
296	28° 13' 36"E	36° 44' 21"N	5/31/1975	12:41 PM	4.1	34.3	2

Table A-1 (continued)

297	29° 10' 44"E	37° 44' 51"N	12/29/1974	6:45 PM	4.1	10	2
298	28° 28' 51"E	36° 38' 02"N	7/9/1974	2:32 AM	4.9	53.8	4
299	29° 13' 02"E	36° 43' 30"N	5/24/1974	9:27 PM	4.4	36.9	2
300	29° 34' 40"E	37° 16' 16"N	3/24/1974	7:9 AM	4.1	7.8	2
301	29° 40' 35"E	37° 19' 50"N	2/5/1974	6:23 PM	4.5	4.9	2
302	29° 36' 00"E	37° 15' 00"N	1/26/1974	5:49 AM	4	34	2
303	29° 45' 07"E	37° 19' 17"N	12/8/1973	7:4 PM	4.4	17.3	2
304	28° 40' 06"E	36° 17' 42"N	11/30/1973	6:47 AM	4.5	25	2
305	29° 03' 05"E	37° 22' 15"N	10/30/1973	7:4 PM	4.3	19	2
306	29° 25' 36"E	37° 34' 58"N	9/21/1973	5:2 AM	4.3	10	2
307	28° 33' 43"E	37° 07' 04"N	7/29/1973	3:1 PM	4	18	2
308	28° 25' 12"E	36° 12' 00"N	6/9/1973	7:9 PM	4	63	2
309	27° 46' 25"E	36° 11' 19"N	12/24/1972	3:39 AM	4.3	35	2
310	29° 08' 37"E	37° 00' 01"N	8/29/1972	2:48 AM	4.4	10	2
311	28° 46' 46"E	36° 52' 25"N	7/30/1972	8:8 PM	4.1	10	2
312	29° 38' 47"E	37° 24' 31"N	1/22/1972	5:17 PM	4.4	9.7	2
313	28° 28' 19"E	36° 37' 40"N	10/16/1971	9:45 AM	4.8	59.3	4
314	28° 47' 29"E	36° 48' 41"N	9/3/1971	1:17 PM	4.6	10	2
315	28° 53' 57"E	36° 52' 26"N	7/30/1971	1:7 PM	4.2	10	2
316	29° 23' 31"E	36° 47' 35"N	7/8/1971	6:35 AM	4	40.4	2
317	29° 38' 12"E	37° 09' 42"N	6/19/1971	12:27 AM	4.7	33.7	2
318	29° 02' 31"E	37° 01' 31"N	6/15/1971	10:55 PM	4.7	2.7	2
319	29° 34' 58"E	37° 26' 11"N	5/16/1971	12:5 PM	4.2	4.3	2
320	29° 36' 36"E	37° 27' 18"N	5/14/1971	10:51 PM	4.6	16.4	4
321	29° 34' 04"E	37° 29' 44"N	5/12/1971	5:48 PM	4.4	48.9	2
322	29° 05' 36"E	37° 03' 22"N	2/25/1971	4:46 AM	4.4	8.5	2
323	28° 59' 49"E	37° 02' 49"N	2/24/1971	2:14 AM	4.5	12.2	2
324	28° 17' 23"E	36° 03' 36"N	2/7/1971	4:59 AM	4.7	25.2	2

Table A-1 (continued)

325	28° 59' 33"E	37° 04' 39"N	1/3/1971	12:46 PM	4.4	25.9	2
326	29° 02' 09"E	37° 03' 54"N	1/2/1971	3:25 AM	4.4	6.6	2
327	29° 00' 00"E	37° 06' 36"N	12/31/1970	10:29 AM	4.4	38	2
328	28° 56' 24"E	36° 57' 36"N	12/30/1970	6:54 PM	5.1	23	2
329	28° 20' 24"E	36° 03' 00"N	12/30/1970	11:32 AM	4.2	36	2
330	28° 20' 24"E	36° 01' 48"N	12/29/1970	9:3 PM	4.6	26	2
331	28° 15' 00"E	35° 58' 48"N	12/29/1970	8:34 PM	4.3	16	2
332	28° 12' 00"E	35° 57' 00"N	12/28/1970	5:48 PM	4.2	33	2
333	28° 12' 36"E	35° 55' 12"N	12/28/1970	5: PM	4.6	28	2
334	28° 54' 36"E	37° 05' 24"N	12/28/1970	12:43 PM	4.4	23	2
335	29° 01' 12"E	37° 03' 36"N	12/28/1970	3:42 AM	4.4	7	2
336	28° 55' 12"E	36° 52' 48"N	11/21/1970	2:13 AM	4.5	10	2
337	28° 14' 24"E	35° 59' 24"N	11/11/1970	8:58 PM	5.1	35	9
338	28° 48' 00"E	36° 51' 36"N	10/24/1970	7:34 PM	4.1	28	2
339	29° 00' 36"E	37° 00' 36"N	10/19/1970	1:32 AM	4.6	11	2
340	28° 35' 24"E	37° 05' 24"N	9/28/1970	7:54 PM	4.6	24	2
341	28° 11' 24"E	36° 16' 12"N	6/16/1970	9:46 AM	4	33	2
342	28° 39' 50"E	36° 46' 30"N	4/24/1970	2:37 PM	4.6	39.5	4
343	28° 21' 36"E	36° 01' 48"N	3/27/1970	11:47 PM	4.5	10	2
344	28° 48' 00"E	36° 48' 00"N	3/2/1970	6:57 AM	4.6	49	2
345	29° 06' 00"E	36° 54' 00"N	3/1/1970	12:54 PM	4.5	10	2
346	27° 56' 24"E	36° 22' 12"N	2/24/1970	1:44 AM	4.2	102	2
347	28° 30' 00"E	37° 00' 00"N	1/26/1970	5:29 AM	5.1	10	2
348	28° 25' 12"E	36° 39' 36"N	12/21/1969	10:1 PM	4.6	69	2
349	29° 26' 24"E	37° 16' 12"N	11/15/1969	5:5 AM	4.8	45	2
350	28° 00' 36"E	36° 34' 12"N	9/22/1969	8:17 AM	4.6	86	2
351	28° 16' 26"E	36° 45' 07"N	9/6/1969	8:3 PM	5	68.3	4
352	29° 00' 00"E	37° 00' 00"N	8/3/1969	8:28 AM	4.1	57	2

Table A-1 (continued)

353	28° 10' 51"E	36° 30' 36"N	4/27/1969	10:58 AM	4.7	35.3	4
354	28° 30' 00"E	36° 42' 36"N	4/26/1969	8:25 AM	4.3	13	2
355	28° 39' 54"E	36° 21' 25"N	4/24/1969	2:45 PM	4.7	54.8	4
356	28° 16' 12"E	36° 13' 12"N	4/21/1969	8:57 PM	4.6	11	2
357	28° 36' 00"E	36° 36' 00"N	3/24/1969	12:44 PM	4.6	10	2
358	29° 30' 00"E	37° 18' 00"N	1/26/1969	6:56 AM	4.3	53	2
359	29° 13' 12"E	36° 41' 24"N	11/16/1968	11:25 PM	4	10	2
360	28° 12' 00"E	36° 36' 00"N	10/16/1968	2:47 PM	4	41	2
361	29° 12' 00"E	36° 30' 00"N	10/10/1968	5:16 AM	4.5	10	2
362	29° 01' 48"E	36° 46' 12"N	7/4/1968	2:27 AM	4.4	94	2
363	29° 40' 12"E	37° 16' 12"N	3/13/1968	2:26 AM	4.4	10	2
364	27° 54' 00"E	36° 18' 00"N	1/13/1968	10:46 PM	4.4	71	2
365	29° 06' 43"E	37° 15' 00"N	10/26/1967	4:55 AM	5	49.3	4
366	29° 19' 48"E	36° 43' 12"N	9/5/1967	8:31 AM	4.5	24	2
367	28° 24' 00"E	36° 58' 48"N	8/9/1967	12:33 AM	4.8	64	2
368	29° 19' 12"E	36° 46' 48"N	6/18/1967	5:28 AM	4.9	35	2
369	29° 18' 00"E	36° 53' 24"N	6/2/1967	12:5 AM	4.3	10	2
370	29° 19' 51"E	36° 49' 30"N	6/1/1967	10:39 AM	5	39.9	4
371	29° 16' 12"E	36° 40' 48"N	4/4/1967	4:39 AM	4.9	24	2
372	27° 49' 48"E	36° 08' 24"N	10/13/1966	1:23 AM	4.5	7	2
373	29° 16' 48"E	37° 28' 12"N	8/16/1966	9:1 PM	4.4	79	2
374	28° 04' 40"E	36° 18' 03"N	2/8/1966	1:16 PM	4.5	84	4
375	29° 19' 12"E	37° 36' 36"N	12/2/1965	6:45 AM	4.7	38	2
376	29° 21' 00"E	37° 37' 12"N	7/12/1965	9:51 AM	4.6	50	2
377	29° 21' 10"E	37° 44' 20"N	6/17/1965	2:58 AM	4.7	40.9	4
378	29° 18' 50"E	37° 46' 40"N	6/13/1965	8:1 PM	5.1	36.6	4
379	28° 17' 24"E	36° 56' 24"N	10/13/1964	10:3 AM	4.5	76	2
380	29° 12' 00"E	36° 42' 00"N	9/28/1964	9: PM	4.4	63	2

Table A-1 (continued)

381	28° 15' 36"E	36° 15' 36"N	6/8/1964	4:49 PM	4.6	62	2
382	28° 12' 36"E	36° 16' 48"N	5/13/1964	5:6 PM	4.5	82	2
383	28° 46' 48"E	36° 25' 48"N	3/31/1964	9:33 AM	4.8	57	2
384	28° 54' 00"E	36° 24' 00"N	1/29/1964	10:28 PM	4.7	70	2
385	29° 40' 48"E	37° 04' 12"N	11/22/1963	8:26 PM	4.7	60	9
386	29° 00' 00"E	36° 30' 00"N	9/29/1963	1:35 PM	4.5	60	8
387	28° 45' 36"E	36° 50' 24"N	7/26/1963	7:46 PM	5.1	80	9
388	27° 52' 48"E	36° 28' 48"N	7/8/1963	4:2 PM	4.7	80	9
389	28° 29' 24"E	36° 42' 00"N	5/23/1961	2:45 AM	6.3	70	9
390	28° 36' 36"E	36° 53' 24"N	1/26/1960	1:13 PM	4.6	30	9
391	28° 55' 48"E	37° 00' 00"N	1/26/1960	1:5 PM	5.2	72	9
392	28° 54' 00"E	37° 04' 12"N	1/9/1960	3:58 AM	4.9	49	9
393	29° 04' 12"E	36° 54' 36"N	12/8/1959	9:35 AM	5	70	9
394	29° 04' 48"E	36° 48' 36"N	6/9/1959	11:21 AM	4.7	20	9
395	28° 36' 00"E	36° 55' 12"N	4/25/1959	1:5 AM	5.3	40	9
396	28° 34' 48"E	36° 56' 24"N	4/25/1959	12:26 AM	5.9	30	9
397	29° 00' 00"E	36° 42' 00"N	1/26/1959	4:15 PM	4.5	30	9
398	29° 01' 12"E	36° 46' 48"N	1/26/1959	11:38 AM	5	47	9
399	28° 42' 00"E	36° 42' 00"N	1/20/1959	8:4 PM	4.8	30	9
400	29° 07' 12"E	36° 38' 24"N	1/11/1959	4:27 AM	4.7	50	9
401	29° 12' 36"E	36° 42' 36"N	1/7/1959	10:22 PM	4.8	40	9
402	29° 06' 36"E	36° 39' 36"N	1/6/1959	2:28 PM	4.8	30	9
403	29° 09' 36"E	36° 51' 00"N	1/6/1959	4:6 AM	4.5	20	9
404	28° 09' 36"E	36° 33' 36"N	12/9/1958	8:54 AM	4.5	50	9
405	27° 51' 00"E	36° 20' 24"N	3/4/1958	11:32 AM	5.2	120	9
406	28° 48' 00"E	36° 24' 36"N	4/26/1957	4:9 PM	4.7	10	9
407	28° 52' 12"E	36° 13' 12"N	4/26/1957	6:33 AM	5.9	50	9
408	28° 36' 00"E	36° 07' 12"N	4/25/1957	7:52 AM	5	10	9

Table A-1 (continued)

409	28° 40' 48"E	36° 25' 12"N	4/25/1957	2:25 AM	7.1	80	10
410	28° 37' 48"E	36° 25' 48"N	4/24/1957	7:1 PM	6.8	80	10
411	28° 52' 48"E	36° 22' 12"N	2/5/1957	5:2 PM	5.2	60	9
412	28° 37' 48"E	36° 59' 24"N	5/5/1956	8:42 PM	4.7	40	9
413	29° 31' 48"E	37° 16' 12"N	4/8/1954	4:18 AM	4.8	10	9
414	28° 00' 00"E	36° 00' 00"N	1/12/1953	9:31 AM	4.8	30	9
415	29° 34' 48"E	36° 54' 00"N	9/23/1952	8:3 PM	4.8	10	9
416	28° 50' 24"E	36° 31' 48"N	6/4/1950	2:11 PM	4.8	30	9
417	28° 21' 36"E	36° 33' 00"N	11/20/1943	10:1 AM	5.5	35	9
418	28° 50' 24"E	36° 48' 36"N	11/15/1943	11:43 AM	5.2	83	9
419	27° 56' 24"E	36° 27' 00"N	10/16/1943	1:8 PM	5.8	120	9
420	29° 26' 24"E	37° 26' 24"N	8/12/1936	10:24 PM	5	130	9
421	28° 49' 12"E	37° 21' 36"N	8/17/1933	6:24 AM	4.5	10	9
422	28° 00' 00"E	36° 00' 00"N	6/27/1926	2:13 AM	4.9	10	9
423	29° 24' 00"E	37° 00' 00"N	3/3/1926	6:58 AM	5	10	9
424	29° 25' 48"E	37° 01' 48"N	3/1/1926	8:2 PM	6.1	50	10
425	29° 10' 12"E	37° 33' 36"N	9/1/1925	8:16 AM	5.4	130	9
426	29° 00' 00"E	37° 30' 00"N	12/6/1922	2:1 PM	5.2	15	9
427	29° 00' 00"E	37° 30' 00"N	11/20/1922	4:24 AM	4.9	10	9
428	28° 00' 00"E	36° 00' 00"N	8/17/1922	3:3 PM	5	15	9
429	28° 39' 00"E	36° 29' 24"N	6/3/1922	4:14 AM	4.9	10	9
430	28° 42' 00"E	37° 00' 00"N	5/22/1921	9:23 PM	5.1	32	9
431	28° 00' 00"E	36° 00' 00"N	1/27/1921	11:3 AM	5.4	15	9
432	29° 00' 00"E	37° 30' 00"N	7/4/1920	8:45 PM	5.2	15	9
433	29° 00' 00"E	37° 30' 00"N	7/4/1920	12:17 PM	5	15	9
434	28° 42' 00"E	37° 00' 00"N	5/1/1920	6:34 AM	5	30	9
435	28° 00' 00"E	36° 00' 00"N	8/24/1919	6:16 PM	5.4	15	9
436	28° 00' 00"E	36° 00' 00"N	7/20/1919	12:3 AM	4.8	10	9

Table A-1 (continued)

437	28° 00' 00"E	36° 00' 00"N	7/18/1919	7:1 AM	5.2	15	9
438	28° 00' 00"E	36° 00' 00"N	6/13/1917	12:15 PM	4.6	10	9
439	28° 28' 12"E	36° 54' 00"N	11/25/1906	12: AM	4.6	10	11
440	28° 54' 00"E	36° 30' 00"N	12/5/1905	5:13 PM	5.2	10	11
References are:1, AFAD-DDH; 2, ISC; 3, KRDEA-ISK; 4, EHB; 5, EMSC-CSEM; 6, NISC; 7, ETH; 8, BCIS; 9, Ayhan et al., 1981; 10 Alsan et al., 1975; 11 Ambressey-Finkel, 1987							

APPENDIX B

EQUIPMENT LIST AND PARAMETERS USED IN SEISMIC SURVEY

Table B-1 The equipment list were used during seismic data collection.

SIG2Mille sparker seismic power supply
17 m long streamer
Sparker-electrodes 500 to 1000 joules
Triton SBlogger seismic recording system
NaviPac integrated navigation system
Crescent A100 standard GPS receiver

Table B-2 The parameters were used during seismic data collection.

Seismic System	SIG2Mille sparker
Output Voltage	3.2 kV
Power	500 J
Ship Speed (nautical miles per hour)	4 knot
Length of streamer	17 m
Number of hydrophone	12
Inline offset	0 m
X-line offset	5 m
Setback Distance	20 m
Recorder	Triton SBlogger
Seismic Data Format	32 Bit SegY
Shotpoint Interval	1000 ms
Record Length	1000 ms
Sampling Interval	0.25 ms
Sample/Trace	4000

Table B-3 Location length and azimuth of seismic lines.

Line ID	Starting Point		Ending Point		Length (m)	Azimuth (degree)
	x	y	x	y		
FT14-01a	684683.47	4055358.08	682828.80	4055878.51	1926.30	278
FT14-01b	682732.82	4055905.76	672504.22	4058851.76	10644.40	286
FT14-02	671699.05	4057569.02	680404.88	4053311.48	9691.14	117
FT14-03	669890.70	4055661.39	680256.23	4051950.19	11009.87	113
FT14-04	672676.82	4052446.82	668293.31	4054569.57	4870.44	298
FT14-09	686557.27	4058845.41	671150.69	4065971.93	16974.99	297
FT14-10	672423.28	4066645.74	667571.71	4058841.40	9272.51	207
FT14-12	669245.65	4057778.12	665607.46	4058967.73	3827.75	290
FT14-13	666720.27	4060708.88	669450.64	4058041.45	3817.08	130
FT14-14	670378.03	4060307.62	666579.49	4060810.99	3831.77	287
FT14-15	666775.52	4062783.30	670502.35	4060574.55	4332.18	125
FT14-16a	684203.28	4057141.53	669947.88	4062483.27	15223.36	293
FT14-16b	669779.79	4062553.84	667864.51	4063136.40	2001.92	285
FT14-17	674074.16	4059838.32	684501.83	4056229.18	11034.59	112
FT14-18	668533.60	4052830.75	677472.35	4064267.69	14515.68	38
FT14-24a	674202.50	4050654.82	672393.52	4051394.54	1954.37	290
FT14-24b	672386.27	4051373.15	667438.99	4053863.98	5538.94	295
FT14-25	667864.21	4053544.04	669398.35	4055509.72	2493.48	40
FT14-26	669602.76	4055126.87	673446.97	4053292.90	4259.27	110
FT14-27	679669.82	4053950.20	686415.43	4059633.36	8825.84	48
FT14-30	681292.52	4062108.88	674835.31	4050434.22	13341.41	210
FT14-31	673918.34	4063029.43	680783.08	4059991.11	7507.07	110
FT14-32	677296.88	4064308.94	673922.38	4063126.08	3575.80	250
FT14-33	683635.60	4061013.90	677615.41	4053689.21	9481.24	225
FT14-34	680093.03	4052752.80	670813.31	4056697.71	10083.43	294
FT14-35	673674.76	4055026.05	679250.20	4064288.98	10811.45	34
FT14-36	679396.99	4063409.88	675285.22	4064951.34	4392.07	290
FT14-37	675859.13	4066100.16	672962.90	4061075.72	5799.41	210
FT14-38	671955.39	4058314.46	681502.63	4054628.76	10234.56	115
FT14-39	676889.61	4053956.74	679820.70	4055293.07	3569.73	75
FT14-40	680006.70	4054073.77	680228.29	4053304.85	800.22	168
FT14-41	683502.39	4054436.14	683524.25	4056698.43	2263.55	3

APPENDIX C

PALEOSTESS RECONSTRUCTION RESULTS

Table C-1 The locations of fault slip data measurements, number of slickenside were collected from each locations, the orientation of the three principle stress axes and the calculated R ratio as a results of paleostress reconstruction analyses.

ID	Longitude	Latitude	n/nt	σ_1 dip/dip-dir		σ_2 dip/dip-dir		σ_3 dip/dip-dir		R
G1	29.2349186	36.7567406	28/28	58	118	21	0.44	350	23	251
G2	28.9490891	36.8075485	48/48	61	340	28	0.43	142	8	236
G3	29.2333296	36.7647895	33/33	61	351	20	0.48	122	20	220
G4	29.2068293	36.7841033	59/59	63	24	1	0.43	293	27	202
G5	29.2013403	36.7890212	173/173	65	76	13	0.42	316	21	221
G6	29.1965202	36.7845266	109/109	67	358	12	0.45	117	20	212
G7	29.1935792	36.790167	98/98	50	145	38	0.5	300	13	40
G8	29.1843714	36.8016205	61/61	46	76	44	0.47	257	1	167
G9	29.1801044	36.8139723	132/132	75	122	2	0.48	24	15	294
G10	29.1848206	36.8312649	91/91	36	102	54	0.5	295	6	197
G11	29.2221007	36.82318	92/92	64	355	17	0.39	124	19	220
G12	29.1962741	36.8389006	101/101	36	181	54	0.5	355	3	89
G12.1	29.1959896	36.8382912	34/34	31	202	58	0.71	3	9	107
G12a	29.1961994	36.8381615	87/87	23	198	65	0.59	352	10	104
G13	29.1735916	36.8629305	35/35	59	62	31	0.23	237	3	328
G14	29.1767357	36.8523753	18/18	58	54	32	0.4	243	4	150
G15	29.1268792	36.8350827	48/48	58	301	31	0.34	142	9	46
G16	29.0843334	36.8457031	8/8	17	144	69	0.5	2	12	238
G17	29.0171738	36.8653221	31/31	39	47	51	0.48	217	5	313
G17-2	29.0171394	36.8653297	36/36	36	66	52	0.5	264	9	162
G18-1	29.0071621	36.8321114	139/139	69	136	7	0.39	245	19	337

Table C-1 (continued)

G19-1	28.9856949	36.8225517	51/51	66	111	9	0.37	1	23	267
G20	28.9815767	36.8213834	132/132	74	216	14	0.53	66	8	334
G21	28.9674283	36.8052137	31/31	68	269	20	0.23	68	7	161
G22	28.949462	36.8247125	33/33	80	330	10	0.25	134	3	225
G23	28.9020759	36.8665236	102/102	81	194	2	0.41	92	9	2
G24	29.1253072	36.5022569	82/82	87	104	3	0.37	286	0	196
G25	29.1259809	36.5083205	40/40	45	213	44	0.5	47	7	310
G26	29.4060307	36.7717515	158/158	70	179	14	0.57	45	14	311
G26 dextral	29.4060307	36.7717515	23/23	12	54	78	0.5	238	1	145
G26-dext	29.4060307	36.7717515	37/37	22	93	68	0.5	274	0	183
G27	29.3945772	36.7811838	61/61	70	47	15	0.1	271	14	177
G27 dext	29.3945772	36.7811838	31/31	15	139	74	0.5	306	3	48
G27.1	29.3945772	36.7811838	7/7	23	140	66	0.5	335	6	232
G28	29.3565267	36.7848061	98/98	66	93	24	0.32	277	1	187
G29	29.2853461	36.7941117	80/80	71	196	5	0.5	302	18	33
G30	29.2868044	36.7839728	73/73	84	147	5	0.48	349	2	259
G31	29.2836794	36.7941117	121/121	85	183	2	0.56	69	5	338
G32	29.262551	36.79409	57/57	19	56	67	0.5	269	12	150
G33	29.2398424	36.764565	28/28	82	182	6	0.54	44	6	314
G34	29.2107492	36.7394345	134/134	87	239	3	0.43	71	1	341
G35	29.1833254	36.7172784	156/156	83	142	2	0.58	31	6	301
G36	29.0941403	36.6886087	102/102	75	96	15	0.46	272	1	2
G37	29.0858697	36.7163578	71/71	77	99	3	0.5	202	13	293
G38	29.08986	36.7264728	161/161	84	80	3	0.44	202	5	292
G39	29.1136794	36.75432	40/40	70	42	20	0.42	222	0	132
G40	29.114235	36.7563339	73/73	65	254	10	0.39	6	23	100
G41	29.1388878	36.7684867	49/49	57	122	5	0.44	219	32	312
G42	29.1481933	36.7748061	161/161	57	49	33	0.6	232	1	141
G43	29.1678461	36.7902922	39/39	60	320	9	0.42	67	28	162
G44	29.1693044	36.7925839	42/42	11	230	79	0.62	66	3	320
G44.normal	29.1693044	36.7925839	119/119	67	174	5	0.5	277	22	10
G45	29.1761794	36.7965422	124/124	61	124	1	0.3	32	29	301
G46	29.14444	36.82488	34/34	47	58	38	0.48	270	16	167
G47	29.1402767	36.8180006	121/121	70	173	7	0.48	64	19	332
G48	29.13611	36.81682	88/88	62	118	7	0.32	14	26	280
G49	29.1252072	36.8129311	103/103	78	38	9	0.47	263	9	171
G50	29.1105417	36.8040319	91/91	55	59	24	0.33	190	23	291
G51	29.1074696	36.8009595	96/96	22	169	68	0.5	359	4	260
G52	29.1187489	36.7950839	176/176	53	131	30	0.41	352	20	249
G53	29.0620516	36.7319876	82/82	57	86	29	0.47	233	15	332
G54	29.059235	36.7286256	122/122	65	125	24	0.46	321	6	228

Table C-1 (continued)

G55	29.0152636	36.7807346	102/102	71	234	14	0.51	8	13	101
G56	29.0110406	36.7764033	101/101	50	236	27	0.43	3	27	108
G57	28.9794124	36.7707762	35/35	66	178	8	0.5	70	23	337
G58	28.9792882	36.766055	100/100	76	95	4	0.39	349	13	258
G70	28.8794621	36.7508945	31/31	70	92	5	0.38	195	19	287
G71	28.8774409	36.7446063	40/40	63	25	13	0.33	141	23	237
G72	28.8527372	36.7311315	24/24	57	230	9	0.5	335	31	71
G73	28.8579025	36.7248433	35/35	58	108	18	0.5	348	26	249
G74	28.8626187	36.719678	37/37	50	186	37	0.5	341	13	81
G75	28.8689069	36.7088982	21/21	86	138	4	0.64	306	1	36
G76	28.87025	36.70822	52/52	60	162	9	0.37	56	28	322
G77	28.8772163	36.7082245	32/32	33	116	57	0.52	299	2	207
G78	28.8859749	36.7084491	47/47	33	315	56	0.5	122	6	221
G79	28.8594746	36.706877	82/82	81	165	7	0.5	31	7	300
G80	28.8473473	36.7336019	43/43	64	54	16	0.5	179	20	275
G81	28.8354446	36.7443817	18/18	53	59	16	0.43	172	32	272
G82	28.8354446	36.698343	95/95	77	146	8	0.49	17	10	186
G83	28.8367921	36.6927286	39/39	52	95	5	0.58	359	37	265
G84	28.8338726	36.6853175	39/39	58	97	1	0.21	188	332	279
G85	28.8345463	36.6814996	64/64	67	130	13	0.46	7	19	272
G86	28.8484702	36.6666774	18/18	66	312	11	0.47	196	21	102
G87	28.6928371	36.7071016	32/32	86	211	2	0.5	94	4	4
G88	28.6831802	36.7023854	90/90	63	339	4	0.5	241	27	149
G89	28.7752575	36.8339886	44/44	59	85	30	0.55	253	5	346
G90	28.7806474	36.8310691	69/69	68	0	20	0.49	154	9	248
G91	28.8062494	36.8133274	105/105	79	278	10	0.5	81	3	171
G92	28.8161309	36.8045688	82/82	63	82	1	0.28	173	27	264
G93	28.8237666	36.7951365	84/84	59	33	31	0.09	216	1	126
G94	28.8998988	36.7661658	45/45	73	72	15	0.48	281	8	189
G95	29.022968	36.7356231	68/68	48	248	38	0.52	37	16	140
G96	29.0339723	36.7115932	76/76	37	62	53	0.5	247	3	154
G97	29.0344215	36.7127161	100/100	61	305	29	0.43	135	4	43
G98	29.0476716	36.7062033	66/66	59	344	31	0.5	155	4	247
G99	29.0503666	36.7021609	60/60	41	302	49	0.5	125	1	33
G100	29.1247022	36.6192913	32/32	50	353	20	0.4	237	33	133
G101	29.0874221	36.6219862	29/29	87	84	1	0.4	193	3	283
G102	29.0786635	36.6287236	53/53	77	69	9	0.5	295	9	203
G103	29.0813585	36.6320923	58/58	66	142	15	0.51	268	18	3
G104	29.0950578	36.6374822	55/55	47	194	36	0.46	335	20	80
G105	29.0946086	36.6350118	47/47	51	238	31	0.49	18	21	121
G106	29.0955069	36.6318677	44/44	60	122	26	0.45	271	13	7

Table C-1 (continued)

G107	29.1083079	36.6743131	47/47	54	221	11	0.21	327	34	64
G108	29.0887696	36.6105327	62/62	52	70	3	0.49	336	38	244
G109	29.0905662	36.6040199	82/82	60	99	4	0.39	196	30	289
G110	29.0939349	36.6011004	39/39	61	353	8	0.44	98	27	193
G111	29.0548582	36.5640449	76/76	64	9	3	0.5	273	26	181
G112	29.0999985	36.5768459	44/44	67	162	11	0.5	45	20	311
G113	29.1123503	36.575723	34/34	60	211	25	0.41	356	15	93
G114	29.1231301	36.5705577	66/66	75	309	0	0.41	41	15	131
G115	29.1768045	36.5564092	41/41	13	64	71	0.5	290	13	157
G116	29.181745	36.550346	47/47	63	113	24	0.46	322	12	226
G117	29.1330116	36.5622483	134/134	77	229	10	0.47	12	7	104
G118	29.1260496	36.4986925	17/17	75	83	15	0.47	257	2	347
G119	29.1298675	36.5009382	67/67	52	306	9	0.45	204	37	108
G120	29.1260496	36.5155359	72/72	73	124	4	0.51	21	16	290
G121	29.1282954	36.5198029	76/76	35	93	55	0.49	264	4	0
G122	29.126948	36.5422607	48/48	68	107	6	0.5	1	21	269
G123	29.1067359	36.6868895	97/97	61	77	29	0.45	261	2	170
G124	29.0322687	36.7141877	89/89	75	355	3	0.44	96	15	186
G125	29.0227451	36.7339155	82/82	53	359	36	0.47	167	6	261
G127	29.0139848	36.7466275	57/57	81	40	8	0.38	248	4	158
G128	28.9407721	36.7583056	60/60	65	335	22	0.14	123	12	218
G129	28.9423442	36.7610005	63/63	78	261	7	0.72	24	10	115
G130	28.9398738	36.7562844	86/86	71	283	3	0.49	186	19	95
G131	28.9306661	36.7706574	97/97	54	210	13	0.42	318	33	57
G132	28.9344839	36.7677379	60/60	49	146	20	0.49	32	34	287
G133	29.0299299	36.7201272	92/92	57	111	24	0.43	338	21	238
G134	28.9665987	36.7338265	172/172	71	299	14	0.42	163	12	70
G135	28.9648021	36.7288857	135/135	72	302	5	0.67	197	17	105
G136	28.9715394	36.7311315	98/98	41	31	49	0.38	213	1	122
G137	28.9288694	36.7565089	38/38	59	263	1	0.19	355	30	85
G138	28.9259499	36.7529157	133/133	70	257	9	0.44	11	18	104
G139	28.9234795	36.749547	86/86	66	190	21	0.5	340	11	74
G140	28.9093311	36.7641446	73/73	79	259	0	0.27	351	11	81
G141	28.7615582	36.8573448	58/58	75	140	11	0.42	274	11	6
G143	29.1502386	36.6048761	61/61	56	69	20	0.48	192	26	292
S1	28.9281957	36.7358477	40/40	64	321	24	0.46	162	8	69
S2	28.929094	36.7340511	95/95	62	341	27	0.49	180	8	86
S3	28.9255008	36.7342756	148/148	85	232	4	0.3	18	3	108
S4	28.9210092	36.7297841	34/34	84	13	6	0.5	196	0	106
S5	28.9138227	36.722373	74/74	76	300	11	0.23	155	8	63
S6	28.9109031	36.7190043	104/104	67	344	21	0.32	183	7	91

Table C-1 (continued)

S7	29.0878712	36.6794784	76/76	67	250	17	0.34	27	14	122
S8	29.0836042	36.6779064	28/28	77	67	7	0.51	305	10	213
S9	29.0341969	36.6956481	51/51	75	131	15	0.48	303	2	34
S10	29.0337477	36.6972201	67/67	74	346	16	0.48	182	4	91
S11	29.033074	36.6981184	56/56	76	152	12	0.52	304	6	35
S12	29.033074	36.7039575	30/30	88	11	2	0.49	195	0	105
S13	29.0341969	36.705305	88/88	44	44	45	0.29	212	6	308
S14	29.0335232	36.7079999	70/70	70	120	17	0.51	335	10	241
S15	29.0303791	36.7066524	84/84	79	158	1	0.47	63	11	333
S16	29.0299299	36.7059787	104/104	65	267	20	0.49	48	15	143
s17	28.9508782	36.7369706	50/50	86	255	4	0.71	64	1	154
S18	28.9526748	36.7353985	42/42	80	184	10	0.48	16	2	286
S19	28.9537977	36.735174	85/85	84	103	2	0.27	211	6	301
S20	28.9549206	36.7349494	57/57	71	25	9	0.76	266	16	173
S21	28.9580647	36.7322544	89/89	73	179	2	0.51	83	17	353
S22	28.9623317	36.7284366	75/75	48	79	20	0.49	201	31	307
S23	28.96323	36.7248433	63/63	64	69	22	0.27	283	13	187
S24	28.9645775	36.7230467	42/42	51	70	36	0.5	228	11	326
S25	28.9650266	36.7237204	49/49	57	321	19	0.51	85	25	184
S26	28.9895057	36.7169831	47/47	56	24	20	0.5	262	27	162
S27	28.9980397	36.7100211	126/126	83	329	1	0.16	232	7	142
S28	28.9978151	36.7136144	55/55	66	244	20	0.31	29	13	124
S29	29.0169043	36.70261	46/46	84	0	5	0.48	211	3	121
S30	29.0106161	36.6936269	100/100	79	304	11	0.52	114	2	204
S31	29.0070229	36.694076	96/96	79	102	11	0.48	274	2	4
S32	29.0110653	36.6958727	59/59	61	346	27	0.39	190	10	95
S34	29.07934	36.64489	31/31	76	235	13	0.48	37	4	128
S35	29.0775406	36.6457916	36/36	78	81	9	0.53	303	8	212
S36	29.075744	36.6435458	109/109	67	204	12	0.51	85	20	351
S37	29.0368919	36.609859	59/59	39	194	45	0.51	50	19	300
S38	29.050142	36.6561222	40/40	79	15	5	0.45	256	9	165
S39	29.0447521	36.6547747	49/49	53	267	9	0.45	9	35	105
S40	29.0456504	36.6635333	93/93	79	322	7	0.45	90	9	181
S41	29.0418326	36.6610629	57/57	67	122	11	0.55	238	21	332
S42	29.0438538	36.6570205	12/12	69	327	1	0.39	60	21	151
S43	29.0364427	36.6675757	61/61	70	101	20	0.49	281	0	191
S44	29.0344215	36.6671266	38/38	65	24	23	0.31	225	8	132
S45	29.0306036	36.6713936	20/20	45	153	39	0.5	11	20	264
S46	29.0880958	36.6794784	49/49	45	337	40	0.49	190	17	85
S47	29.1083079	36.675436	34/34	42	292	45	0.5	135	12	33
S48	28.9088819	36.7131652	142/142	76	165	1	0.69	261	14	351

Table C-1 (continued)

S49	28.906187	36.7055296	28/28	69	314	20	0.5	116	6	208
S50	28.9010217	36.6987922	54/54	57	221	30	0.5	14	12	111
S51	28.8835045	36.7008134	54/54	59	298	30	0.49	139	10	44
S52	28.8810342	36.7001397	54/54	58	314	22	0.42	84	22	184
S53	28.8675594	36.6868895	24/24	55	265	29	0.49	123	18	22
S54	28.8686823	36.7088982	74/74	67	355	21	0.35	201	9	107
S55	28.882157	36.70261	77/77	65	19	6	0.39	121	24	213
S56	28.8662119	36.6841946	51/51	82	299	7	0.46	153	4	62
S60	28.8005662	36.6751826	37/37	65	178	24	0.48	16	7	283
S61	28.8007908	36.6718139	116/116	68	203	20	0.49	48	8	315
S62	28.8073036	36.6682207	34/34	83	96	1	0.32	192	7	282
S63	28.7947272	36.6585638	39/39	62	172	4	0.48	268	28	0
S64	28.7998925	36.6525001	38/38	3	128	70	0.5	227	20	37
S65	28.802812	36.6558688	124/124	55	289	25	0.37	157	23	56
S65.1	28.803093	36.6558876	55/55	82	302	2	0.5	198	7	107
S65_dex	28.804781	36.6561623	26/26	37	280	50	0.49	128	14	21
S66	28.8037103	36.6560934	61/61	84	238	3	0.5	360	5	90
S67	28.8263928	36.6522756	98/98	58	339	25	0.52	201	19	102
S68	28.9362118	36.7189755	42/42	73	313	11	0.09	182	12	89
S69	28.9377839	36.7192	42/42	80	210	7	0.47	72	7	341
S69.1	28.9386822	36.7189755	59/59	70	85	9	0.35	203	17	296
S70	28.9440721	36.7079711	45/45	75	324	9	0.5	90	12	182
S71	28.9442967	36.7077465	84/84	49	49	40	0.5	224	2	316
S72	28.9337415	36.6960684	155/155	59	202	18	0.59	79	24	341
S74	28.929699	36.6976405	18/18	62	250	12	0.5	2	25	98
S75	28.9337415	36.7007846	61/61	65	132	25	0.55	314	1	224
S76	28.9350889	36.7066236	37/37	86	289	4	0.5	99	1	189
S77	28.9305974	36.7068482	45/45	74	294	10	0	65	12	157
S78	28.9305974	36.7093186	112/112	68	347	4	0.25	86	22	178
S79	28.9400297	36.7194246	30/30	71	214	19	0.47	39	1	308
S80	28.9420509	36.7209967	28/28	76	307	10	0.43	171	9	79
S81	28.9429492	36.7227933	45/45	79	256	8	0.41	32	7	123
S82	28.9445212	36.7250391	50/50	79	97	11	0.36	275	0	5
S83	28.946767	36.7252637	32/32	62	235	27	0.42	44	5	136
S84	28.8784447	36.6438484	23/23	70	206	15	0.62	69	13	335
S85	28.8989317	36.6608096	57/57	86	82	1	0.48	183	4	273
S86	28.8935418	36.6688944	36/36	56	315	34	0.51	131	2	222

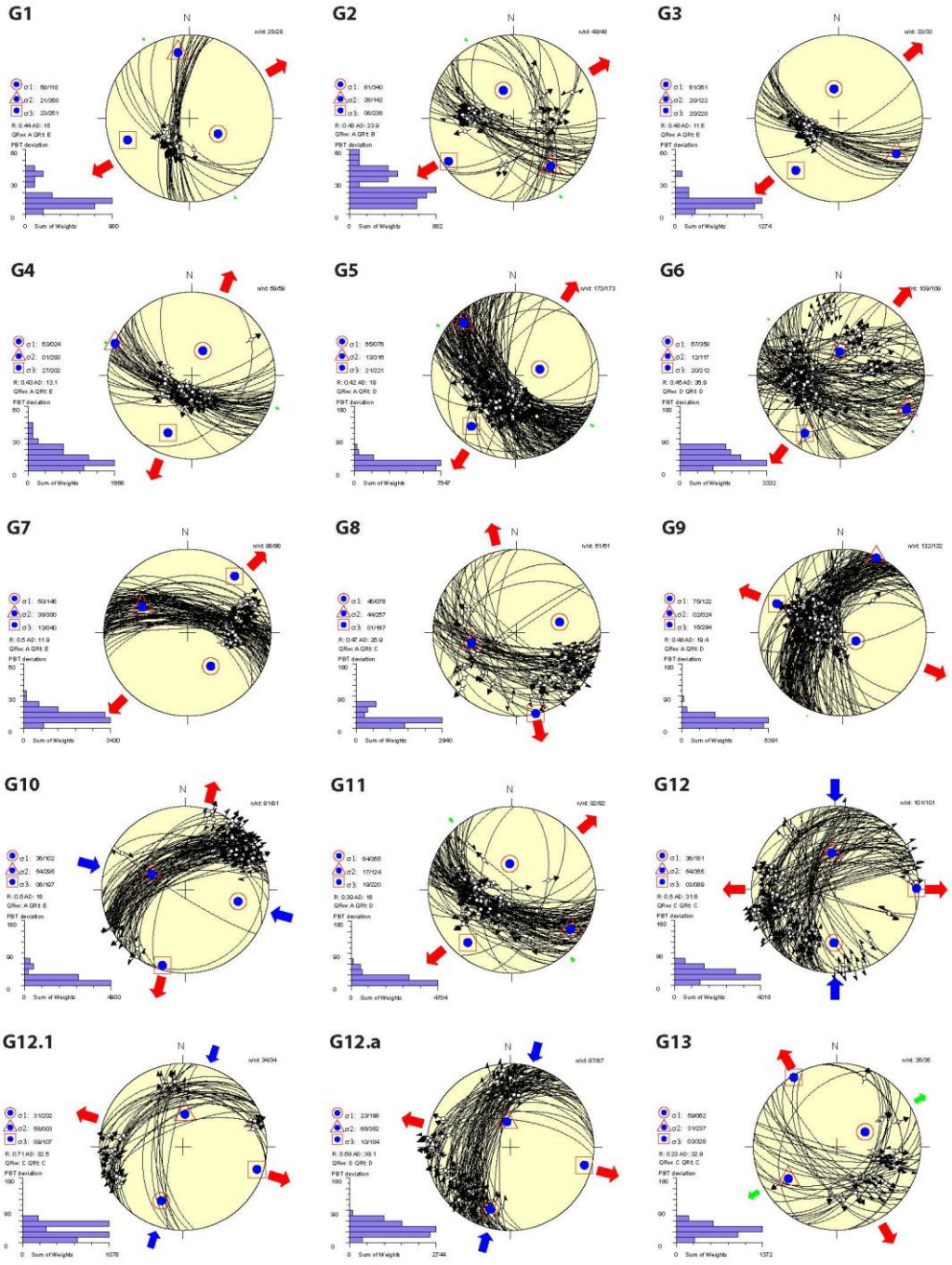
G1
G2
G3
G4
G5
G6
G7
G8
G9
G10
G11
G12
G12.1
G12.a
G13

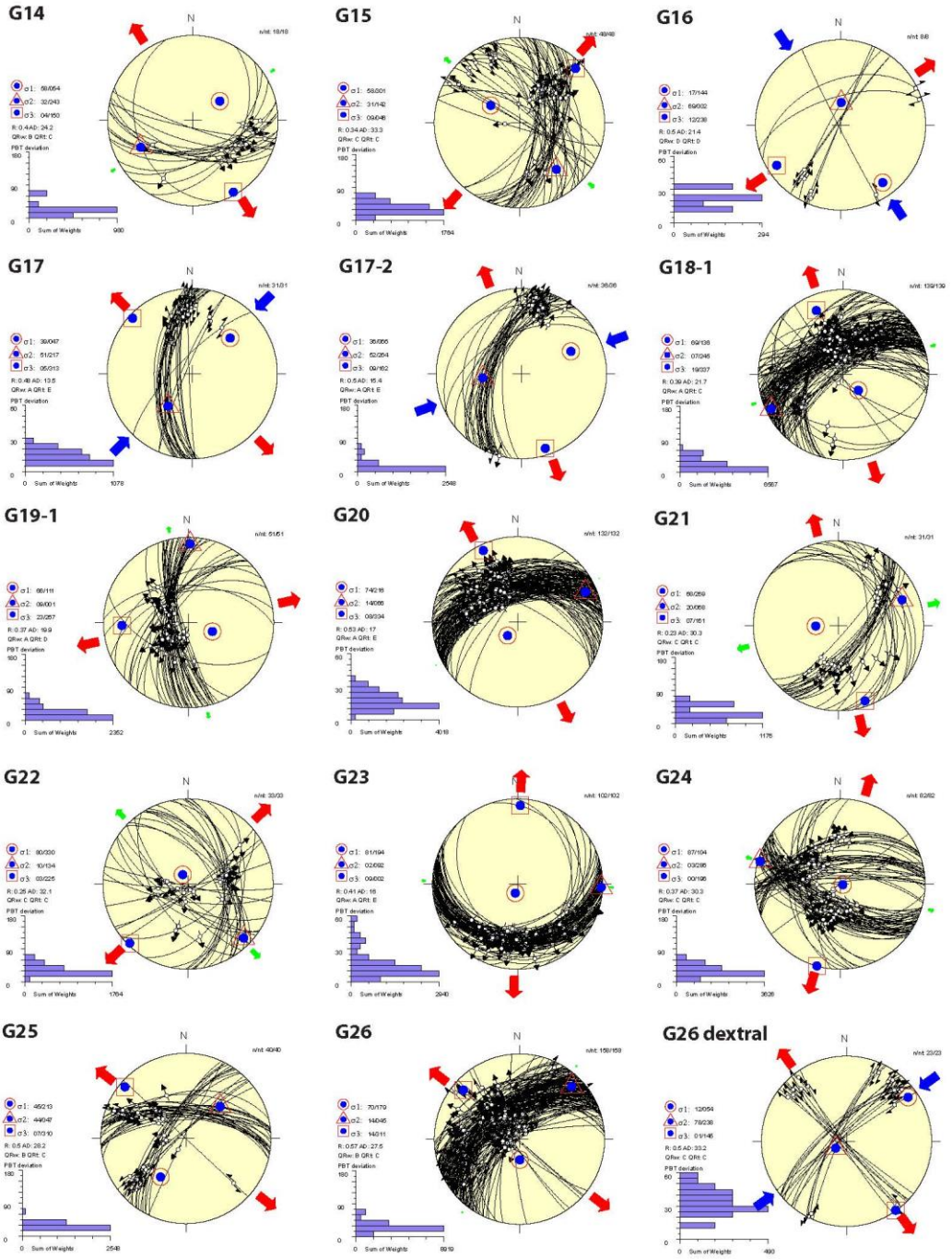
G14
G15
G16
G17
G17-2
G18-1
G19-1
G20
G21
G22
G23
G24
G25
G26
G26 dextral

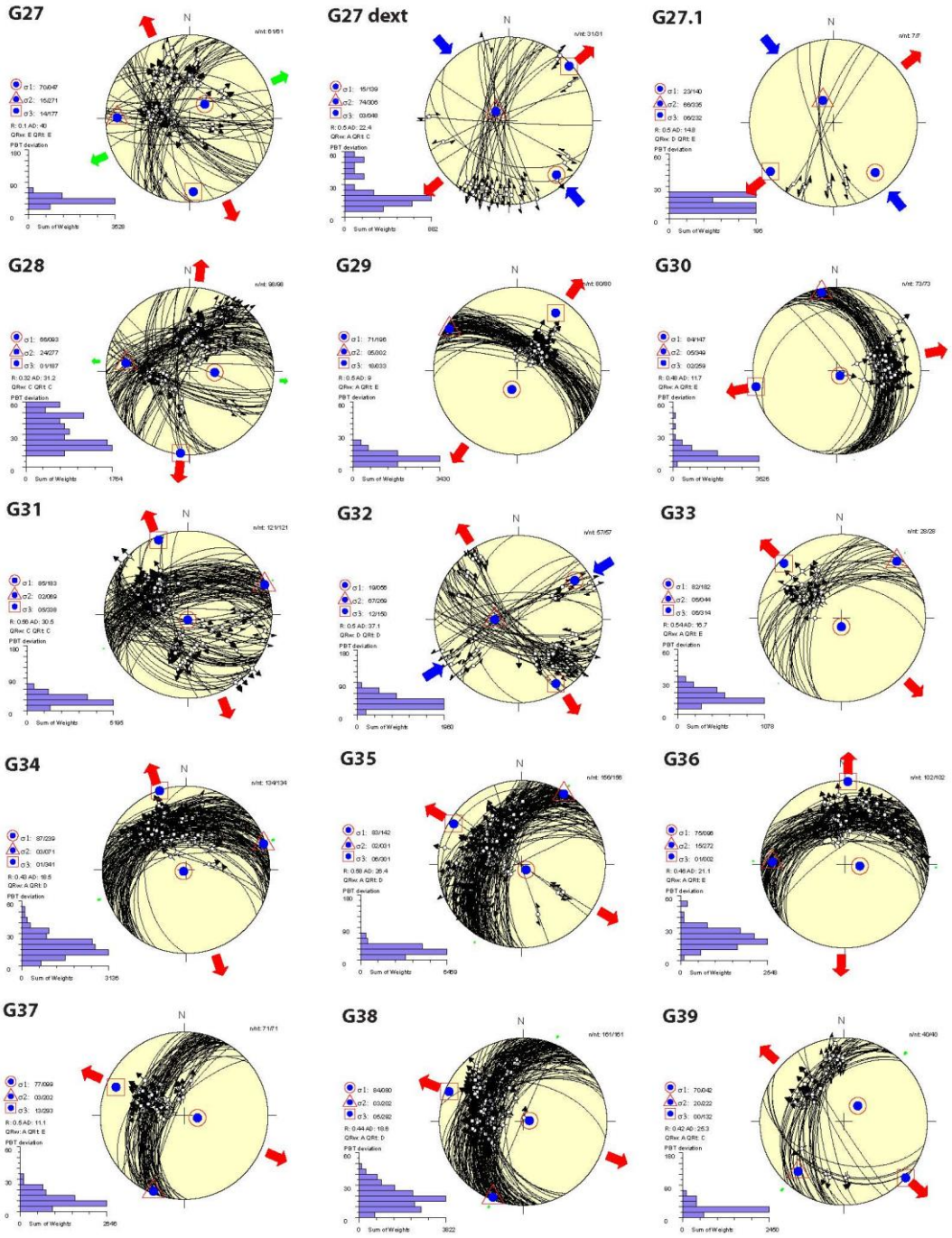
G27
G27 dext
G27.1
G28
G29
G30
G31
G32
G33
G34
G35
G36
G37
G38
G39

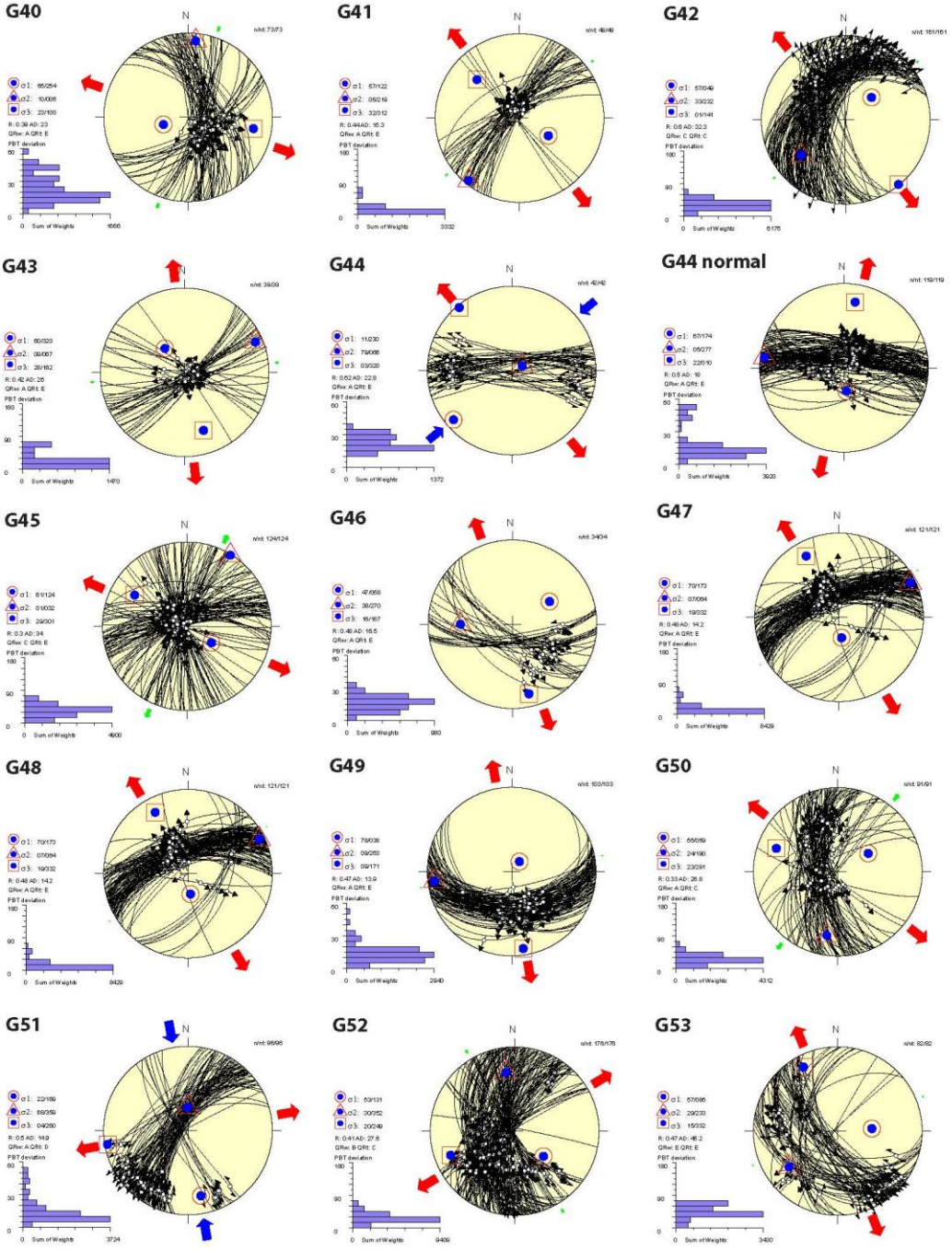
G40
G41
G42
G43
G44
G44 normal
G45
G46
G47
G48
G49
G50
G51
G52
G53

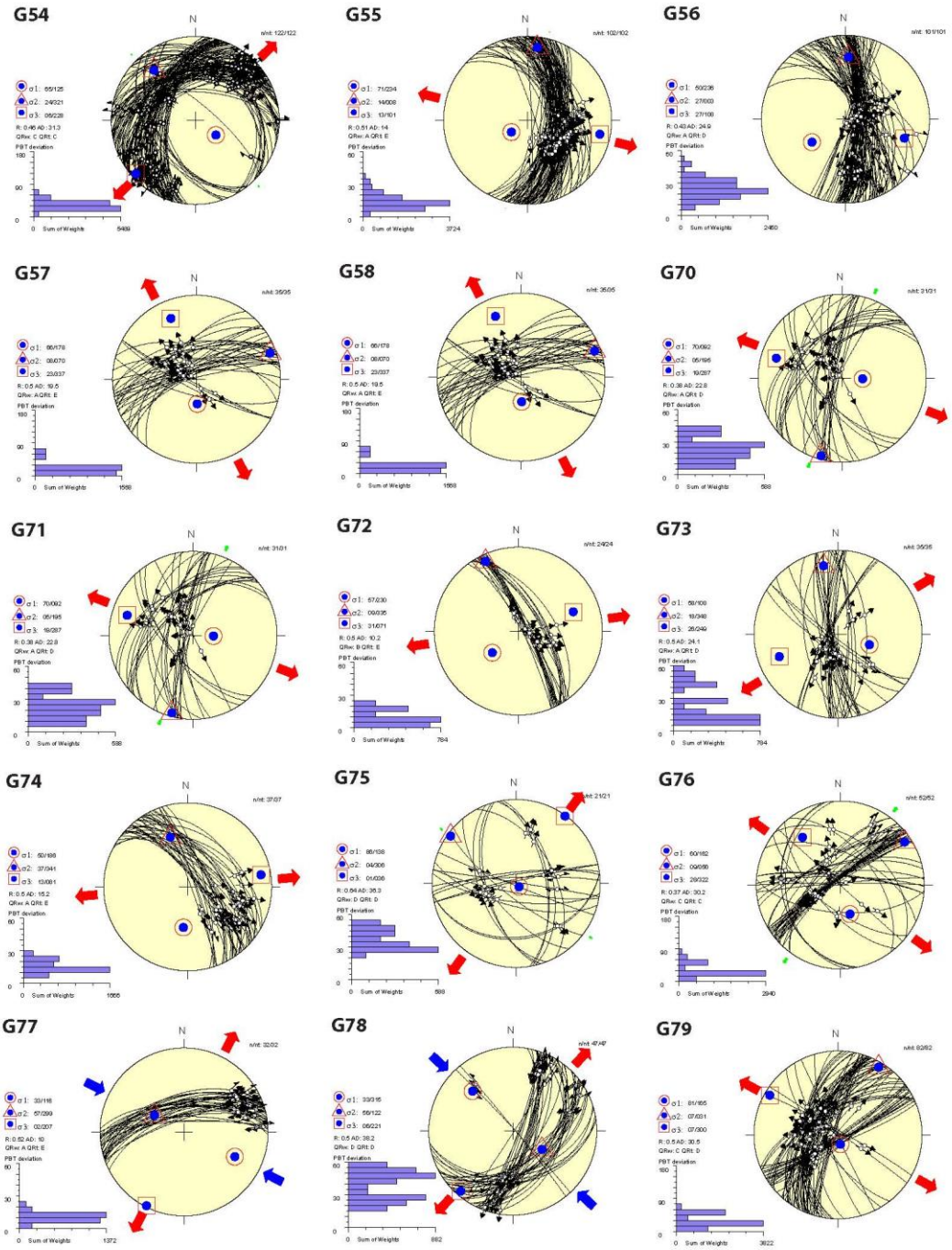
G54
G55
G56
G57
G58
G70
G71
G72
G73
G74
G75
G76
G77
G78
G79

G80

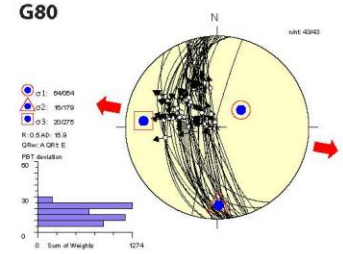

G81

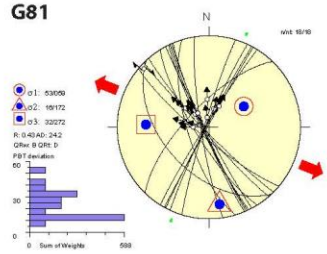

G82

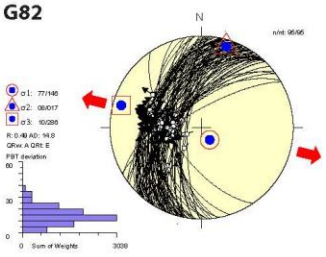

G83

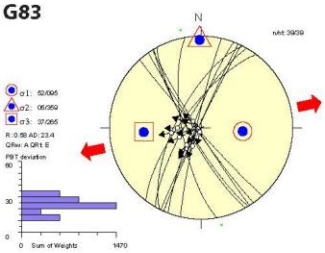

G84

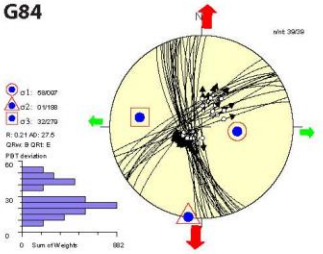

G85

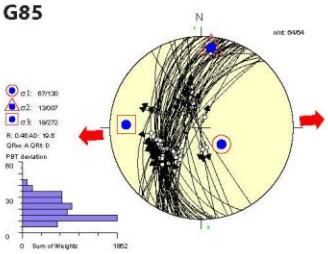

G86

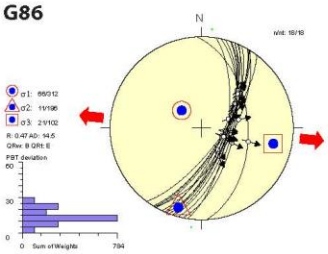

G87

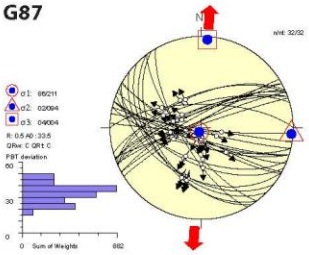

G88

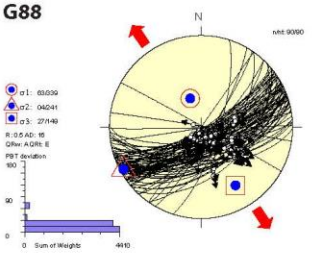

G89

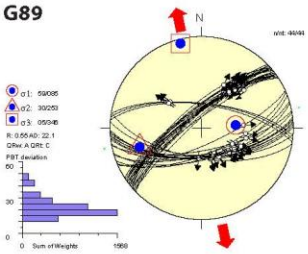

G90

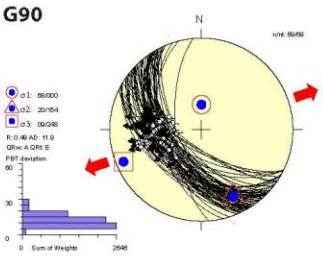

G91

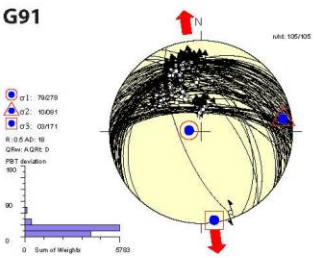

G92

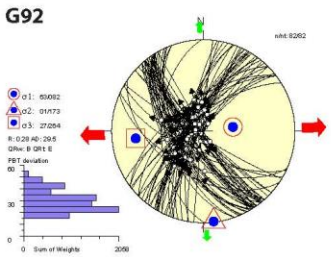

G93

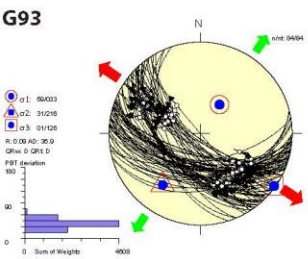

G94

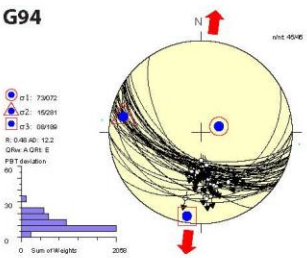

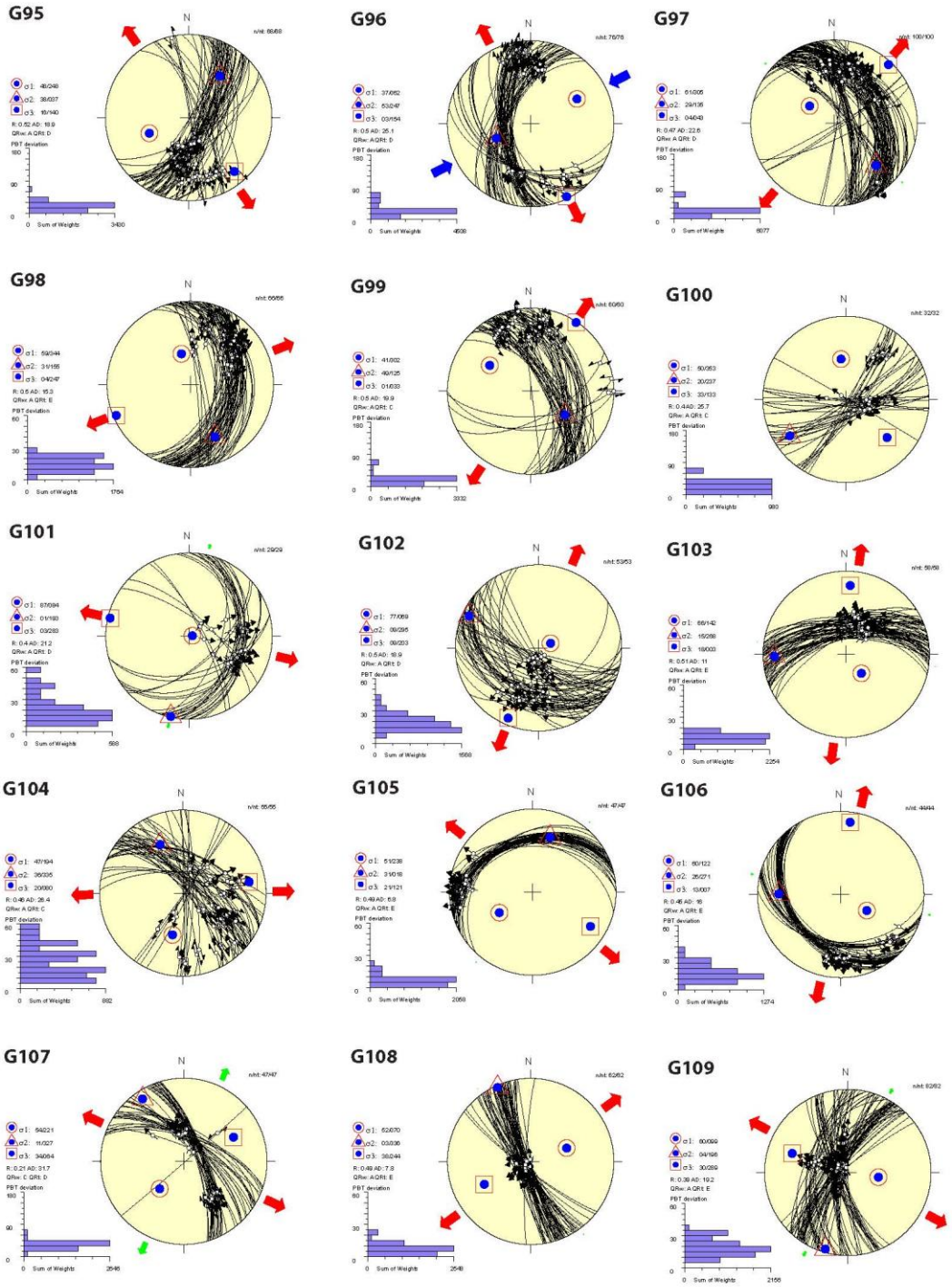
G95
G96
G97
G98
G99
G100
G101
G102
G103
G104
G105
G106
G107
G108
G109

G110

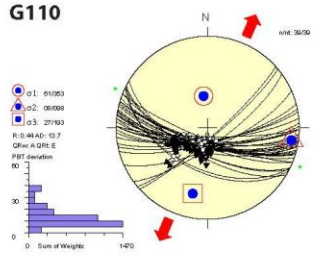

G111

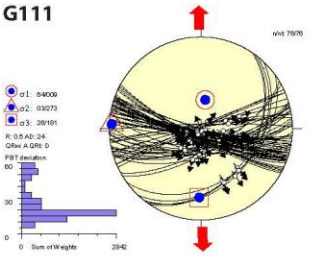

G112

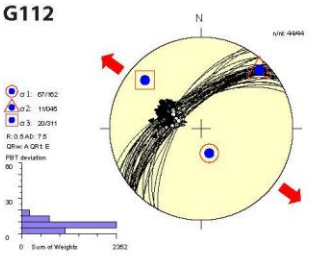

G113

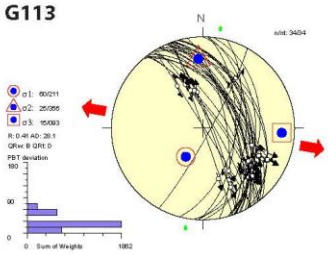

G114

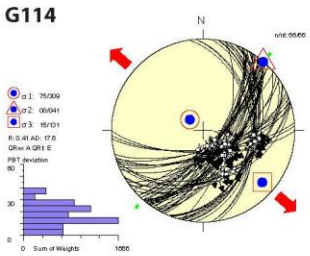

G115

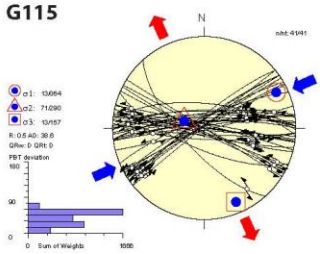

G116

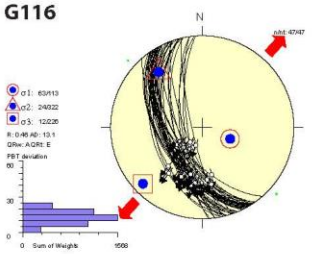

G117

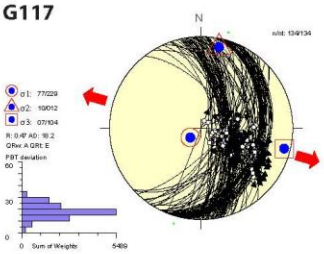

G118

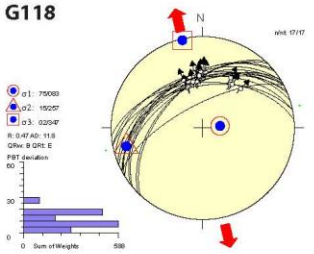

G119

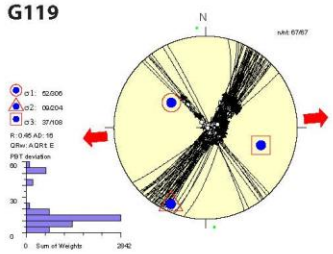

G120

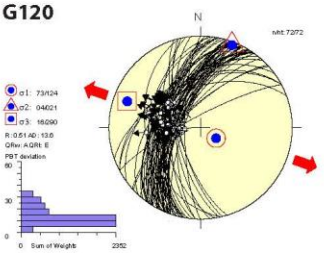

G121

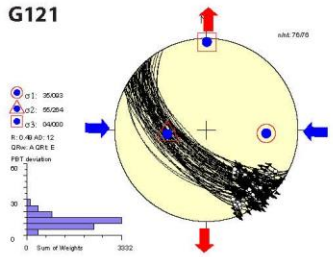

G122

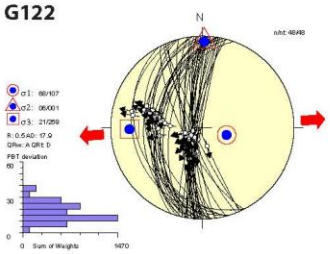

G123

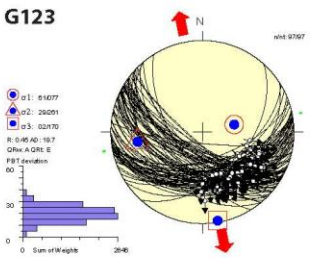

G124

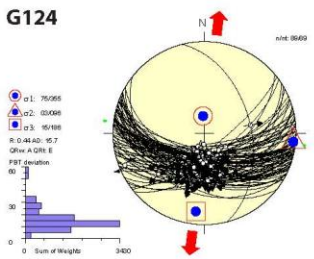

G125

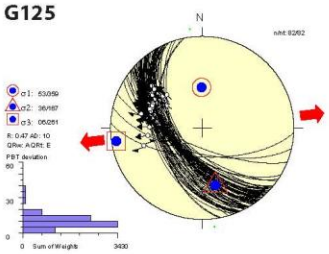

G127

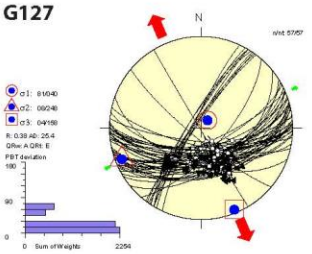

G128

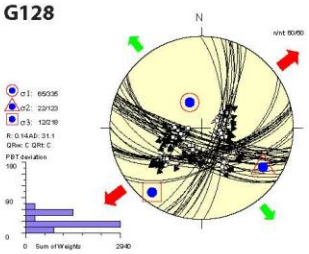

G129

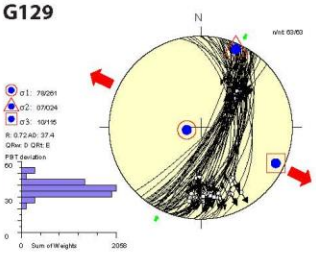

G130

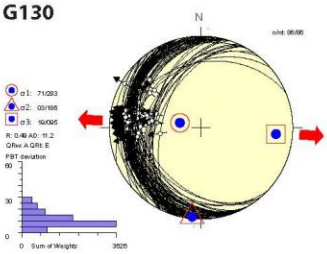

G131

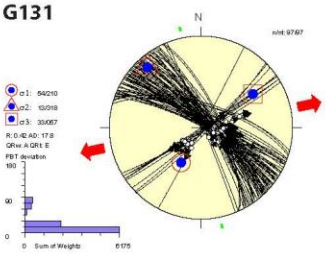

G132

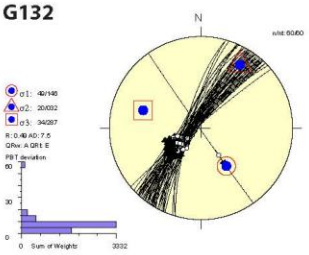

G133

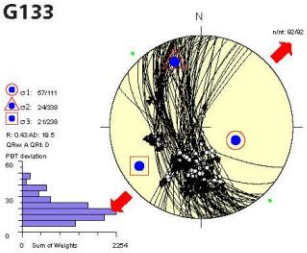

G134

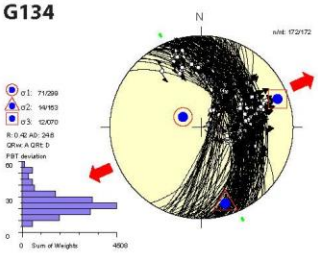

G135

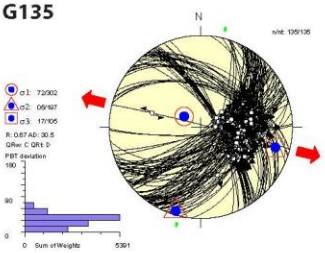

G136

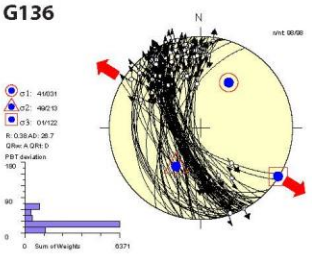

G137

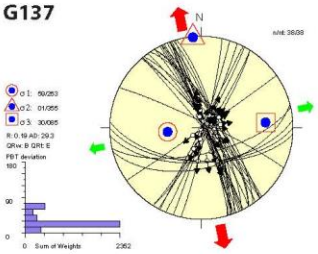

G138

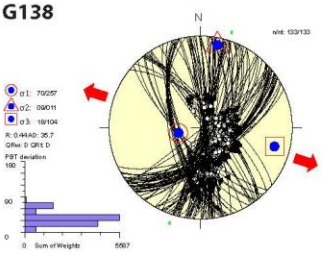

G139

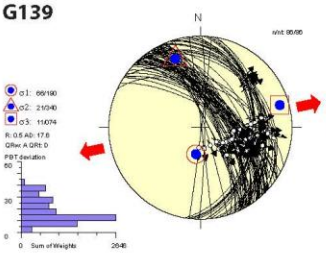

G140

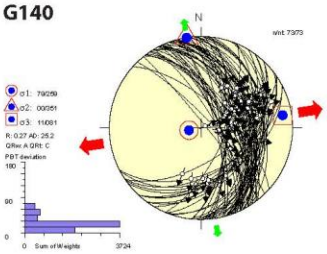

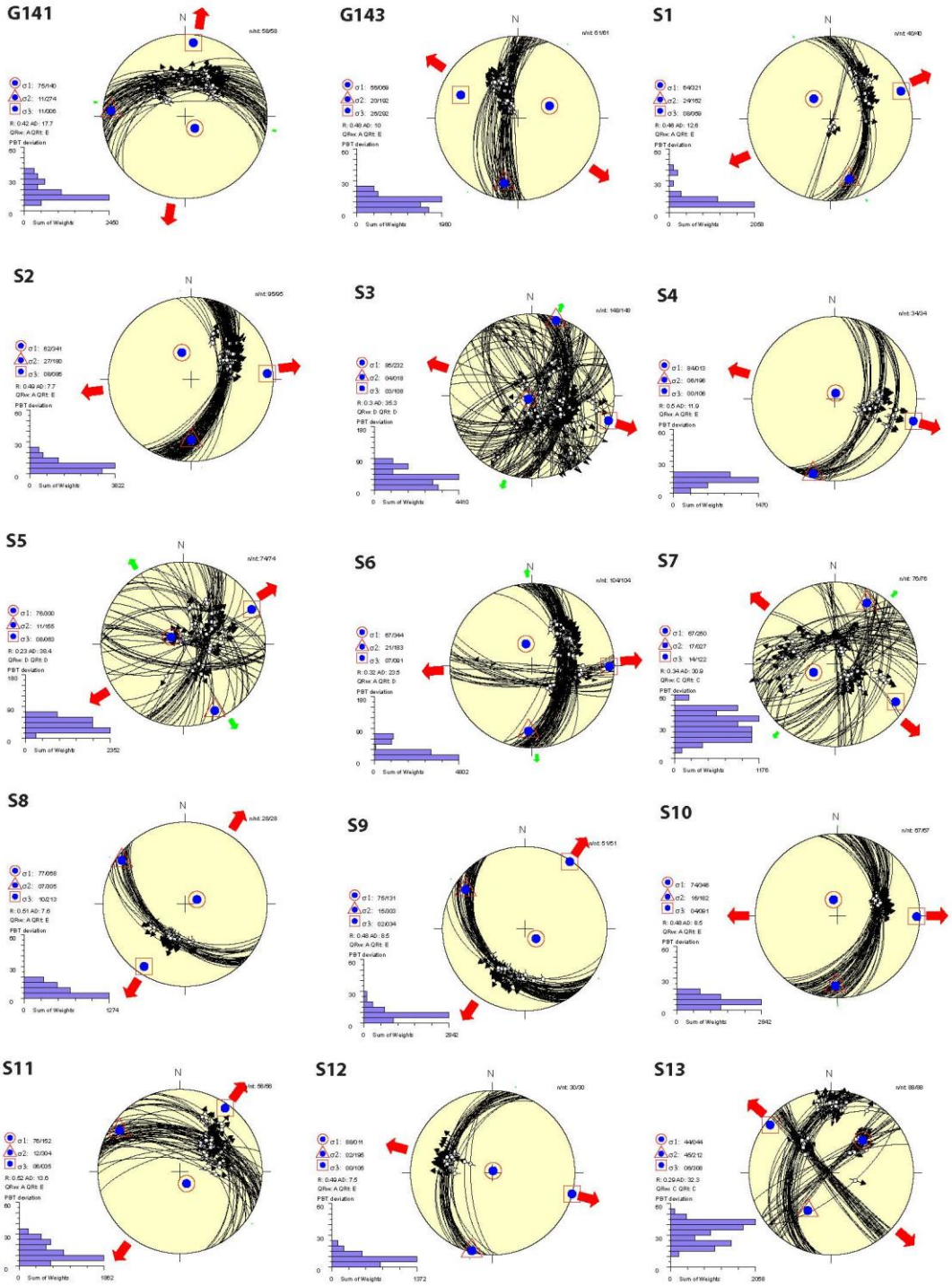
G141
G143
S1
S2
S3
S4
S5
S6
S7
S8
S9
S10
S11
S12
S13

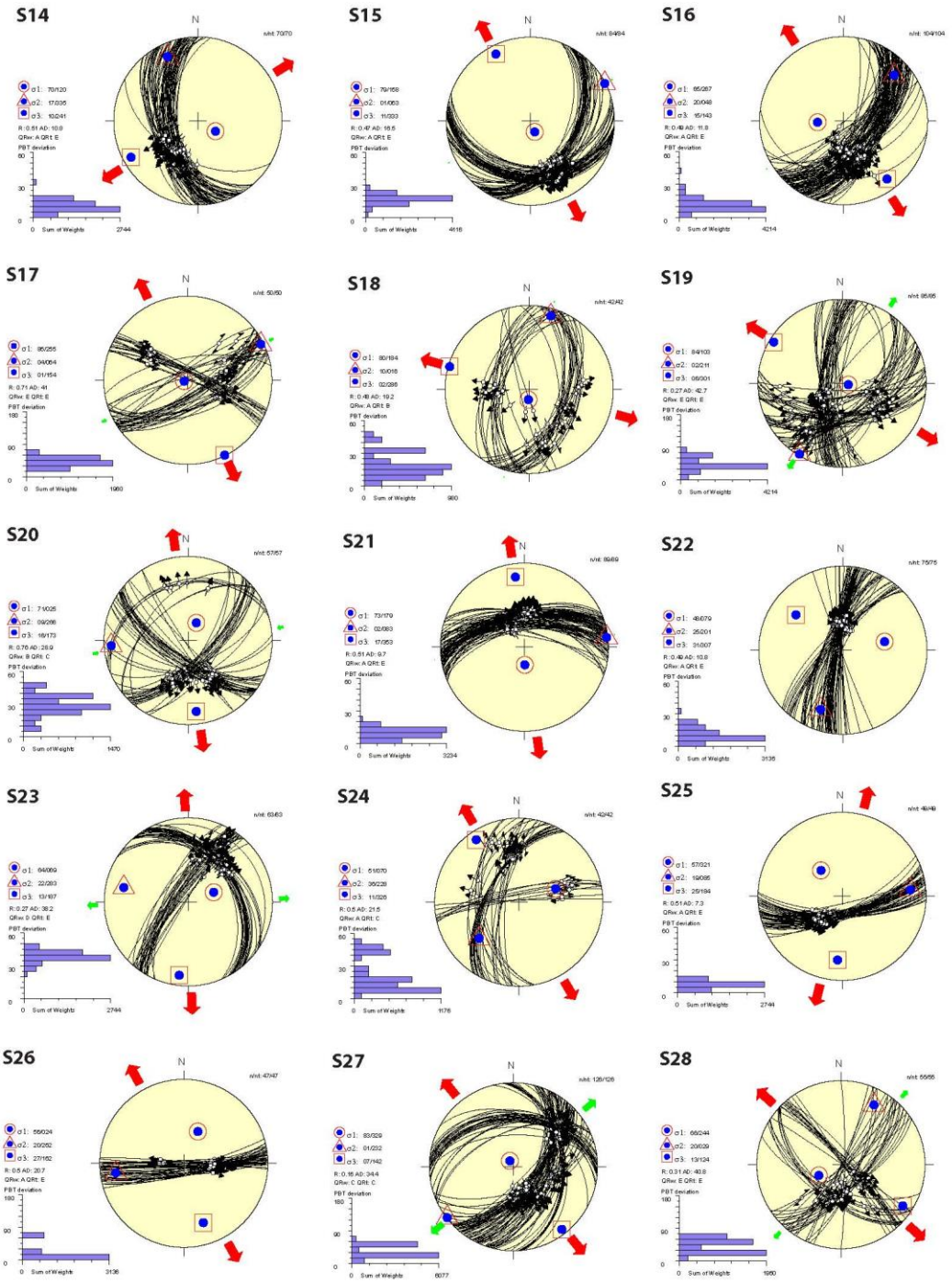
S14
S15
S16
S17
S18
S19
S20
S21
S22
S23
S24
S25
S26
S27
S28

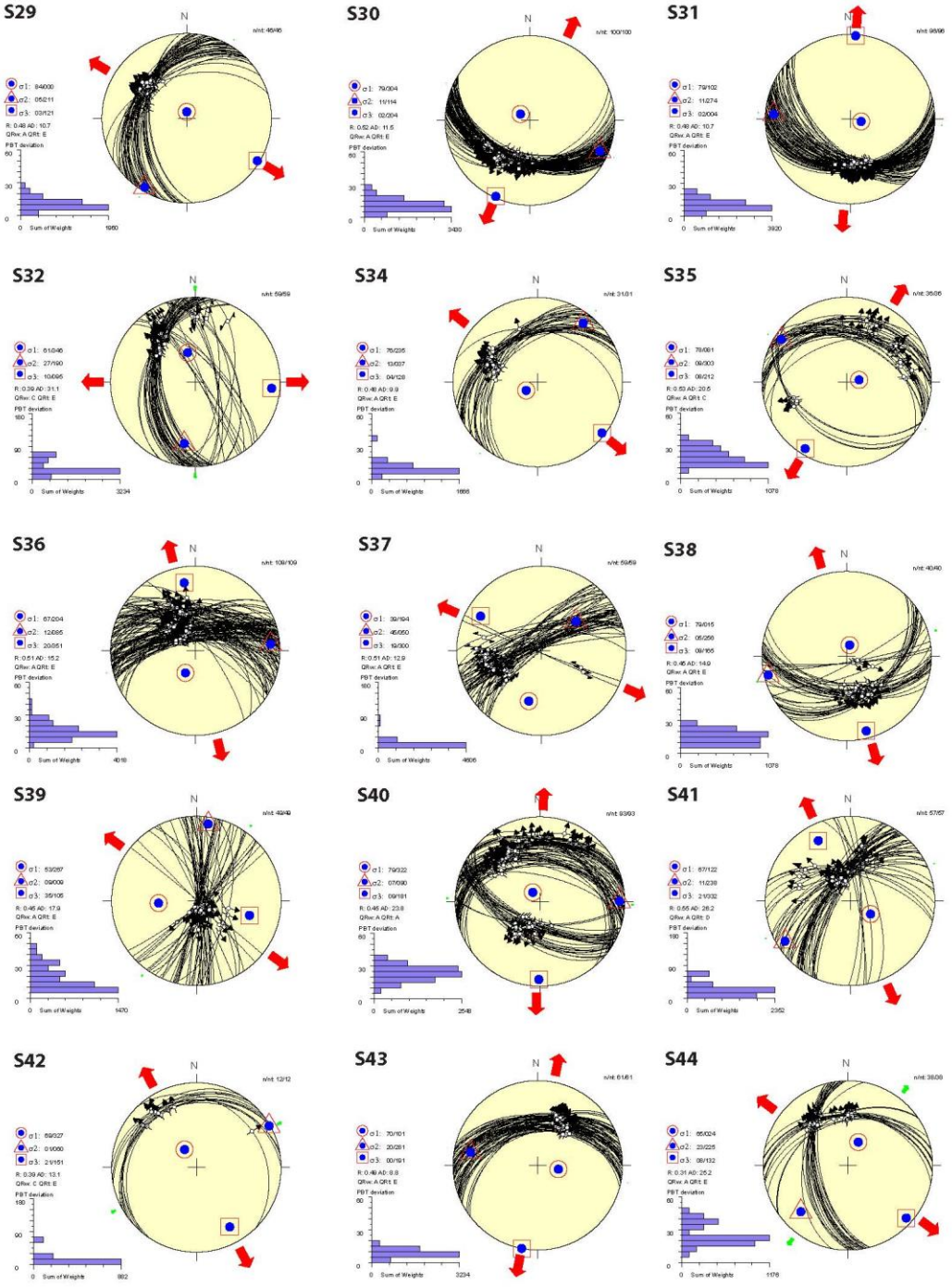
S29
S30
S31
S32
S34
S35
S36
S37
S38
S39
S40
S41
S42
S43
S44

S45

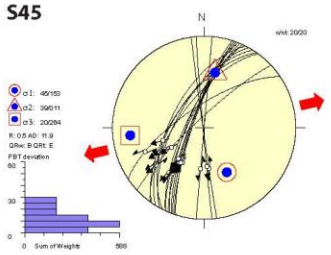

S46

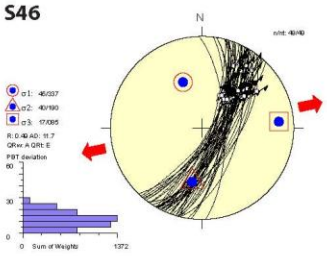

S47

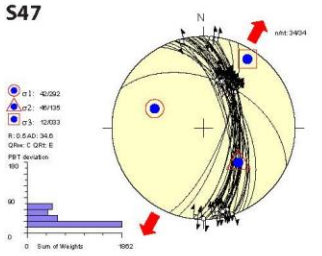

S48

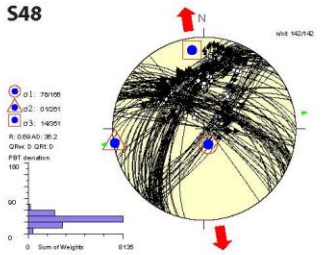

S49

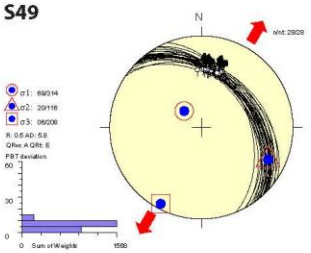

S50

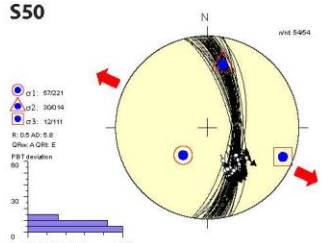

S51

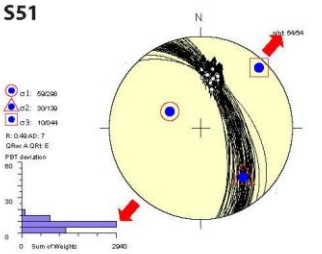

S52

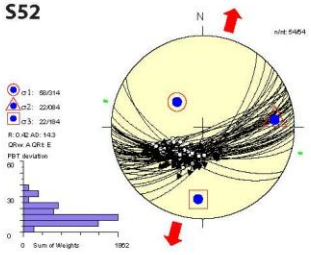

S53

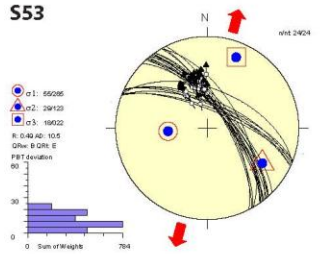

S54

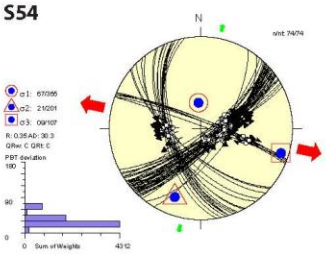

S55

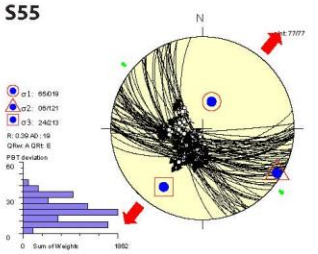

S56

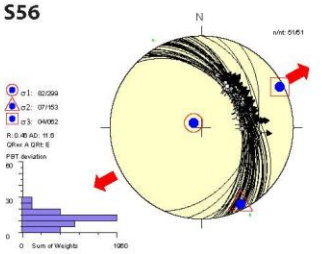

S60

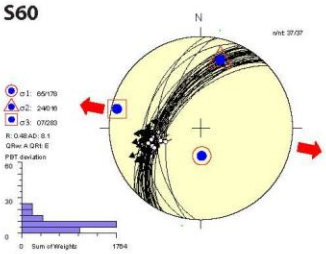

S61

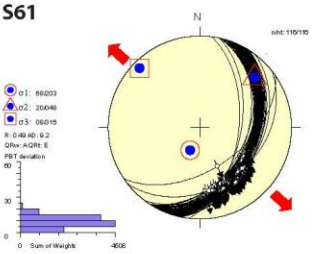

S62

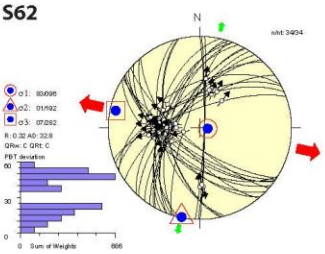

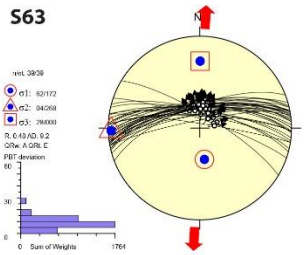
S63
N

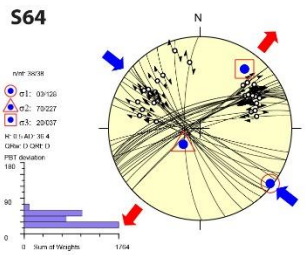
S64
N

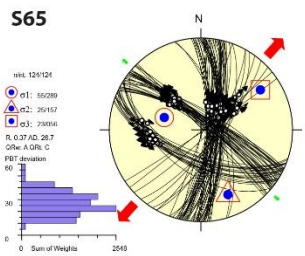
S65
N

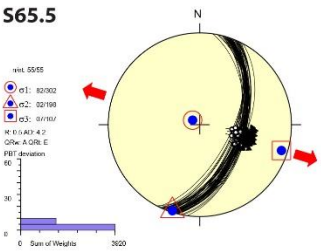
S65.5
N

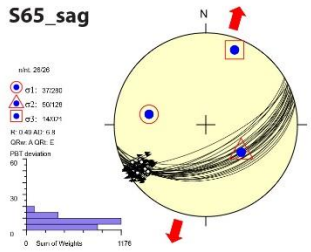
S65_sag
N

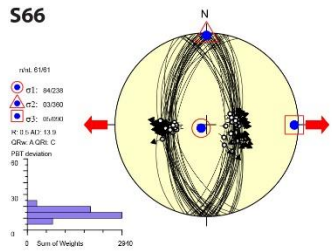
S66
N

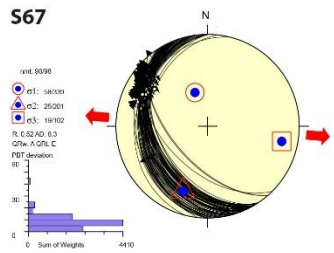
S67
N

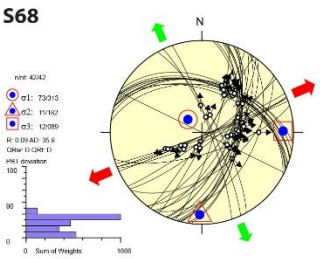
S68
N

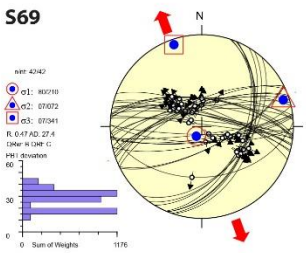
S69
N

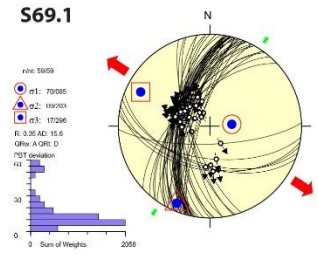
S69.1
N

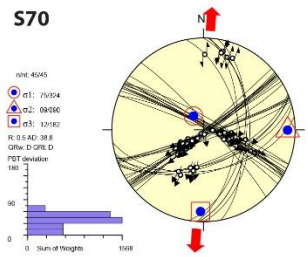
S70
N

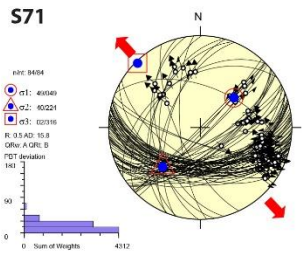
S71
N

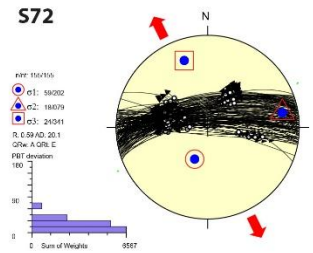
S72
N

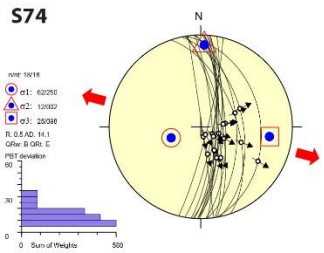
S74
N

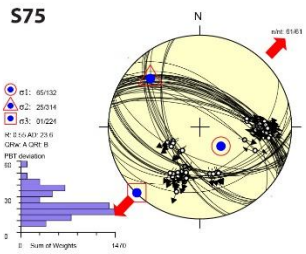
S75
N

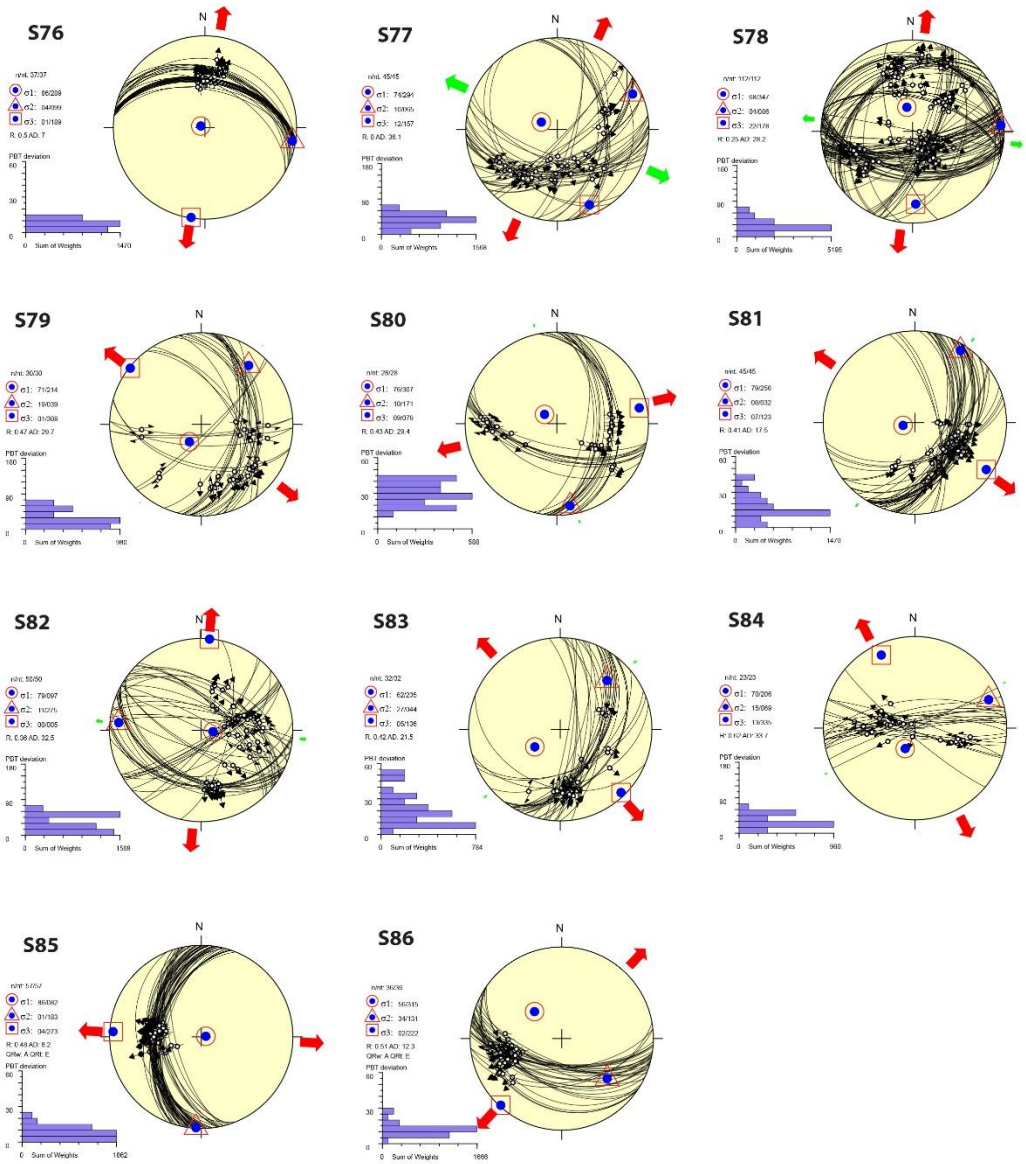
S76
S77
S78
S79
S80
S81
S82
S83
S84
S85
S86
N